UNIVERSITY OF CALIFORNIA,
IRVINE

Functional implications for novel gaits and substrates in anurans

DISSERTATION

submitted in partial satisfaction of the requirements
for the degree of

DOCTOR OF PHILOSOPHY

in Biological Sciences

by

Crystal M. Reynaga

Dissertation Committee:
Associate Professor Emanuel Azizi, Chair
Associate Professor Matthew J. McHenry
Associate Professor Donovan P. German

2018

DEDICATION

To

my parents, Sandra and Miguel,

in recognition of their endless hard-work
to provide me with every opportunity they never had;

my siblings, Madeleine and René

for their continued guidance, advice, and encouragement to continuously grow.

"Never be limited by other people's limited imaginations."
-Dr. Mae Jemison

"We draw our strength from the very despair
in which we have been forced to live. We shall endure."
-César Chávez

TABLE OF CONTENTS

LIST OF FIGURES

LIST OF TABLES

ACKNOWLEDGMENTS

First and foremost, I would like to thank my advisor and mentor Dr. Manny Azizi for his continued care and support throughout my PhD. Thank you for teaching me to become a better scientist, to think critically, and structure my time. In addition, I would like to thank my dissertation committee members, Drs. Matt McHenry and Donovan German for their insights in the development of my dissertation projects and career advice throughout the years. I would like to thank the UCI Physiology Group, a truly unique community of professors, postdocs, and graduate students. Thank you for the critical and constructive feedback on presentations, research projects, and career development. Thank you to my advancement committee, Drs. Kate Loudon and David Reinkensmeyer, your research continues to fascinate and inspire me, I am thankful for the time you spent serving on my advancement committee.

Thank you to the Azizi Lab, from post-docs to graduate students to undergraduates, I am grateful for our everyday interactions, helpful discussions, and learning from one another. I look forward to the new comraderies, the growth, and discoveries made from this lab and the unique contributions of the individuals that move it. I am thankful to various members who have helped with data collection (Nicole Danos, Caitrin Eaton, Marla Goodfellow, Yasmin Gutierrez, Ashley Hughes, Jeff Olberding, Ben Pearlman, Priyanka Satish, Kris Stover) and animal husbandry (Jordan Balaban, Alex Dunman, Marla Goodfellow, Yasmin Gutierrez, Ashely Hughes, Elizabeth Mendoza, Matthew Mickle, Choloe, Nouzille, Ben Pearlman, Thadora Poo, Pouyan Pouresfandiari, Priyanka Satish, Galatea Strong, Nuria Varela).

I am grateful to Greg Pauly, assistant curator, and Neftali Comacho, collections manager of Herpotology, Los Angeles County Museum of Natural History (LACM) for access to frog species and use of the collections space for my first chapter. I would like to thank Joseph Heras for useful discussions and insights for my first chapter. I am thankful for the critical discussions that have further developed chapters 2 and 3 from the members of the MURI team (Sarah Bergbreiter, Al Crosby, Mark Ilton, Greg Sutton, and Sathvik Divi).

In addition, a big thank you to Dr. Frances Leslie, Dr. Court Crowther, Daniel Fabrega, Phong Luong, Neda Moayedi, Bri McWhorter, Dr. Celina Mojica, Dr. Douglas Haynes, Dr. Roxane Cohen Silver, Dr. Nancy Aguilar-Roca, Dr. Ann Sakai, the Diversity Council, the DECADE community, and CARE center. I am thankful for their abundant resources, which have shaped me into the academic I am today. Their support through conversions and individual meetings have been crucial in my advocacy for diversity and inclusion, and action to develop strategies and programs that ensure minority population success. It is because of these people that I finally felt included and found my place at UCI, not just friendships, support, and fellowship but a group of professionals that truly cared for my success and have helped me fundamentally change and influence the academic administration at UCI. I doubt I would have continued the PhD without your influence and efforts, which has dramatically increased my pride and confidence in the Latina scholar I am today.

Thank you to Ms. Aida Gonzalez for sharing your second-grade classroom with me every year, to inspire the next generation, as I was uniquely inspired at Naples Elementary to become the scientist I am today. Thank you to Mr. Ronald Bournes for incorporating me into your youth

programs at George Washington Middle School. Thank you for allowing me to shape middle school minds and erase of the sigma of "What a Scientist Looks Like" and to know that this too can be them.

Dr. Colin Rathbun, my number one scientific supporter, friend, and partner. Grad school has been a fun adventure because of you. Thank you for also allowing me to reap the benefits of the Chemistry Department, share your friends, and become an honorary Prescher lab member. I look forward to the amazing discoveries you will engineer and our exciting new chapter as postdocs.

Chapter 1 was published with the permission of Wiley and Sons. The text in Chapter 1 is a reprint of the material as it appears in the following peer-reviewed article: Reynaga CM, Astley HC, Azizi E. Morphological and kinematic specializations of walking frogs. *JExpZool*. 2018;329:87–98, which has been published in final form at https://doi.org/10.1002/jez.2182. This article may be used for non-commercial purposes in accordance with Wiley Terms and Conditions for Use of Self-Archived Versions. The others listed in this publication directed and supervised research that forms the basis for the dissertation. Other coauthors from unpublished Chapters 2 and 3 are listed in Author Contributions sections at the end of each chapter.

I would like to thank fellow collaborators/coauthors from unpublished Chapters 2 and 3. Thank you, Henry Astley, for being a fantastic collaborator, your invaluable data, and your help and feedback throughout the development of Chapter 1. Thank you, Caitrin Eaton, for your compliant substrate innovation and help throughout Chapter 2. Thank you, Galatea Strong, for your incredible efforts with digitization in Chapter 2 and help with surgeries. Lastly, thank you to the MURI team, for our many conversations about my third chapter, which has led to many exciting new directions and I look forward to delving deeper.

All of this work would not have been possible without funding provided by: The National Science Foundation [DGE-1321846], the Department of Education [FG-18491], US Army Research Laboratory and the US Army Research Office, the Department of Ecology and Evolutionary Biology, the School of Biological Sciences, the Graduate Division, and the Chancellor's Club at UCI. Thank you for your generous funding of my research and dissertation.

CURRICULUM VITAE

CRYSTAL M. REYNAGA

Department of Ecology and Evolutionary Biology • University of California, Irvine
321 Steinhaus Hall, Irvine, CA 92697, USA • reynagac@uci.edu
crystalreynaga.weebly.com

EDUCATION

UNIVERSITY OF CALIFORNIA, IRVINE 2013 - 2018
Ph.D. in Biological Sciences
Dissertation: Functional implications for novel gaits and substrates in terrestrial vertebrates
Advisor: Dr. *Manny Azizi*

UNIVERSITY OF CALIFORNIA, SANTA CRUZ 2010 - 2012
B.S. in Marine Biology, with Honors Thesis
Advisor: Dr. *Rita S. Mehta*

UNIVERSITY OF CHICAGO 2008 - 2010
Anticipated Major(s): Biological Sciences and Romance Languages & Literatures (Spanish)
Completed 1st and 2nd year college education

RESEARCH EXPERIENCE

UNIVERSITY OF CALIFORNIA, IRVINE 2013 - 2018
PhD Candidate, Department of Ecology & Evolutionary Biology
Advisor: Dr. *Manny Azizi*
Collaborators: Drs. *Henry Astley*, *Caitrin Eaton*, *Mark Ilton*, *Sathvik Divi* & *Sarah Bergbreiter*

CALIFORNIA STATE UNIVERSITY, LONG BEACH 2012 - 2013
Research Assistant, Department of Biological Sciences
PIs: *Kimberly Dolphin* & Dr. *Ashley Carter*

UNIVERSITY OF WASHINGTON Summer 2012
Student Fellow, Functional Morphology & Ecology of Marine Fishes Course
Friday Harbor Laboratories
Advisors: Drs. *Lara Ferry* & *Andrew Clark*

UNIVERSITY OF CALIFORNIA, SANTA CRUZ 2010 - 2012
Undergraduate Research Assistant, Department of Ecology & Evolutionary Biology
Advisor: Dr. *Rita Mehta*
Collaborators: Drs. *Andrea Ward* & *David Collar*

UNIVERSITY OF CHICAGO 2008 - 2010
Laboratory Assistant, Department of Organismal Biology & Anatomy
Advisor: Dr. *Victoria Prince*

PUBLICATIONS

2. **Reynaga, C.M.**, Astley, H.C., and Azizi, E. (2018). Morphological and kinematic specializations of walking frogs. ***Journal of Experimental Zoology A: Ecological and Integrative Physiology*** 329:87-98. DOI: 10.1002/jez.2182

1. Collar, D. C., **Reynaga, C.M.**, Ward, A.B., and Mehta, R.S. (2013). A revised metric for quantifying body shape in vertebrates. ***Zoology*** 116:246-257.

MANUSCRIPTS IN REVISION AND PREPARATION

Available upon request

2. **Reynaga, C.M.**, Strong, G., Eaton, C. and Azizi, E. Jump mechanics and control on compliant substrates in the Cuban tree frog. *In preparation*.

1. **Reynaga, C.M.**, Ilton, M., Divi, S., Crosby, A.J., Bergbreiter, S., and Azizi, E. Trade-offs of power amplification on compliant substrates. *In preparation*.

PUBLISHED ABSTRACTS

7. **Reynaga, C.M.**, Eaton, C., Strong, G., Azizi, E. (2018). Hindlimb mechanics and motor pattern response to varying compliant substrates in the Cuban tree frog. *Integrative and Comparative Biology* 58, E186-E186.
6. **Reynaga, C.M.**, Eaton, C., Azizi, E. (2017). Effects of compliance on hindlimb kinematics of jumping Cuban tree frogs (*Osteopilus septentrionalis*). *Integrative and Comparative Biology* 57, E138-E138.
5. **Reynaga, C.M.**, Astley, H., Azizi, E. (2016). Morphological and kinematic constraints of quadrupedal walking in frogs. *Integrative and Comparative Biology* 56, E182-E182.
4. **Reynaga, C.M.**, Azizi, E. (2015). Force transmission pathways in the axial muscles of the common carp, *Cyprinus carpio*. *Integrative and Comparative Biology* 55, E320-E320.
3. **Reynaga, C.M.**, Danos, N., Azizi, E. (2014). Conflicts between locomotor modes: terrestrial and aquatic locomotion in the Senegal running frog, *Kassina senegalensis*. *Integrative and Comparative Biology* 54, E337-E337.
2. **Reynaga, C.M.**, Ferry, L.A., Clark, A.J. (2013). A comparative study of body shape and swimming kinematics in pholid and stichaeid fishes. *Integrative and Comparative Biology* 53, E3337-E337.
1. **Reynaga, C.M.**, Collar, D.C., Ward, A.B., Mehta, R.S. (2012). A revised metric to quantify body shape diversity in vertebrates. *Integrative and Comparative Biology* 52, E145-E145.

PRESENTATIONS

**Award winning presentation*

25. ***Crystal M. Reynaga** (2018). Frog Olympics: Jumping off unsteady diving boards. Oral presentation competition at the *UC Irvine Campus-wide Finals*, Irvine CA.
24. ***Crystal M. Reynaga** (2018). Frog Olympics: Jumping off unsteady diving boards. Oral presentation competition at the *UC Irvine Campus-wide Grad Slam Semi-finals*, Irvine CA.
23. **Crystal M. Reynaga**, Galatea Strong, Caitrin Eaton & Emanuel Azizi (2018). Hindlimb mechanics and motor pattern response to varying compliant substrates in Cuban tree frogs. Oral presentation at the *Society for Integrative and Comparative Biology*, San Francisco CA.
22. **Crystal M. Reynaga** & Emanuel Azizi (2017). Effects of compliance on elastic energy recovery in the bullfrog plantaris muscle. Oral presentation at the Southwest Regional Meeting for the *Society for Integrative and Comparative Biology*, Harvey Mudd College, Claremont CA.

21. **Crystal M. Reynaga,** Caitrin Eaton & Emanuel Azizi (2017). Hindlimb mechanics and response of jumping from compliant substrates in tree frogs. Oral presentation at the *Society for Experimental Biology Annual Meeting*, Gothenburg, Sweden.
20. ***Crystal M. Reynaga,** Caitrin Eaton & Emanuel Azizi (2017). Effects of compliant substrates on jumping. Oral presentation at the *NSF-GRFP Research Symposium*, UC Irvine, Irvine CA.
19. **Crystal M. Reynaga,** Caitrin Eaton & Emanuel Azizi (2017). Frog Olympics: Jumping off unsteady diving boards. Oral presentation at the *Associated Graduate Students (AGS) Symposium*, UC Irvine, Irvine CA.
18. **Crystal M. Reynaga,** Caitrin Eaton & Emaunel Azizi (2017). Effects of substrate compliance during jumping in the Cuban tree frog. Oral presentation at the *Winter Ecology and Evolutionary Biology Graduate Student Symposium (WEEBGSS)*, UC Irvine, Irvine CA.
17. **Crystal M. Reynaga**, Caitrin Eaton & Emanuel Azizi (2017). Effects of substrate compliance on hindlimb kinematics of jumping in Cuban tree frogs, *Osteopilus septentrionalis*. Poster presentation at the *Society for Integrative and Comparative Biology Annual Meeting*, New Orleans LA.
16. **Crystal M. Reynaga**, Caitrin Eaton & Emanuel Azizi (2016). Investigating the effects of substrate compliance on jumping in Cuban tree frogs. Oral presentation at the Southwest Regional Meeting for the *Society for Integrative and Comparative Biology*, California State University Fullerton, Fullerton CA.
15. **Crystal M. Reynaga**, Caitrin Eaton & Emanuel Azizi (2016). Effects of substrate compliance during Jumping in the Cuban tree frog, *Osteopilus septentrionalis*. Poster presentation at the *Society for Advancing Chicanos/Hispanics and Native Americans (SACNAS) in Science: The National Diversity in STEM Conference*, Long Beach CA.
14. **Crystal M. Reynaga**, Henry Astley & Emanuel Azizi (2016). Morphological and kinematic constraints of quadrupedal walking in frogs. Oral presentation at the *Society for Integrative and Comparative Biology Annual Meeting*, Portland OR.
13. **Crystal M. Reynaga**, Henry Astley & Emanuel Azizi (2015). Morphological and kinematic constraints of quadrupedal walking in frogs. Oral presentation at Southwest Regional Meeting of the *Society for Integrative and Comparative Biology*, Cal Poly Pomona, Pomona CA.
12. **Crystal M. Reynaga** & Emanuel Azizi (2015). Force transmission pathways in axial muscles of the common carp, *Cyprinus carpio*. Oral presentation at *Winter Ecology and Evolutionary Biology Graduate Student Symposium*, UC Irvine, Irvine CA.
11. **Crystal M. Reynaga** & Emanuel Azizi (2015). Force transmission pathways in axial muscles of the common carp, *Cyprinus carpio*. Poster presentation at *Society for Integrative and Comparative Biology Annual Meeting*, West Palm Beach FL.
10. **Crystal M. Reynaga**, Nicole Danos, Emanuel Azizi (2014). Conflicts between locomotor modes: running and jumping locomotion in the Senegal running frog, *Kassina senegalensis*. Poster presentation at the *Society for Integrative and Comparative Biology Annual Meeting*, Austin TX.
9. **Crystal M. Reynaga**, Nicole Danos, Emanuel Azizi (2013). Conflicts between locomotor modes: terrestrial and aquatic locomotion in the Senegal running frog, *Kassina senegalensis*. Oral presentation at the Southwest Regional Meeting of the *Society for Integrative and Comparative Biology*, UC Riverside, Riverside CA.
8. **Crystal M. Reynaga**, Nicole Danos, Emanuel Azizi (2013). Limb kinematics during terrestrial and aquatic locomotion in the Senegal running frog, *Kassina senegalensis*. Oral presentation at the *Competitive Edge Summer Symposium*, UC Irvine, Irvine CA.
7. **Crystal M. Reynaga**, Lara Ferry, Andrew Clark (2013). A comparative study of body shape and swimming kinematics in pholid and stichaeid fishes. Poster presentation at the *Society for Integrative and Comparative Biology Annual Meeting*, San Francisco CA.

6. **Crystal M. Reynaga**, Lara Ferry, Andrew Clark (2012). A comparative study of body shape and swimming kinematics in pholid and stichaeid fishes. Oral presentation at the *Southwest Regional Meeting of the Society for Integrative and Comparative Biology*, CSU San Bernardino, San Bernardino CA.
5. **Crystal M.Reynaga**, David Collar, Andrea Ward, Rita Mehta (2012). A revised metric to quantify body shape diversity in vertebrates. Poster presentation at the *CAMP Statewide Research Symposium*, UC Irvine, Irvine CA.
4. **Crystal M. Reynaga**, David Collar, Andrea Ward, Rita Mehta (2012). A revised metric to quantify body shape diversity in vertebrates. Oral presentation at the *Society for Integrative and Comparative Biology Annual Meeting*, Charleston SC.
3. **Crystal M. Reynaga**, David Collar, Andrea Ward, Rita Mehta (2011). A revised metric to quantify body shape diversity in vertebrates. Oral presentation at the *Wainwright Functional Morphology Meeting*, Carmel Valley CA.
2. **Crystal M. Reynaga**, David Collar, Andrea Ward, Rita Mehta (2011). A revised metric to quantify body shape diversity in vertebrates. Poster presentation at the *SACNAS National Conference*, San Jose CA.
1. **Crystal M. Reynaga**, David Collar, Andrea Ward, Rita Mehta (2011). A revised metric to quantify body shape diversity in vertebrates. Poster presentation at the *Undergraduate Summer Research Symposium*, UC Santa Cruz, Santa Cruz CA.

GRANTS, AWARDS & FELLOWSHIPS

Research grants: 10 total; $175,815

2018	**Chancellor's Club Fund for Excellence Fellowship**, UC Irvine, Recognizes and rewards the most academically superior doctoral students who exhibit outstanding promise as scholars, researchers and public leaders, $6,000.
2018	**Grad Slam Campus-wide Finalist**, UC Irvine, Campus-wide competition that showcases and awards the top ten, best three-minute research presentations by graduate scholars.
2018	**Diverse Educational Community and Doctoral Experience (DECADE) Travel Award**, UC Irvine, Graduate Division, $2,000
2017	**Best Oral Research Presentation**, NSF GRFP Research Symposium, UC Irvine, $100.
2017	**Society of Experimental Biology (SEB) Travel Grant**, £140.
2014-2017	**Broadening Participation Committee Travel Award**, Society for Integrative and Comparative Biology (SICB), $2,000
2014-2017	**Dept. of Ecology and Evolutionary Biology Travel Award**, UC Irvine, $1,500.
2014-2017	**Biological Sciences Dean's Office Travel Award**, UC Irvine, $1,000.
2016	**Graduate Assistance in Areas of National Need (GAANN) Research Fellowship**, US Dept. of Education, $1,000
2016	**GAANN Fellowship**, US Dept. of Education, $10,486
2015	**Diverse Educational Community and Doctoral Experience (DECADE) Research Award**, UC Irvine, Graduate Division, $1,800
2013-2018	**National Science Foundation Graduate Research Fellowship Award (NSF-GRFP)**, $136,000
2013-2017	**Graduate Opportunities Fellowship**, UC Irvine, Graduate Division, $17,000
2011,	**Charlotte Mangum Student Housing Award**
2013-2015	Society for Integrative and Comparative Biology (SICB)
2011-2012	**Initiative for Maximizing Student Diversity Fellowship (IMSD)**, UC Santa Cruz, National Institutes of Health, $3,500

2011-2012 **California Alliance for Minority Participation Fellowship (CAMP)**, UC Santa Cruz, National Science Foundation, $4,800

2012 **Friday Harbor Marine Lab Scholarship**, University of Washington, $1,800

2011 **National Science Foundation Research Experiences for Undergraduates (NSF-REU 0819009)**, UC Santa Cruz, $3,915

2009-2010 **Sam and Roslyn Berkman Scholarship**, University of Chicago

TEACHING EXPERIENCE

2016 **Guest Lecturer**, *Exercise Science Seminar*, UC Irvine, Irvine CA.
Lectured and lead discussion on the diversity of muscle function, and how muscles perform as motors, struts, and brakes. This seminar included about 20 students. Instructor of Record: Dr. *Manny Azizi*.

2016 **Teaching Assistant**, *Biology of Birds Laboratory*, UC Irvine, Irvine CA.
Supervised field (lab) bird observations throughout Orange County Parks. Additionally, involved in course administration: graded exams and final papers. Instructor of Record: Dr. *John Avise*.

2013-2015 **Teaching Assistant**, *Physiology Laboratory*, UC Irvine, Irvine CA.
Prepared, instructed, and supervised weekly physiology laboratory experiments and assignments. Graded lab reports and exams. Assisted students outside of class with course material, assignments, and scientific writing. Instructor of Record: Dr. *Nancy Aguilar-Roca.* Evaluated highly by student evaluations:

> "*She is a very diligent instructor and would always provide us good feedback on our assignments. She goes above and beyond compared to other TA's to prepare us for the current assignments (homework, lab reports) or for future assignments (future lab reports). Her feedback helps me become a better writer, more specifically lab report writing, which is extremely important here at UCI. In addition, she is very enthusiastic lecturer and makes students more interested in participating in the lab.*"

2014 **Teaching Assistant**, *Marine Biology*, UC Irvine, Irvine CA.
Assisted students outside of class with course material and was involved in course administration. Instructors of Record: Drs. *Nancy Aguilar-Roca* & *Donovan German.*

STUDENT MENTORING

*(33 students for ~ 720 total hours; *Undergraduate research project; ⌘Current career in STEM)*

Galatea Strong* (2016-2018), Ashley Hughes* (2014-2015), Yasmin Gutierrez* (2014-2015), Elizabeth Mendoza⌘ (2016), Alica Correales (2016), Luc D'Hauthuille (2016), Kenny Huynh (2016), Kirolos Kelada (2016), Lupita Lopez (2016), Aylin Mojica (2016), Nuria Perez Varela (2016), Jordyn Rodwell (2016), Dany Atallah (2015), Alexander Beechko⌘ (2015), Thomas Carpino⌘ (2015), Noah Ghossein⌘ (2015), Jourdan Mason (2015), Jasmin Melara (2015), Courtney Powell⌘ (2015), Joli Quinceno (2015), Bianka Dominguez (2014-2015), Judith Granados (2014-2015), Leidy Cruz (2014-2015), Andrew DiMauro⌘ (2014), Melvin Lorenzo⌘ (2014), David Novo (2014), Ivory Paulk⌘ (2014), Flora Wang (2014), Nicholas White⌘ (2014), Sarah Valles⌘ (2013-2014)

UNIVERSITY AND PROFESSIONAL SERVICE

Graduate Representative, *Graduate Dean's Advisory Council on Diversity*, UC Irvine, 2015-2018.
Composed of distinguished faculty with a record of commitment to diversity, with participation by selected graduate students and professional staff. The primary function of this group provides ideas, insight, and expertise to expand and enhance the Graduate Division's efforts to recruit and retain outstanding students from diverse backgrounds. Notable works include the development of "Learning Community for Future Faculty at UC Irvine", a proposal to develop learning

communities to prepare graduate students from underrepresented backgrounds to successfully pursue faculty careers at research intensive universities. A pilot program based upon this proposal will go into effect starting Fall 2019.

UC LEADS Poster Presentation Judge, for the Annual University of California Leadership Excellence through Advanced Degrees (UC LEADS) program 2018, *Santa Barbara* CA.

Physiology Oral and Poster Presentation Judge, for the Annual Biomedical Research Conference for Minority Students (ABRCMS) 2017 in *Phoenix* AZ.

UC Irvine Graduate Division Student Representative, for the Annual Biomedical Research Conference for Minority Students (ABRCMS) 2017, *Phoenix* AZ.

NSF-GRFP Graduate Student Panelist, *UC Irvine School of Biological Sciences*, 2014-2017. Provided words of wisdom to first and second year UCI graduate students based upon my personal experience preparing a successful NSF-GRFP proposal.

McNair Graduate Student Panelist, *UC Irvine Graduate Division*, 2016-2017. Provided words of wisdom to third to fourth year undergraduates from UC Davis and University of Central Florida based upon personal experience applying to graduate school and transitioning from undergraduate to graduate life.

UC Irvine Graduate Division Student Representative, for the Annual Biomedical Research Conference for Minority Students (ABRCMS) 2016, *Tampa* FL.

Graduate Student Lead Mentor, *UC Irvine Graduate Division*, Summer(s) 2014-2016. Mentored 6-10 undergraduate students each summer in the Summer Undergraduate & Masters Research Program. This program is designed to prepare students from diverse backgrounds for graduate school. Mentoring covered successfully applying for graduate school, applying for fellowships, academic writing, preparing academic presentations, academic career planning, advice on all aspects of life as a graduate student, and academic research methods.

Ecology & Evolutionary Biology Brown-Bag Lunch, *UCI Dept. of Ecology & Evolutionary Biology*, Spring 2016. Established and developed a brown-bag dialogue series for graduate students to access a supportive community, tailored resources, and professional development opportunities through invited speakers. In coordination with Dr. *Ann Sakai*, DECADE Faculty Mentor.

UC Irvine Graduate Division Student Representative, for the Northern California Forum for Diversity in Graduate Education, 2016, San Jose State University, *San Jose* CA.

DECADE Student Council STEM Co-Chair, for the UCI Diverse Educational Community and Doctoral Experience (DECADE), *UC Irvine*, 2015-2016. Notable works include the development of the "DECADE Student Council Strategic Plan" this document provides university-wide strategies to help effectively address challenges for academic enhancement and inclusion for all graduate students at UCI.

Member of organizational committee, for the Graduate Student Invited Speaker (GSIS), Dept. Ecology and Evolutionary Biology, UC Irvine, Fall 2015.

Leadership mentor, for Diverse Educational Community and Doctoral Experience: Partnering in Leadership for Undergraduate Students (DECADE-PLUS) Program, *UC Irvine*, 2014-2015. Mentored seven first year undergraduate Chancellor's Excellence Scholars. The focus of this program is to increase retention of incoming minority and underrepresented scholars through mentoring, with a focus on academics.

NSF-GRFP Writing Mentor, *UC Irvine School of Biological Sciences*, 2014. Provided one-on-one writing workshops to provide feedback on NSF-GRFP personal and research statement proposals.

UC Irvine Graduate Division Student Representative, for the Annual Biomedical Research Conference for Minority Students (ABRCMS) 2014, *San Antonio* TX.

Member of organizational committee, for the Winter Dept. of Ecology and Evolutionary Biology Graduate Student Symposium (WEEBGSS), *UC Irvine*, Winter 2015.

PROFESSIONAL DEVELOPMENT

Activate to Captivate Public Speaking, *UC Irvine*, Fall 2018. Eight-week certification program, addressed how to effectively communicate your research in a compelling way. Instructed by communications specialist, Bri McWhorter, MFA.

Safe Zone Training, *UC Irvine*, Spring 2016. Program empowers individuals as Allies to remain informed, supportive, and affirming of the LGBTQQIA+ Community at UCI.

Science Communication, *UC Irvine*, Spring 2015. Trainee under NPR's Sandra Tsing Loh, host of the syndicated radio show "The Loh Down on Science". This program explores the art and science of effective writing, performance, and audience interaction.

Certified Undergraduate Research Mentor in the Laboratory, *UC Irvine*, Fall 2014. Training and development workshop series on undergraduate research mentoring in the laboratory setting. A curriculum developed by the Wisconsin Program for Scientific Teaching with support from the Howard Hughes Medical Institute.

Mentor Excellence Program, *UC Irvine*, Summer 2013. Training and development workshop series on building a mentoring relationship, communication and interpersonal connections, ethics in academics, research and personal decisions, and resilience in balancing academics and wellness through mentorship. Programing offered by the Graduate Division.

Teaching Assistant Professional Development Workshops, *UC Irvine*, Summer 2013. Training and development workshop series on instructional design, responsibilities, pedagogical theory and practice, and university policies and resources. Programing offered by the Teaching, Learning & Technology Center.

UCI Graduate Division Competitive Edge Summer Research Program, *UC Irvine*, Summer 2013. A summer pre-entry program for incoming female and underrepresented PhD students to conduct research under the direct supervision and guidance of a faculty member, Dr. *Manny Azizi*. This program featured workshops and seminars about campus resources, fostering professional development, establishing peer support networks, and developing academic strategies to enhance the graduate education experience.

PUBLIC OUTREACH

American Physiological Society (APS) Physiology Understanding (PhUn) Week, *Long Beach* CA. 2018. A nationwide outreach program building connections between scientists and local schools. Partnered with *Dr. Nancy Aguilar-Roca* (UCI faculty), *Ms. Aida Gonzalez*, (2nd grade teacher), and APS to develop discovery and hands-on learning using small group "laboratory" activities on "Muscles, Movement, and Our Skeleton".

Naples Elementary School— Second Grade Outreach, *Long Beach* CA. 2014-2018. Partnered with *Ms. Aida Gonzalez* to develop interactive presentations, curriculum, and laboratory activities that addressed my research. Topics included: natural history of the Senegal running frog, muscle and vertebrate anatomy, anatomical measurements, and simple model building.

Washington Middle School— 7th and 8th Grade Outreach, *Long Beach* CA. 2016-2018. Developed an interactive presentation on my research, "How our muscles move and activate". With a post-discussion on STEM diversity in the sciences proposing questions like "What does a scientist look like?"

Helen Bernstein High School STEM Volunteer Tutor, *Hollywood* CA. 2013. Provided after school tutoring in a variety of STEM disciplines to students in a low-income/low-performing high school.

Haiti Compassion Volunteer with Ambassadors Fellowship, *Port-au-Prince*, Haiti. Summer 2011. Provided financial assistance and service to students and people within a neighborhood affected by the January 2010 earthquake, by organizing and administering a children's summer day camp which involved teaching English, crafts, and various educational activities.

Volunteer Camp Assistant at Hope Unlimited, *Campinas*, Brazil. Summer 2010. Prepared and supervised outreach activities prepared for orphan and street children through educational activities and provided a loving homelike environment designed to cultivate their trust and encourage growth.

Girls' Cross-Country Coaches' Assistant and Camp Councilor, *Long Beach Polytechnic High School*. Summer 2008. *Catalina Island*, CA. Guided daily workouts, activities, monitored athlete activity, and safety of 50 female high school athletes.

JOURNALS SERVED AS MANUSCRIPT REVIEWER

Anatomia, Histologia, Embryologia

PROFESSIONAL MEMBERSHIPS

American Physiological Society (APS)
Society for Experimental Biology (SEB)
Society for Integrative and Comparative Biology (SICB)
Society for Advancing Chicanos and Native Americans in the Sciences (SACNAS)

SKILLS

Laboratory: *in vitro* muscle preparations, high-speed motion analysis, fish, amphibian, and reptilian handling, small animal surgery and dissections, fine-wire electromyography (EMG), processing specimens, clearing and double staining specimens, radiography, morphometrics and meristics, pressure and force transducers, materials testing, microscopy including SEM, soldering, 3D printing, laser cutting
Computer/Programming Experience: Statistical programing in "R", statistical program "JMP", data acquisition and analysis with IGOR, data mining, analysis, scripting, and programing in Matlab, ImageJ, LabView, Adobe Photoshop, Adobe Illustrator, Google SketchUp, Affinity Designer.
Language: Studied Spanish for 6 years— fluency in reading, writing, and conversational speaking.
Recreational: Enjoy running, cycling, climbing, and hiking. Classically trained violinist; studied 13 years under Mr. Allan Carter.

REFERENCES

Available upon request.

ABSTRACT OF THE DISSERTATION

Functional implication for novel gaits and substrates in terrestrial vertebrates

By

Crystal M. Reynaga

Doctor of Philosophy in Biological Sciences

University of California, Irvine, 2018

Associate Professor Emanuel Azizi, Chair

The evolution of novel locomotor modes has played a crucial role in the evolution of vertebrates. A shift in an organisms' primary mode of locomotion or changes in the mechanical properties of the external environment require adjustments to kinematic and motor patterns. These adaptations are often associated with distinct morphological changes. Such modifications are necessary for maintaining performance in response to variation in the external physical environment. This provides the foundation for the evolution of novel modes of locomotion. Understanding this adaptability, the mechanistic, and functional implications of novel gaits and the substrates that shape biological systems can provide further insights for design parameters in synthetic and engineered systems. My dissertation seeks to understand this adaptability and the functional implications of novel gaits and substrates that affect them. I examined how the evolution of novel locomotor modes shape variation in: (Chapter 1) limb morphology, (Chapter 2) motor control strategies, and (Chapter 3) muscle properties in frogs. I used morphological, biomechanical, and physiological approaches to understand modulation of organismal locomotor patterns and responses to varying external conditions.

First, we explore how quadrupedal walking gaits are achieved in four frog species that are ancestrally specialized for jumping. We examine how the prominence of this gait correlates with a shift in limb morphology and limb posture. We find frogs specialized for walking accommodate a quadrupedal gait with an increase in relative forelimb length compared to the average anuran body plan and maintain greater vertical retraction in the hindlimb compared to the forelimb during walking. Second, I investigate the effects of substrate compliance on limb kinematics and motor control patterns of jumping Cuban tree frogs. We found evidence Cuban tree frogs use a feedforward control program and compliance substrates potentially disrupt the inertial catch mechanism used to store elastic energy. Last, I explore the effects of substrate compliance on elastic energy storage at the muscle-tendon level. We develop a spring-loaded latch analogue model using an *in vitro* muscle preparation. We find slower rates of energy release, less optimal latches, allow for greater energy recovery from compliant substrates.

INTRODUCTION

The mechanical properties of the environment shape an organisms' locomotor mode. Adaptation to a new environment can bring various challenges, for example predator avoidance, navigating physical obstacles, and the unpredictable mechanical perturbations associated with various substrate interactions. As a result, organisms have evolved novel ways of movement to overcome such obstacles (Shubin et al. 2015; Reilly et al. 2006). Strategies range from active behavioral changes in gait (or movement) patterns (Lemelin et al. 2003; Reynaga et al. 2018), motor recruitment patterns, to physiological changes that take place over a longer evolutionary time scales (Taylor, 1978; Garland and Losos, 1994; Gomes et al. 2009). Uncovering the evolutionary, ecological, and physiological pressures or determinates that motivate these changes are critical in understanding organismal locomotor performance. Engineered systems often gain inspiration from the unique designs and adaptations of biological systems (e.g. Haldane et al. 2016). However, an optimal design for one environment may not be for another, inevitably there are design trade-offs (e.g. Blum et al. 2011).

The mechanism one organism uses to navigate a complex habitat may be achieved differently than another, nonetheless both organisms achieve the same outcome, moving from point A to point B. There are multiple ways to achieve these outcomes that can be achieved at different levels of organization, and each have their associated trade-offs. A prime example are frogs, a clade whose ancestral form of locomotion has been derived from jumping (Jenkins and Shubin 2004). Still known for their robust jump performance, some species have independently adapted unique forms of movement from walking and running to burrowing, hopping, gliding, swimming, and climbing (Reilly and Jorgensen 2011). These ways of movement have varying mechanics and ground reaction forces that variably affect metabolic demand (Heglund et al.

1982a, b; Anderson et al. 1991; Hoyt et al. 2006; Fedak et al. 1982), however the underlying anatomical structures are similar, even discrete changes in morphology can correlate to directional changes in movement (Emerson 1979; Hackert et al. 2006). Evolution has developed multiple strategies, however understanding whether these functional consequences are optimally tuned and what kind of trade-offs incur is an active and developing field motivated by these questions. We review and examine the mechanistic basis of these changes, to investigate the underlying mechanical principals potentially driving locomotor movement and subsequently organismal ecology and evolution.

I aim to investigate how the evolution of novel locomotor patterns and shifts in the environment drive variation in:

1. Novel gaits in independently derived specialized quadrupedal walking frogs.
2. Mechanical variation and control strategies in tree frogs on variable substrates.
3. Muscle function and energy efficiency in ballistic locomotor systems.

1. Locomotor Mode

The anuran body plan is defined by morphological features associated with saltatory locomotion, but these specializations may have functional consequences for other modes of locomotion (Shubin and Jenkins 1995; Jenkins and Shubin 1998). Several frog species use a quadrupedal walking gait as their primary mode of locomotion, characterized by limbs that move in diagonal pairs (Ahn, et al. 2004). In the first part of my dissertation, we examine how walking species may deviate from the ancestral body plan and how the kinematics of a quadrupedal gait are modified to accommodate the anuran body plan. We use a comparative analysis of limb

lengths to test the hypothesis that quadrupedal anurans shift away from the standard anuran condition defined by short fore-limbs and long hindlimbs. We also use three-dimensional high-speed videography in four anuran species (*Kassina senegalensis*, *Melanophryniscus stelzneri*, *Phrynomantis bifasciatus*, and *Phyllomedusa hypochondrialis*) to characterize footfall patterns and body posture during quadrupedal locomotion, measuring the angle and timing of joint excursions in the fore- and hindlimb during walking to compare kinematics between limbs of disparate lengths. Our results show frogs specialized for walking tend to have less disparity in the lengths of their fore- and hindlimbs compared with other anurans. We find quadrupedal walking species use a vertically retracted hindlimb posture to accommodate their relatively longer hindlimbs and minimize body pitch angle during a stride. Overall, this novel quadrupedal gait can be accommodated by changes in limb posture during loco-motion and changes in the relative limb lengths of walking specialists.

2. Control

Organisms control locomotor outcomes via feedforward motor control patterns and neural feedback of muscle activation (Dickinson et al. 2000). However, mechanical properties of the musculoskeletal system can also control whole-body and muscle kinetics beyond the limits of the nervous system (Dickinson et al. 2000; Roberts and Azizi, 2011). For instance, arboreal frogs navigate complex environments and can face various changes in mechanical properties of their physical environment. An optimal, well-coordinated jump allows for the recovery of elastic energy stored in a springy substrate to amplify mechanical power; effectively adding an in-series spring to the hindlimbs (Astley et al. 2015; Gilman and Irsckick 2012). The second part of my dissertation tests the hypothesis that effective use of springy substrates requires active changes in

muscle activation and changes to limb kinematics to effectively regain energy from a compliant substrate. We design an actuated force platform, modulated with a real-time feedback BeagleBone controller to vary the stiffness of the substrate. We quantified the kinetics and kinematics of Cuban tree frogs (*Osteopilus septentrionalis*) jumping-off platforms at four different stiffness conditions. Additionally, we used electromyography to examine the relationship between muscle activation patterns and substrate compliance during take-off in a knee extensor (*m. cruralis*) and an ankle extensor (*m. plantaris*). We find *O. septentrionalis* do not significantly modulate motor patterns in response to substrate compliance. However, changes in the rate of limb extension highlight a trade-off in power amplification, suggesting compliant substrates disrupt the inertial catch mechanism that allows the organism to store elastic energy in the tendon. This work serves to broaden our understanding of how the use of elastic energy storage may alter the responsiveness of an organism to react to perturbations.

3. Physiological Changes

From frogs to fleas, many biological systems utilize power amplifying mechanisms to achieve fast accelerations. Power amplification can have varied performance outputs using the same machinery or theoretical components (llton, et al. 2018). Finally, to better understand the mechanical properties of power amplification and the latching mechanism, we reduce the complexity to a lower level of organization where we can control the latch dynamics and properties by simply adjusting substrate mechanics. Here, we ask how latch quality and substrate stiffness affects elastic energy recovery from compliant substrates. We present a simple hypothetical model that explains key features of latch dynamics on compliant substrates. We test this model, which suggests less-rigid latches perform optimally on complaint substrates. We

develop a reduced in vitro muscle preparation to test the performance of the catch mechanism on compliant substrates. We use the plantaris muscle-tendon-unit of a bullfrog (*Lethobates catesbeianus*) as the actuator, motor, and spring in-series between two servomotors; one that simulates unlatching (rapid muscle shortening as a result of joint extension) and a second that simulates a reactive complaint substrate. We test elastic energy recovery during tendon recoil from various compliant substrates and latch velocities. We found slower latch velocities recover more energy from compliant substrates. Our results show a trade-off in power amplification with increased compliance relative to tendon stiffness, however latch dynamics only affect the amount of energy stored and not the efficiency of energy recovered. Our work decouples the latching mechanism to test key features of latch and spring dynamics on variable substrates. We suggest 'less-ideal' latches may be most optimal for efficient performance on variable substrates regardless of relative compliance.

REFERENCES

Anderson, B. D. Feder, M. E., and Full, R. J. (1991). Consequences of a gait change during locomotion in toads (*Bufo woodhousii fowleri*). *Journal of Experimental Biology* 158:133-148.

Ahn, A. N., Furrow, E., & Biewener, A. A. (2004). Walking and running in the red-legged running frog, *Kassina maculata*. *Journal of Experimental Biology*, 207, 399–410. https://doi.org/10.1242/jeb.00761

Astley, H. C., Haruta, A., and Roberts, T. J. (2015). Robust jumping performance and elastic energy recovery from compliant perches in tree frogs. *Journal of Experimental Biology* 218, 3360-3363.

Blum, Y., Birn-Jeffery, A., Daley, M. A., and Seyfarth, A. (2011). Does a crouched leg posture enhance running stability and robustness? *Journal of Theoretical Biology* 281:97-106.

Emerson, S. B. (1979). The ilio-sacral articulation in frogs: form and function. *Biological Journal of the Linean Society* 11:153-168.

Fedak, M. A., Heglund, N. C., and Taylor, C. R. (1982). Energetics and mechanics of terrestrial locomotion. II. Kinetic energy changes of the limbs and body as a function of speed and body size in birds and mammals. *Journal of Experimental Biology* 79:23-40.

Garland, T. and Losos, J. B. (2014). Ecological Morphology of Locomotor Performance in Squamate Reptiles. Pages 240-302 in P. C. Wainwright and S. M Reilly, eds. Ecological morphology: integrative organismal biology. University of Chicago Press, Chicago.

Gillman, C. A. and Irschick, D. J. (2012). Foils of flexion: the effects of perch compliance on lizard locomotion and perch choice in the wild. *Functional Ecology* 27: 374-381.

Gomes, F.R., Rezende, E.L., Grizante, M.B. and Navas, C.A. (2009). The evolution of jumping performance in anurans: morphological correlates and ecological implications. *Journal of Evolutionary Biology*, 22(5), 1088-1097. doi: 10.1111/j.1420-9101.2009.01718.x

Hackert, R., Schilling, N., and Fischer, M. S. (2006). Mechanical self-stabilization a working hypothesis for the study of the evolution of body proportions in terrestrial mammals? *Comptes Rendus Palevol* 5:541-549.

Haldane, D. W., Plecnik, M. M., Yim, J. K. and Fearing, R. S. (2016). Robotic vertical jumping agility via series-elastic power modulation. *Science Robotics* 1: eaag2048.

Hoyt, D. F., Wickler, S. J., Dutto, D. J., Catterfeld, G. E., and Johnsen, D. (2006). What are the relations between mechanics, gait parameters, and energetics in terrestrial locomotion? *Journal of Experimental Zoology* 305A:912-922.

Heglund, N. C., Cavagna, G. A., and Taylor, C. R. (1982a). Energetics and mechanics of terrestrial locomotion. III. Energy changes of the centre of mass as a function of speed and body size in birds and mammals. 79:41-56.

Heglund, N. C., Fedak, M. A., Taylor, C. R., and Cavagna, G. A. (1982b). Energetics and mechanics of terrestrial locomotion. IV. Total mechanical energy changes as a function of speed and body size in birds and mammals. *Journal of Experimental Biology* 97:57-66.

Ilton, M., Bhamla, M. S., Ma, X., Cox, S. M., Fitchett, L. L., Kim, Y., Koh, J., Krishnamurthy, D., Kuo, C., Temel, F. Z., Crosby, A. J., Parkash, M., Sutton, G. P., Wood, R. J., Azizi, E., Bergbreiter, S., and Patek, S.N. (2018). The principles of

cascading power limits in small, fast biological and engineering systems. *Science* 360, eaao1082.

Jenkins, F. A., & Shubin, N. H. (1998). *Prosalirus bitis* and the anuran caudopelvic mechanism. *Journal of Vertebrate Paleontology*, 18(3), 495–510. https://doi.org/10.1080/02724634.1998.10011077

Lemeline, P., Schmitt, D., and Cartmil, M. (2003). Footfall patterns and interlimb co-ordination in oppossums (Family Didelphidae): evidence for the evolution of diagonal-sequence walking gaits in primates. *The Zoological Society of London* 260:423-429.

Reilly, S.M. and Jorgensen, M.E. (2011). The evolution of jumping in frogs: Morphological evidence for the basal anuran locomotor condition and the radiation of locomotor systems in crown group anurans. Journal of Morphology, 272(2), 149-168. doi: 10.1002/jmor.10902

Reilly, S.M., McElroy, E.J., Odum, R.A., and Hornyak, V.A. (2006). Tuataras and salamanders show that walking and running mechanics are ancient features of tetrapod locomotion. *Proceedings of the Royal Society B: Biological Science*, 273(1593), 1563-1568. doi: 10.1098/rspb.2006.3489

Reynaga, C. M., Astley, H. C., and Azizi, E. (2018). Morphological and kinematic specializaitons of walking frogs. *Journal of Experimental Zoology A: Ecological and Integrative Physiology*. 329: 87-89.

Shubin, N. H., Daeschler, E. B., and Jenkins, F. A. (2014). Pelvic girdle and fin of *Tiktaalik roseae. PNAS*. 111(3): 893-898.

Taylor, R. C. (1978). Why change gaits? Recruitment of muscles and muscle fibers as a function of speed and gait. *American Zoologist* 18:153-161.

CHAPTER 1

Morphological and kinematic specializations of walking frogs

1.1 INTRODUCTION

The ancestral anuran body plan is thought to reflect specializations associated with jumping, with many morphological features retained in modern frogs (Emerson, 1988; Gans & Parsons, 1966; Jenkins & Shubin, 1998; Shubin & Jenkins, 1995). Anurans tend to have short and stout bodies with relatively short forelimbs and long powerful hindlimbs, which are used to perform work against the ground during the jump take-off phase (Emerson, 1988; Peplowski & Marsh, 1997; Zug, 1972). Previous work suggests these anatomical mechanisms contribute significantly to frog jump performance (Astley, 2016; Choi, Shim, & Ricklefs, 2003; Gomes, Rezende, Grizante, & Navas, 2009; Marsh, 1994; Zug, 1978).

Despite the conservation of the ancestral body plan, anuran species have evolved several locomotor modes, each associated with novel morphological features. For example, a group of specialized burrowers have evolved tough metatarsal tubercles (spades) that aid in excavating dry soil (Emerson, 1976), a feature that appears to date back to the Paleocene (Chen, Bever, Yi, & Norell, 2016). Moreover, two arboreal families have independently evolved the ability to glide from the canopy by increasing the surface area of hands and feet with increased webbing between digits (Emerson & Koehl, 1990). The pelvic girdle morphology is one feature that does vary substantially across anurans (Emerson, 1979; Jorgensen & Reilly, 2013; Reilly & Jorgensen, 2011). Emerson (1979) described three pelvic configurations that were proposed to correlate with locomotor mode, which shows a strong correlation between the sacral diapophyses width and an animal's locomotor specialization (Jorgenson and Reilly, 2013). The evolution of novel locomotor modes rarely eliminates jumping from an anuran's locomotor repertoire,

resulting in specific morphological modifications without large-scale changes in the general body plan (Emerson, 1988).

Several frog species have independently evolved walking as a primary mode of locomotion. This gait is characterized by limbs moving in alternating, diagonal pairs (Ahn, Furrow, & Biewener, 2004; Emerson, 1979). In one species, *Kassina maculata*, the kinetics and energy exchange of the quadrupedal gait resemble a walk at slow speeds and shift to a run-like gait at higher speeds (Ahn et al., 2004). Although the authors did not quantify joint level limb kinematics, they noted the limb posture appeared highly crouched across speeds (Ahn et al., 2004). A crouched limb posture is quite common in smaller quadrupedal mammals (Biewener, 1989a). In contrast, larger mammals with more extended limbs operate with higher effective muscle mechanical advantage, allowing them to support a larger body mass during locomotion (Biewener, 1989a).

Interestingly, a comparative analysis also suggests limb posture (effective mechanical advantage) does not differ between the mammalian fore- and hindlimbs (Biewener, 2005). This observation is not particularly surprising given the fore- and hindlimbs of many quadrupedal mammals are typically of similar length (Biewener, 1983). The symmetry in limb length does decrease in smaller mammals that tend to have slightly longer hindlimbs compared with their forelimbs (Biewener, 2005). This shift away from symmetric limb lengths is not restricted to smaller quadrupedal mammals but also extends to locomotor specializations such as bipedal running, hopping, vertical clinging and leaping. One such example is the *Galago senegalensis*, which is an arboreal primate with legs almost twice the length of its forelimbs (Preuschoft, Witte, & Fischer, 1995). The asymmetry in the limb lengths of the galago is associated with its ability to perform exceptionally powerful jumps (Aerts, 1998), but this species largely avoids the

use of a quadrupedal walking gait (Napier & Walker, 1967). It is therefore likely that high asymmetry in limb length fundamentally alters the limb posture, limb mechanical advantage, and body posture in species that utilize a quadrupedal gait.

The independent evolution of walking in many anuran lineages presents a unique opportunity to investigate how the ancestral body plan, associated with jumping, likely constrains limb and body postures during a quadrupedal gait. We combine a broad comparative morphological approach with detailed kinematics of four independently derived species of specialized anuran walkers to determine how the conflicts associated with an anuran body plan are accommodated by species that commonly use a quadrupedal gait (Figure 1.1). We propose three potential mechanisms that may be associated with quadrupedal walking. First, we predict species specialized for walking have more symmetric fore- and hindlimb lengths compared with other anuran species (Figure 1.2A). Second, we predict that if limb lengths remain asymmetric, frogs may adjust body posture by using a significant downward pitch during locomotion (Figure 1.2B). Finally, we predict the posture of longer hindlimbs will likely be significantly more crouched compared with the shorter forelimbs (Figure 1.2C). These predictions are not mutually exclusive and species may combine these strategies to circumvent the constraints of the anuran body plan. This work seeks to highlight morphological and kinematic strategies associated with the evolution of quadrupedal walking and reveal potential conflicts and trade-offs between disparate locomotor modes.

1.2 MATERIALS AND METHODS

We test our predictions on four independently derived lineages of specialized quadrupedal walking frogs to study variation in limb posture (Astley, 2016; Emerson, 1979;

Figure 1.1). We combine meta-analysis, direct limb measurements, and online database collections to examine evolutionary changes in limb length and use three-dimensional (3D) high-speed kinematic video analysis to characterize the specialized walking gait, including detailed analysis of limb and body postures.

1.2.1 Quadrupedal walking frogs

This study used four specialized walking frogs: the Senegal running frog, *Kassina senegalensis* (*n* = 5); the bumblebee toad, *Melanophrynis- cus stelzneri* (*n* = 2); the red-banded rubber frog, *Phrynomantis bifasciatus* (*n* = 3); and the tiger-legged monkey frog, *Phyllomedusa hypochondrialis* (*n* = 2). These species were chosen for their capability to perform diverse modes of locomotion (e.g., swimming, jumping); however, all four predominately utilize a quadrupedal walking gait for terrestrial, non-escape locomotion, as well as arboreal locomotion in the case of *Phy. hypochondrialis*. An extreme example is *Phr. bifasciatus*, which we rarely observed jump (personal observation). Although some other species of anurans will walk on rare occasions, this behavior is extremely infrequent and difficult to elicit consistently, particularly for repeated cycles; prior experiments by one author failed to produce walking behavior in numerous other species in the lab (Astley, 2016). Although the rarer three species had lower sample sizes, we filmed a number of trials per individual within a species to reduce intraspecific error via repeated-measures statistics (see Table 1.1).

Filming and animal husbandry for *K. senegalensis* were conducted at the University of California, Irvine (UCI) and approved by the UCI Institutional Animal Care and Use Committee (IACUC). Filming and animal husbandry for *M. stelzneri*, *Phr. bifasciatus*, and *Phy. hypochondrialis* were conducted at Brown University and approved by the Brown University

IACUC. Videos filmed at Brown University were originally used for previous study by Astley (2016). All species were wild-caught and purchased from commercial vendors.

1.2.2 Limb morphological measurements

We sampled a diverse array of anurans to assess whether species that specialize in quadrupedal walking have more symmetric fore- and hindlimb lengths compared with a range of other anuran species. Specimens came from the collections of Herpetology at the Natural History Museum of Los Angeles County (LACM), the online National Science Foundation Digital Library at the University of Texas at Austin (DigiMorph), and personal collections. We collected fore- and hindlimb measurements from 56 anuran species spread across 14 major families. For specimen information, see Appendix Table A.4. Whenever possible, we examined multiple individuals per species (n = 1–10) to characterize the range of limb dimensions. We examined either cleared and stained specimens, dry skeletal preparations, or 3D X-ray computed tomography (CT) scans.

We calculated limb lengths from the sum of the lengths of each individual limb element. All measurements were straight line measurements of the skeletal elements; the distance from the most proximal end to the most distal end. We measured three forelimb segments: the humerus, radio-ulna, and metacarpophalangeal segment; and in the hindlimb: the femur, tibiofibula, proximal tarsal, and metatarsophalangeal segment. We measured the most distal segment length as the linear distance from the proximal end of the metacarpus (or metatarsus) to the distal end of the longest phalanx. We measured all prepared specimens with digital calipers, and recorded to the nearest 0.01 mm. For measurements on 3D X-ray CT specimens, we used

Java slice applet viewer application, the UTCT inspeCTor (Digital Morphology, Austin, TX). We used X, Y, Z coordinates to calculate limb segment lengths.

Furthermore, we used meta-data from Mammalia to assess whether specialized walking anuran species have similar limb length symmetry to mammalian quadrupeds. Data came from a previously published study by Biewener (1983). These data from 33 mammalian quadrupedal locomotors approximate mammalian limb lengths from measurements of the radius, humerus, tibia, and femur lengths. For mammals, the bones contained in the terminal end of the fore- and hindlimb, such as tarsals, metatarsals, and phalanges, were not included in total limb length calculations. However, the bony elements that make up the associated metatarsal joint below the foot or ankle contribute negligibly to the total limb length or center of mass in mammals (Steudel & Beattie, 1993).

1.2.3 Walking kinematics and analysis

We collected all 3D video kinematic data under standardized conditions at approximately 23 ± 2◦C at UCI and 28 ± 2◦C at Brown University. In spite of temperature differences, there was some overlap in walking speed between the *K. senegalensis* trials in this study and those in Astley, 2016. We recorded the 3D kinematics of quadrupedal walking events for each species with two high-speed video cameras. We filmed events at UCI with Phantom M120 Cameras (Vision Research Inc., Wayne, NJ), whereas events filmed at Brown University used Photron 1024 PCI Cameras (Photon Inc., Tokyo, Japan). The cameras, positioned laterally and dorsally to the individual, recorded at 500 frames s^{-1} at UCI and 125 frames s^{-1} at Brown University, and were calibrated with a custom calibration cube (32 non-planar points) with direct-linear transformation software (Hedrick, 2008) in MATLAB (The MathWorks, Natick, MA).

We recorded walking events as the animal moved freely throughout the arena (30 × 15 cm^2). For each frog, two-dimensional (2D) data were collected from both cameras to characterize body and limb postures within a stride. To do this, we manually tracked the following joint center landmarks along one side of the body, in each frame for both recordings: the wrist, elbow, and shoulder joints in the forelimb; the ankle, knee, and hip joints in the hindlimb; the distal end of the longest phalange for each limb; the sacroiliac joint; and the centers of both eyes. 2D camera data were reconstructed to 3D with MATLAB digitizing scripts (Hedrick, 2008). We defined the arena surface as the *x*–*y* plane, with the *z*-axis perpendicular to the plane. We performed further kinematic analysis of the 3D coordinates from these anatomical landmarks using MATLAB, IGOR Pro (Wavemetrics, Inc., Beaverton, OR) and Excel (Microsoft Corp., Renton, WA). We quantitatively analyzed multiple walking stride trials per individual for each species (Table 1.1). Analyzed trials were carefully selected to ensure all anatomical landmarks were visible to both cameras and frogs completed at least one stride cycle without any impediments. However, frogs rarely walked exactly parallel to the x-axis of the arena, often times walking at a slight diagonal to the axis. Although no drastic turning events were analyzed, slight diagonal walking events introduced a small change of heading within a stride.

We used average footfall patterns within a single stride to ensure similar gait ranges were examined. We defined a single stride cycle as the video frame when the forelimb facing the laterally positioned camera touched-down, lead forelimb (LFL), to the frame just before the same LFL touched down again to begin a new stride. To characterize footfall patterns, we quantified the number of frames where touch-down and lift-off occurred for each foot, and normalized to the total frames within a stride. We used Hildebrand (1985) terminology to characterize gaits. We calculated duty factor as the average percent of a stride a single foot contacted the ground.

We characterized same-side limb phase as the average percent of a stride when the hindfoot contacted the ground until the same-side forelimb contacted the ground.

We used absolute pitch and yaw angles to characterize body posture, with respect to the horizontal ground as a fixed plane of reference. First, we performed global to local coordinate system transformations with a custom-designed script in MATLAB. To define the 3D position of landmarks in the global reference frame, we used coordinates based on the mean position of where three phalanges encountered the platform within the filming arena. We used these landmarks to find the frog position relative to the arena platform, which were fixed with respect to the moving frog body. Second, we defined the body axis as a parasagittal line connecting the eye and the dorsal lateral projection of the sacrum, both located on the same lateral side of the body axis closest to the laterally positioned camera. Third, *Y* coordinates of the sacroiliac joint were subtracted from each eye center coordinate, so the sacroiliac joint acted as the origin of the horizontal plane. As a point of comparison with empirical data, we predicted body pitch angle based on fully extended limbs. For pitch angles, positive values indicated a body posture where the rostrum is elevated relative to the sacrum, whereas negative values indicated the sacrum is elevated relative to the rostrum. Pitch angles of zero indicated a perfectly level body posture relative to the horizontal axis. Lastly, we defined yaw angle as the angle of rotation of the body axis around the horizontal x-axis. For example, if a frog walked in a straight-line trajectory along the positive *x*-axis direction, a yaw angle of zero assumes the body axis is perfectly aligned with the *x*-axis. However, positive changes in yaw indicated the rostrum was angled toward the left side of the sacroiliac joint, whereas negative values indicated the rostrum was directed toward the right side of the sacroiliac joint. Additionally, we accounted for slight changes in heading

within a stride by characterizing the net change in frog head orientation at the start and end of a stride.

We calculated relative 3D joint angles between segments listed below, which were not separated into flexion/extension and adduction/abduction components nor referenced to body position. We measured wrist angle as the angle between the metacarpals and radio-ulna; elbow angle, the angle between the radio-ulna and humerus; shoulder angle, the angle between the humerus and the ipsilateral eye; ankle angle, the angle between the tarsus and tibiofibula; knee angle, the angle between the tibiofibula and femur; and the hip angle, the angle between the femur and the ipsilateral sacroiliac joint. For joint angles, values closer to 0° indicated greater joint flexion and values closer to 180° indicated greater extension.

We also characterized 3D limb postures within the local reference frame of the fore- and hindlimb (Figure 1.3). First, coordinates of the distal phalange were subtracted from either the shoulder or hip joints respectively to make the joints the origins of the coordinate axes for each limb. Then, 3D Cartesian coordinates of the digitized body landmarks were transformed to spherical coordinates. Angular changes in this coordinate system were defined as the radial magnitude (r), elevation, and azimuth. We calculated the aforementioned fore- and hindlimb polar angles from a 3D vector directed from the shoulder or hip to the tip of the longest phalanx. The azimuth angle characterized the lateral abduction or adduction of the limbs where larger angle indicated laterally abducted limb posture. The elevation angle characterized the vertical protraction or retraction of the limb, where a larger angle corresponded with a vertically protracted limb posture. The variable r was defined as the instantaneous distance from the most proximal joint to the most distal digit tip. Elevation, azimuth, and r were calculated for all frames for both fore- and hindlimb. Lastly, we normalized r by dividing the total limb length (r: total

limb length). By normalizing *r*, this measured how flexed or extended the limb was on a scale from 0 to 1, respectively. We evaluated these variables at mid-stance and at maximum *r*, during the period of ground contact for each limb. The timing of maximum *r* within a stride for the forelimb coincided with touch down, whereas for the hindlimb maximum *r* occurred during the take-off phase of the hindlimb within a stride, and thus do not occur at the same instant in time. Relative 3D joint angle measurements were also taken at midstance and maximum *r* relative to each limb. Ranges between midstance and maximum *r* and means during stance phase were also calculated for relative 3D joint angles.

1.2.4 Statistical analysis

We analyzed all data with RStudio (v. 1.0.136, Boston, MA) and IGOR Pro. We calculated all species means and standard errors from individual means. For the comparative analysis, we grouped species into locomotor type: quadrupedal walking anurans, other anuran locomotors, and quadrupedal mammals. Fore- and hindlimb lengths were $\log_{10}$ transformed prior to analysis. We calculated least-squares regressions to determine the relationship between mammalian quadruped fore- and hindlimb lengths. We used phylogenetic generalized least squares (PGLS) to control for similar traits and shared evolutionary history across anuran locomotor groups (Garland & Ives, 2000; Grafen, 1989; Martins & Hansen, 1997). We used packages CAPER, APE, and NLME in R for PGLS and to assess phylogenetic contribution (Orme et al., 2013; Paradis, Claude & Strimmer, 2004; Pinheiro, Bates, DebRoy, & Sarkar, 2017). PGLS used a pruned phylogeny (modified in R) from published phylogenetic analyses (Frost et al., 2006; Isaac, Redding, Meredith, & Safi, 2012). Traits were assumed to evolve by "Brownian motion" evolution (Rohlf, 2001). Furthermore, we used analysis of covariance

(ANCOVA) to test for differences between anuran locomotor groups, with forelimb length as the covariate and locomotor type (walker versus other specialized anuran locomotor) as the fixed factor. ANCOVA was performed on log transformed data not corrected for phylogeny to determine what model best fit the data to test our hypothesis. Fit of PGLS and ANCOVA models were compared with Aikake information criterion (AIC).

For the kinematic data set, we calculated averages and 95% confidence intervals for pitch, yaw, relative joint angles, limb extension magnitude (*r*), and polar limb angles from individual means. We used one-way analysis of variance (ANOVA) to compare pitch and joint angles across species, accounting for variance across individuals. To test for differences in 3D limb postures, *r*, azimuth, and elevation angles, we used repeated measures ANOVA, accounting for variance within individuals, with a false discovery rate post hoc test.

1.3 RESULTS

1.3.1 Limb morphology

We sampled a diverse array of anuran species to characterize the relationship between fore- and hindlimb lengths of four specialized walking anuran species and 55 other anurans (Figure 1.4). For comparison, we included data from 33 mammalian quadruped species (Biewener, 1983). Least-squares regression indicated mammalian quadrupeds exhibit nearly equal fore- and hindlimb lengths with a slope closest to one (slope ± SEM = 0.926 ± 0.0117). We found a strong correlation between the mammalian fore- and hindlimb lengths (R^2 = 0.995; P < 0.0001). In multivariate analyses, anuran hindlimb length scaled nearly isometrically with forelimb length (slope ± SEM = 0.941 ± 0.047; see Appendix Table A.5). The regression lines

show a significant effect of forelimb length and locomotor type, but no significant interaction. These results suggest that the slope between fore- and hindlimb length is similar for all anurans regardless of locomotor type (see Appendix Table A.5; ANCOVA: $P = 0.738$; PGLS: $P = 0.846$). However, locomotor type has a significant effect on hindlimb length, with a significant difference in the regression line intercepts (see Table A.5; ANCOVA: $P = 0.0003$; PGLS: $P = 0.005$). PGLS was the best-fitting regression model based on the smallest AIC value (see Appendix Table A.5). For Anura, Pagel's lambda indicated limb proportions were correlated with phylogeny (see Appendix Table A.5). This confirmed anuran quadrupedal walkers have more equal limb lengths compared with other anurans.

1.3.2 Footfall patterns

We examined footfall patterns to verify whether each species (*K. senegalensis*, *M. stelzneri*, *Phy. hypochondrialis*, and *Phr. bifasciatus*) used a similar walking or running gait (Figure 1.5). All four quadrupedal walking species used a diagonal footfall sequence, where the movement for a given forelimb was followed by the contralateral hindlimb. The gait cycles analyzed between forelimb and contralateral hindlimb pairs alternated in sequence. At any given time within a stride, the frogs had two limbs or more in contact with the ground. According to footfall sequence, duty factor varied across species with the fastest duty factor by *M. stelzneri* and *K. senegalensis*, which overlapped in their range, whereas *Phr. bifasciatus* had the lowest duty factor (Figure 1.6). Although Ahn et al., 2004 observed grounded running in *K. maculata* at duty factors above 50%, we refer to these sequences as “walking” for consistency, based on our measured duty factor. *Phr. bifasciatus* predominately used a single foot sequence walk, whereas

K. senegalensis, *M. stelzneri*, and *Phy. hypochondrialis* mainly used a diagonal couplet footfall sequence.

3.3 Body posture

We measured body pitch across quadrupedal walking species to determine whether these frogs modulate pitch angle to accommodate for the difference between the fore- and hindlimb lengths. Comparisons were made relative to predicted body pitch angles for each species. Predicted body pitch angles were calculated from total anatomical fore- and hindlimb lengths (assuming full limb extension) and illustrated as a point of comparison with the observed body pitch across a stride (Figure 1.7). All quadrupedal walkers showed little variation in pitch. Pitch angles did not deviate from zero enough to reach predicted negative pitch values. Despite limb asymmetry, the boxes combined with whiskers indicated nonsignificant difference in body pitch across species (one-way ANOVA; $P = 0.995$). Although pitch angles did not deviate significantly from a horizontal orientation, we did detect consistent yaw (average range: *K. senegalensis* −15.0 ± 2.5° to 7.4 ± 0.8°; *M. stelzneri* −11.0 ± 3.5° to 4.0 ± 0.2°; *Phr. bifasciatus* −5.7 ± 1.1◦ to 7.1 ± 2.6◦; *Phy. hypochondrialis* −5.4 ± 9.8◦ to 14.5 ± 4.8◦) throughout the stride cycle (Appendix Figure A.1.A–D). Yaw angles frequently returned to a value of zero at the beginning of a new stride. However, when frogs were not walking in a perfectly straight line, yaw angles did not return to zero at the stride transition (Appendix Figure A.1.E–H).

1.3.4 Limb posture

We measured joint kinematics to examine how forelimb extension or hindlimb flexion may compensate for unequal fore- and hindlimb lengths (Figure 8; Appendix Figure A.2 and

Appendix Table S3). From joint coordinates across each limb, we measured relative joint angle extension and flexion across a stride. All frogs used similar fore- and hindlimb joint angle patterns (see Supp. Table A.6). Specifically, forelimb joint angle changes followed a similar pattern in the proximo-distal direction with average joint angles only varying across species at the wrist ($P = 0.0103$). At mid-stance, elbow angle across species significantly differed ($P = 0.0492$), largely driven by greater elbow joint extension in *M. stelzneri* (Appendix Table A.6). Likewise, hindlimb joint angles follow similar magnitudes. However, *Phr. bifasciatus* and *Phy. hypochondrialis* deviate in the timing of hindlimb joint excursion. This shift in hindlimb timing is also reflected their footfall patterns illustrated in Figure 1.5. Average ankle angle significantly differed across species ($P = 0.0024$), largely due to a reduced joint angle in *Phy. hypochondrialis* (Appendix Table A.6). A difference in hip joint range across species resulted from a smaller relative hip joint angle range in *Phr. bifasciatus* (Appendix Table A.6).

We also examined the fore- and hindlimb postures by characterizing the magnitude of limb extension, lateral abduction, and vertical retraction, using spherical coordinates and reducing the limb to a 3D vector characterized by the magnitude of the vector (r), the elevation angle, and the azimuth angle across a stride (Figure 1.3 and Appendix Figure A.3). We measured these variables at mid-stance and at maximum limb extension (Figure 1.9). The ratio of the vector magnitude to the total limb length (r:TL) was used to estimate the amount of limb flexion. At mid-stance, elevation angle across all species were greater in the forelimb relative to the hindlimb (Figure 1.9A; $F = 292.67$, $P < 0.0001$). Post-hoc tests showed differences across species were largely driven by variation in hindlimb retraction (Appendix Table A.7). Moreover, a significant interaction between species and limb suggested the elevation angle difference between the fore- and hindlimbs were different across species ($F = 32.28$, $P = 0.0014$). Between

species azimuth angle in the fore- and hindlimb at mid-stance were different (Figure 1.9B; F = 11.96, P = 0.0124). Consequently, post hoc tests revealed that differences across species were largely driven by greater lateral forelimb abduction in *K. senegalensis* (Appendix Table A.7, P = 0.002). Lastly, *r*:TL differed between species (Figure 1.9C; F = 11.18, P = 0.014), however there was no difference between relative extension of fore- and hindlimbs within species. A significant interaction suggested that the relative extension of the fore- and hindlimb for each species were different (F = 9.369, P = 0.020), likely attributed to the slight variation in forelimb flexion and hindlimb extension in *M. stelzneri* and *Phr. bifasciatus* (Appendix Table A.7).

At maximum limb *r*, elevation angle of the fore- and hindlimb differed between species (Figure 1.9D; F = 6.124, P = 0.045), and within species (F = 60.46, P = 0.0006). There was a significant interaction between species and limb (F = 33.70, P = 0.0013). This result was largely driven by a significant decrease in forelimb elevation angle relative to the hindlimb in *Phr. bifasciatus* (P = 0.005) and *Phy. hypochondrialis* (P = 0.028) whereas, in *K. senegalensis* and *M. stelzneri,* both the fore- and hindlimbs achieved similar elevation angles. Though there was no difference between species in azimuth angle, within species fore- and hindlimb azimuth angles differed (Figure 1.9E; F = 12.82, P = 0.016). There is a significant interaction of species and limb, suggesting this difference between fore- and hindlimb azimuth angle are different across species. At maximum extension, fore- and hindlimb abduction were similar for *K. senegalensis*, whereas fore- and hindlimb azimuth angles began to further differentiate in *M. stelzneri* (P = 0.0006), *Phr. bifasciatus* (P = 0.0009), and *Phy. hypochondrialis* (P = 0.0024). At maximum *r*, *r*:TL, effective use of limbs differed between species (Figure 1.9F; F = 9.738, P = 0.0189), with a significant difference in effective use of fore- and hindlimbs (F = 16.93, P = 0.009). The interaction of species and limb suggests species are changing fore- to hindlimb flexion and

extension relative to one another in different ways at maximum extension ($F = 26.91$, $P = 0.002$), however each species effectively uses the entire length of the fore- and hindlimb similarly.

1.4 DISCUSSION

Our results support the hypothesis that quadrupedal walking frogs have more equal fore- and hindlimb lengths compared with other anurans (Figure 1.4). It is clear that phylogeny and locomotor type are critical predictors of hindlimb lengths in anurans. PGLS regression provides a better fit of the data compared with a standard ANCOVA, and indicate frogs specialized in quadrupedal walking have significantly reduced asymmetry in fore- and hindlimb lengths compared with other anurans (Appendix Table A.5). This pattern is consistent with findings that suggest walking species tend to have shorter hindlimbs relative to snout vent length (Astley, 2016). Our analysis indicates fore- to hindlimb length ratios in our walking frogs are similar to those measured in small cursorial mammals (Figure 1.4; Biewener, 1983). Despite a shift toward symmetric limb dimensions, walkers still retain significantly longer hindlimbs compared with forelimbs. In fact, on several occasions we observed a complete walking stride impeded in *K. senegalensis* when the hindlimb actually stepped on the ipsilateral forelimb, thereby delaying the start of the next stance phase cycle (personal observation). These stride impediments were only observed in *K. senegalensis*. It is likely such interference between the fore- and hindlimbs would be more prevalent without the observed deviation from the ancestral body plan in walking species.

The footfall patterns of all four species can be characterized as a walking gait with alternating limb movements (Figure 1.5). Per Hildebrand's (1985) terminology these species range variably in footfall sequence within a stride (Figure 1.6). This is consistent with the red-

legged running frog (*K. maculata*) and tiger salamander (*Ambystoma tigrinum*), which have similar kinematics to *M. stelzneri* and *K. senegalensis* (Ahn et al., 2004; Reilly, McElroy, Odum, & Hornyak, 2006). This footfall pattern is similar to patterns typically seen in short-legged mammals, which use a single-foot or diagonal-couplet gaits (Hildebrand, 1968). However, Ahn et al., 2004 showed that duty factor and footfall patterns can be inconsistent with energy exchange patterns associated with walking and running, making it somewhat difficult to formally characterize quadrupedal frog gaits. Additionally, our kinematic results indicated that footfall patterns alone do not reflect some of the nuanced features of the gait, limb and body postures arising from the significant fore–hind asymmetry in limb lengths.

We hypothesized to accommodate longer hindlimbs walking frogs may locomote with significantly more crouched hindlimbs than fore- limbs. We find little support for this hypothesis using only observed relative joint angle kinematic comparisons in the fore- and hindlimbs (Figure 1.8 and Appendix Table A.6). However, assessing relative joint angles to characterize limb posture is not entirely appropriate for anurans that use substantial motion along other planes. There are multiple ways to achieve a "crouched" posture by using a combination of flexion, lateral abduction, or vertical retraction in a limb. We examined changes in 3D limb posture to further address our third hypothesis. We found at mid-stance the forelimb was more vertically protracted than the hindlimb (Figure 1.9A), with no clear difference in relative lateral abduction or adduction between the fore- and hindlimb (Figure 1.9B). Across the walking frog species, the effective use of the entire limb was similar in the fore- and hindlimb within a stride (Figure 1.9C and F). Walking frogs utilize the entire length of each limb to a similar degree. However, with slight fore–hind asymmetry in limb lengths these quadrupedal walkers seem to

accommodate this length disparity in the forelimb with greater protraction in the forelimb as shown during mid-stance.

Across a stride cycle these walking frogs seem to adjust the protraction and retraction of the forelimb relative to a constantly retracted hindlimb from mid-stance to maximum extension (Figure 1.9A and D). This is clearly demonstrated with little changes to elevation angle in the hindlimb at mid-stance and maximum *r*, whereas the forelimb elevation almost doubles from maximum *r* to mid-stance. Similar to larger mammals these walking anurans seem to exhibit more upright forelimb postures (Fischer, 2002; Jenkins, 1971). Adjusting for an upright forelimb posture in walking anurans likely minimizes pitch perturbations, lowers joint moments, moderates vertical forces, increases mechanical advantage, and reduces muscular loads in the forelimb (Biewener, 1983, 1989b).

We find little support that walking frog species adjust lateral abduction in the hindlimb relative to the forelimb as a mechanism to accommodate longer hindlimbs. There is little variation in azimuth angle between fore- and hindlimbs at mid-stance, however at maximum *r* the differential in azimuth angle between the fore- and hindlimb grows significant (Figure 1.9B and E). Quadrupedal walking frogs still utilize a sprawling gait, however may maintain a more abducted posture in the hindlimb throughout a stride in concert with a more vertically protracted forelimb, which in part allows them to accommodate for limb length asymmetries. The hindlimb vertical retraction, adjustments in forelimb protraction, and overall sprawled postures allow walking anurans to locomote with minimal pitch adjustments. Additionally, the lateral forces produced by limbs during a sprawled gait have been shown to increase stability in the horizontal plane (Kubow & Full, 1999; Schmitt & Holmes, 2000) and reduce pitching and rolling moments about the center of mass (Chen, Peattie, Autumn, & Full, 2006). Variation in limb postures may

also have some important consequences for the joint moments and muscle forces required during locomotion. These changes in limb postures in the sagittal plane for walking anurans likely alter the limb effective mechanical advantage, with disproportionately retracted and flexed limbs increasing the forces and moments required to support bodyweight during locomotion (Biewener, 1989b). Similarly, a sprawled posture may reduce effective mechanical advantage and require high muscle forces. In running geckos, the abducted limb posture results in ground reaction force vectors that are oriented above the knee and elbow, and well above the hip and shoulder, thereby resulting in higher joint moments (Chen et al., 2006). Future studies focused on the effective mechanical advantage of sprawled gaits will likely elucidate the functional trade-offs associated with this common limb posture.

We initially hypothesized asymmetry in the fore- and hindlimb lengths may result in a constant downward pitch during walking. Our results do not support this hypothesis as the body pitch did not vary significantly from a horizontal orientation (Figure 1.7). However, we did observe somewhat substantial changes in yaw angle over a single stride (Appendix Figure A.1). This observation is somewhat surprising given the short inflexible trunk of anurans. Significant changes in yaw angle are commonly observed in short limbed tetrapods with elongate bodies, where axial bending is thought to increase stride length (Ashley-Ross, 1994; Chen et al., 2006; Farley & Ko, 1997; Hildebrand, 1980). In contrast, the yaw observed in walking frogs is not likely to increase stride length significantly as it does not arise from axial bending but rather the lateral displacement of the body in response to forces generated by the hindlimbs. Since the hindlimbs are laterally displaced during walking they likely generate a relatively large mediolateral reaction force that shifts the trunk position from side to side during subsequent strides. This pattern is most notable in *Phy. hypochondrialis* where the lateral forces generated

by the hindlimb shift the body over the contralateral forelimb during the period when the diagonal pair is in contact with the substrate. Although it is unclear whether the lateral displacement of the body affects stride length, it may minimize physical interference between ipsilateral limbs by tucking the forelimbs under the body and out of the way of the hindlimb.

Our results suggest specialized walkers deviate from the extreme asymmetry in fore- and hindlimb lengths common to most anurans (Figure 1.4; Astley, 2016). Despite this deviation, walking species still have relatively long hindlimbs and retain the ability to jump. Though performance may be somewhat compromised, changes to limb asymmetry may not directly impact jump performance but predominately affect quadrupedal walking ability. For example, we have observed *K. senegalensis*, *M. stelzneri*, and *Phy. hypochondrialis* not limited to walking locomotion but also run, swim, and jump (personal observation). As seen in another specialized anuran walker, *K. maculata* maintains average jumping capabilities in comparison with other anurans (Porro, Collings, Eberhard, Chadwick, & Richards, 2017). In contrast, Astley (2016) found walkers tend to have inferior jump performance and shorter hindlimb lengths relative to body length. Since asymmetry in limb length appears to be maintained to preserve jumping performance as a predator avoidance strategy, then quadrupedal walkers need to make kinematic adjustments to accommodate their body plan. We show that one strategy used by four walking species is to reduce the vertical protraction of their relatively long hindlimbs and locomote with a highly-protracted forelimb posture similar to cursorial mammals (Schmidt, 2005).

Specialized walkers show modifications to limb length and kinematics on local and evolutionary timescales. Although a sprawled posture has benefits, it also creates larger bending loads and subsequently alters mechanical advantage and ground reaction forces. This shift of specialized characteristics for jumping to walking in anurans provides another example of the

difficulties in “re-evolving quadrupedal walking.” In a similar case, vampire bats specialized for flight, have independently evolved a bounding gait (Riskin & Hermanson, 2005). Bats have highly elongated forelimbs, a mechanical adaptation for flight, but no more elongated than brachiating or knuckle-walking primates (Swartz, 1997; Swartz & Middleton, 2007). Such limb asymmetries may have implications for a quadrupeds’ choice in gait and limb posture. These transitions between locomotor modes and limb adaptations offers insight into the timescale of modifications across tetrapod gaits and the associated trade-offs. Our study offers a basis for understanding the conflicts across diverse locomotor modes, and how novel gaits shape limb morphology, kinematics, and motor control strategies.

Table 1.1 Average walking anuran performance values (*mean* ± *s.e.m*).

Species	Individual	Trials	SNVL (mm)	Mass (g)	L_{stride} (cm)	V_{stride} (cm/s)
K. senegalensis	1	5	28.02	1.64	4.42 ± 0.28	21.29 ± 1.95
	2	5	35.41	2.34	3.85 ± 0.26	12.20 ± 2.05
	3	5	29.69	1.87	4.11 ± 0.20	20.66 ± 1.83
	4	5	33.32	2.38	4.32 ± 0.57	19.14 ± 3.34
	5	5	30.94	1.53	3.74 ± 0.38	14.43 ± 2.71
M. stelzneri	1	2	29.47	1.58	2.95 ± 0.22	16.84 ± 1.90
	2	4	22.00	0.82	3.00 ± 0.33	15.65 ± 1.23
Phr. bifasciatus	1	5	41.15	4.17	4.34 ± 0.51	15.65 ± 1.23
	2	5	39.37	3.92	5.13 ± 0.16	23.65 ± 3.58
	3	5	41.99	4.78	3.15 ± 0.13	5.13 ± 0.27
Phy. hypochondrialis	1	5	37.25	2.28	5.43 ± 0.42	11.68 ± 1.50
	2	5	34.25	1.99	4.69 ± 0.13	16.18 ± 2.77

SNVL, snout-vent length; L_{stride}, stride length; V_{stride}, stride velocity. See Supplementary Material Table S1 for average limb length details.

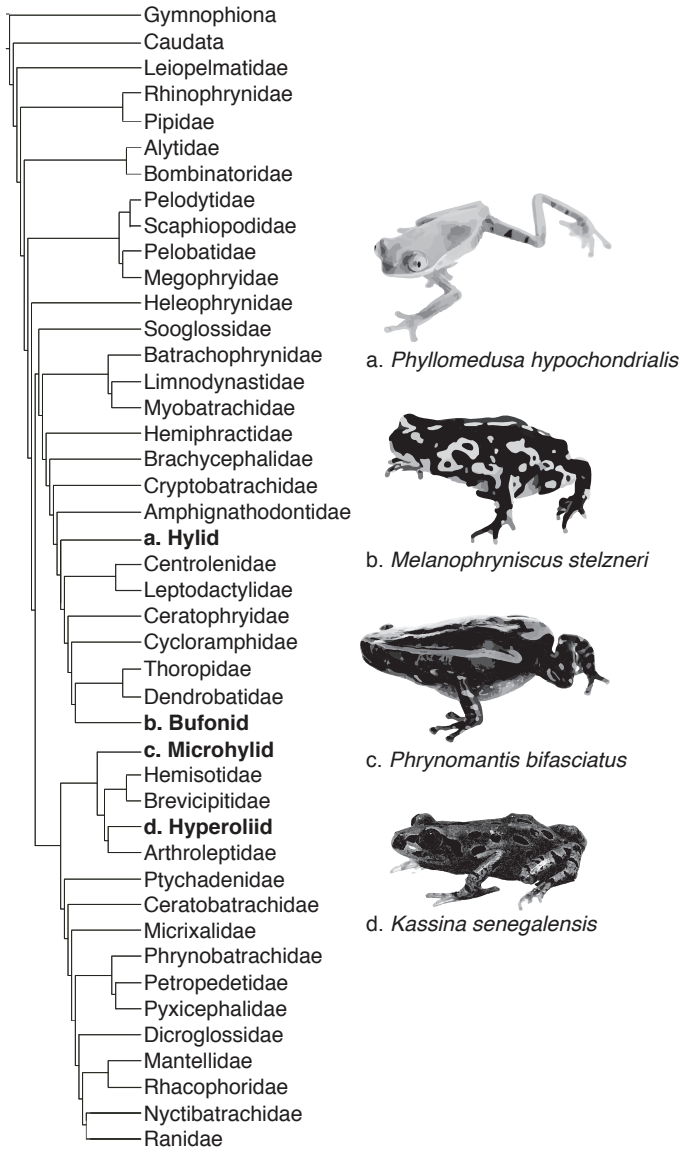

Figure 1.1. Anuran phylogenetic relationships based on Frost et al. (2006) and Isaac et al. (2012). Families of study species are in bold script. Bolded families indicate where quadrupedal walking has evolved. However, not all species within those families are specialized walkers; many still retain the ancestral jumping specialization. Lowercase letters correspond to pictured study species from independently derived lineages: (a) tiger-legged monkey frog (*Phyllomedusa hypochondrialis*), (b) bumblebee toad (*Melanophryniscus stelzneri*), (c) red-banded rubber frog (*Phrynomantis bifasciatus*), and (d) Senegal running frog (*Kassina senegalensis*).

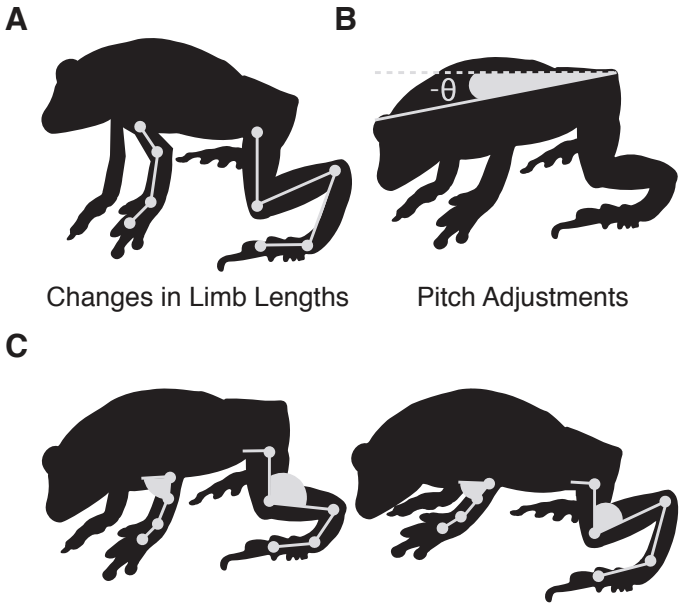

Figure 1.2. Schematic of three hypothetical solutions to how quadrupedal walking frogs circumvent the constraints of an anuran body plan specialized for jumping. The associated changes to achieve a quadrupedal gait can be morphologic or kinematic: (A) One way to achieve this is through more symmetric limb dimensions. Otherwise, if limb dimensions remain asymmetric frogs may adjust (B) with a downward body pitch to accommodate for a longer hindlimb. Alternatively, (C) adjust limb posture; where forelimbs assume a more flexed or extended limb posture than the hindlimbs.

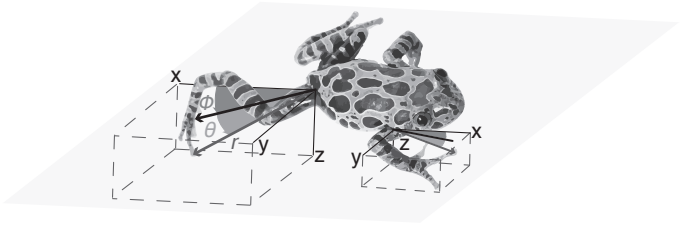

Figure 1.3. Schematic diagram of the coordinate system used to characterize 3D limb posture. Polar coordinates were used to characterize the radial distance (*r*, blue vector), the magnitude of limb extension from the shoulder and hip. Then, the vertical protraction of the limb was characterized by the elevation angle (*q*, yellow angle). Lastly, the lateral abduction of the limb was characterized by the azimuth angle (*f*, green angle).

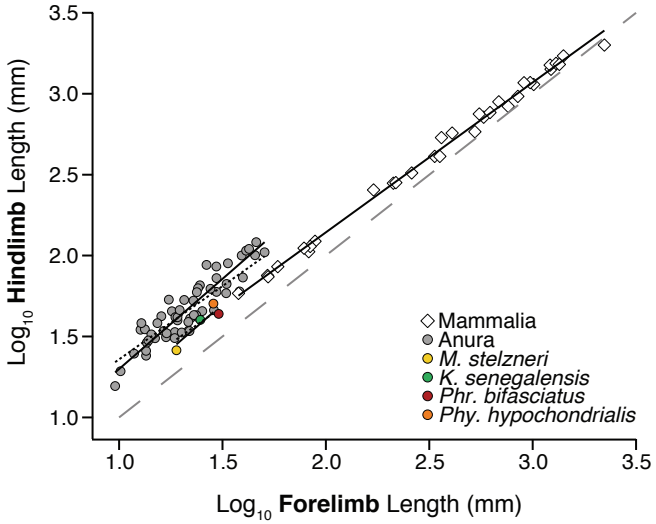

Figure 1.4. The relationship between fore- and hindlimb length of quadrupedal walking frogs (*N*=4), relative to other specialized anuran locomotors (*N*=56) and mammalian quadrupeds (*N*=33). Each symbol represents a different species. See Appendix A.5 for details on plotted anuran species. The gray dashed line is the line of isometry, with a slope of one, it indicates equal lengths between fore- and hindlimb. Approximate limb lengths (radius, humerus, tibia, and femur) of Mammalia are displayed for reference, obtained from Biewener (1983). We calculated solid regression lines from raw data points shown, whereas dotted regression lines are based on PGLS. Results from PGLS between quadrupedal anurans and other non-walking specialized anuran locomotors demonstrate quadrupedal walking anurans appear to have more equal fore- and hindlimb lengths. PGLS statistics are given in Appendix A.5.

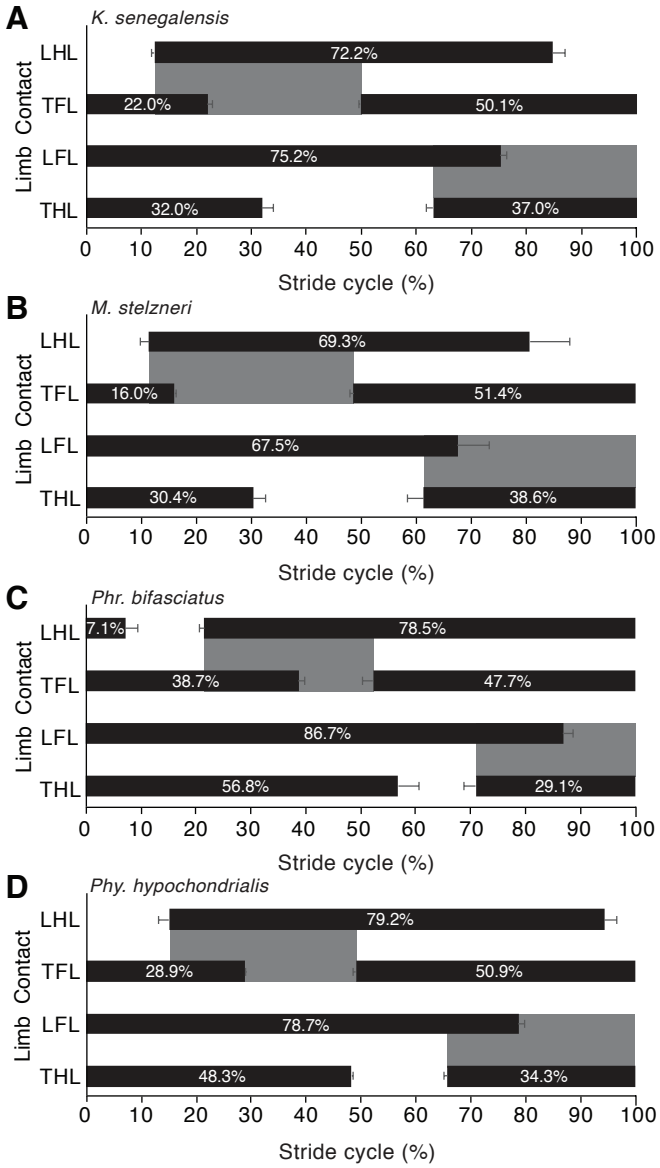

Figure 1.5. Average footfall patterns over a single stride (mean±s.e.m.). Mean and standard error calculated from video frames normalized to stride duration. (A) *Kassina senegalensis* (*n*=5), (B) *Melanophryniscus stelzneri* (*n*=2), (C) *Phrynomantis bifasciatus* (*n*=3), and (D) *Phyllomedusa hypochondrialis* (*n*=2). Stride cycle was defined from the first point of contact from the leading forelimb (LFL), to just before the same LFL touched back down for a new stride. The footfall order is the LFL, leading hindlimb (LHL), trailing forelimb (TFL), and trailing hindlimb (THL). Dashed lines indicate same-side limb phase used to characterize locomotor gait in Fig. 1.6. The footfall patterns show these walking frog species use similar alternating limb movements.

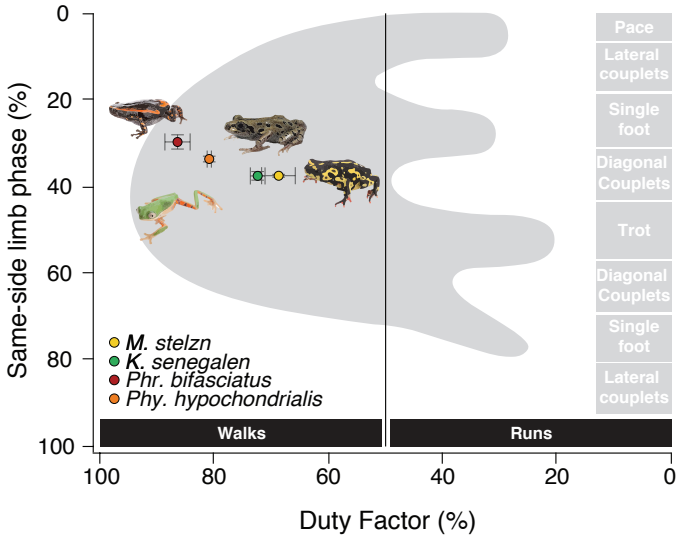

Figure 1.6. Average walking gaits of four quadrupedal walking frog species (mean±s.e.m.): *Kassina senegalensis* (green; *n*=5), *Melanophryniscus stelzneri* (yellow; *n*=2), *Phrynomantis bifasciatus* (maroon; *n*=3), and *Phyllomedusa hypochondrialis* (orange; *n*=2). Footfall patterns were solely used to characterize walking patterns. All species used a walking gait with either single foot or diagonal couplet sequence limb phases. Plot adapted from Hildebrand (1980).

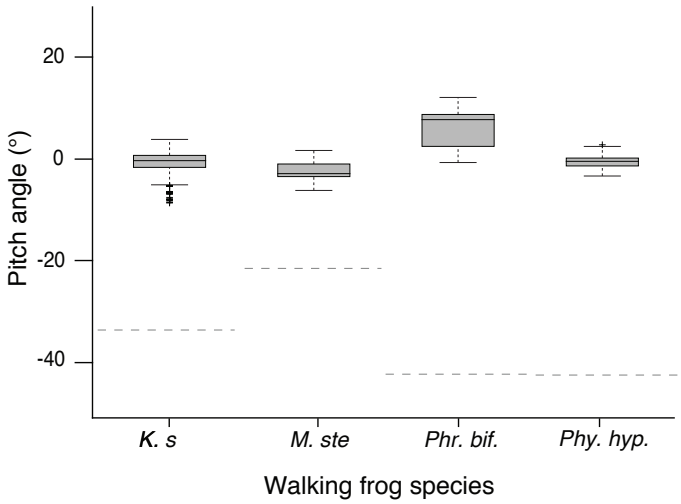

Figure 1.7. Comparison of average body pitch over a single stride and estimated body pitch from total extended limb lengths. (A) *Kassina senegalensis* (green; *n*=5), (B) *Melanophryniscus stelzneri* (yellow; *n*=2), (C) *Phrynomantis bifasciatus* (maroon; *n*=3), and (D) *Phyllomedusa hypochondrialis* (orange; *n*=2). Box plots correspond to changes in body pitch over a stride duration. Box-and-whisker diagrams show body pitch variation within a single stride. The boxes represent 50% of the data range, whiskers represent the interquartile range, bold horizontal bars represent the median, box height and whisker asymmetry indicate skewness of observations. The dashed line is the predicted pitch angle, calculated from total limb length. For all four species, pitch angle hardly deviates from 0 and differed from estimated pitch angles.

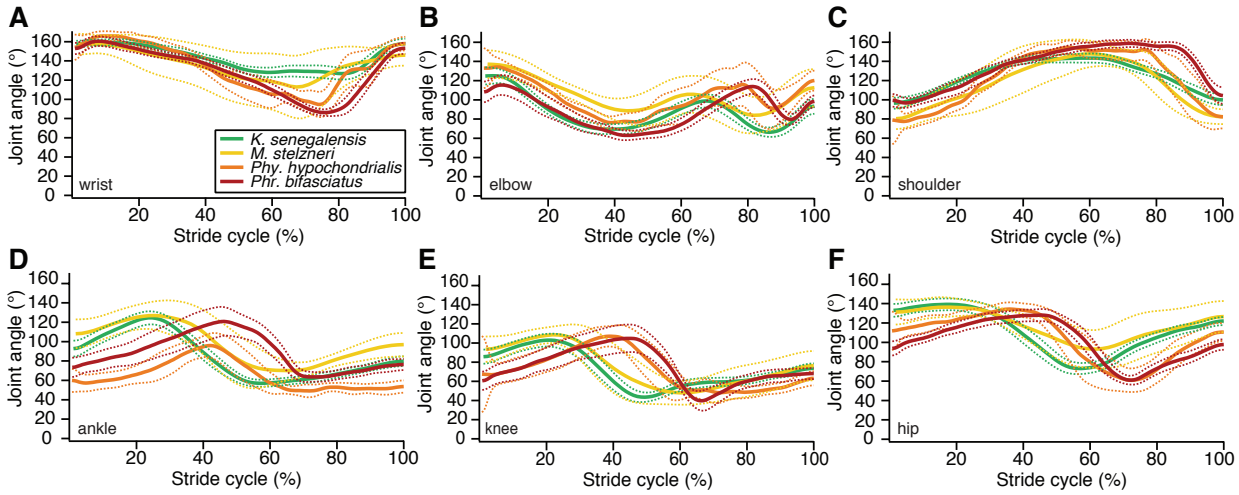

Figure 1.8. Average relative joint angle changes over a stride in the fore- and hindlimb. *Kassina senegalensis* (green; *n*=5), *Melanophryniscus stelzneri* (yellow; *n*=2), *Phrynomantis bifasciatus* (maroon; *n*=3), and *Phyllomedusa hypochondrialis* (orange; *n*=2). The top row of graphs shows the joint angle changes in the forelimb: (A) wrist, (B) elbow, and (C) shoulder. The bottom row of graphs shows joint angle changes in the hindlimb: (D) ankle, (E) knee, and (F) hip. A complete stride cycle is defined from the first point of contact of the leading forelimb to just before the same leading forelimb touches back down. All averaged data are shown as a solid line, with dotted lines that represent 95% confidence intervals. Relative joint angle patterns are similar across species, however deviates in the timing of these changes throughout a stride.

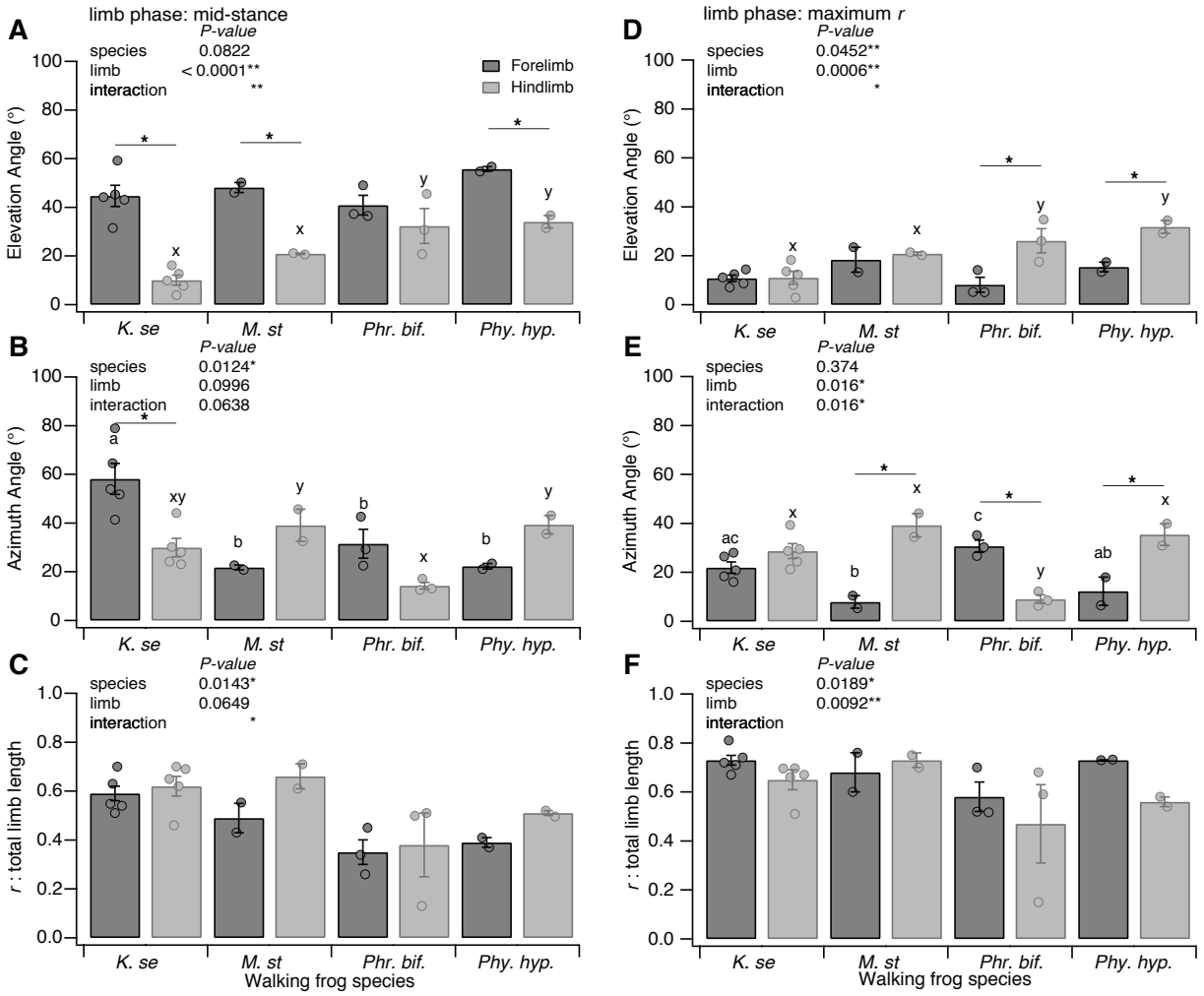

Figure 1.9. Average relative three-dimensional limb posture at mid-stance and maximum limb extension (mean±s.e.m.): *Kassina senegalensis* (*n*=5), *Melanophryniscus stelzneri* (*n*=2), *Phrynomantis bifasciatus* (*n*=3), and *Phyllomedusa hypochondrialis* (*n*=2). Elevation angle, azimuth angle, and normalized radial magnitude (r) measurements of the forelimb and hindlimb were taken at mid-stance of the limb (A, B, C) and at maximum limb radial extension (*r*) (D, E, F). *P*-values are given for each graph. At mid-stance, (A) elevation angle is significantly greater in the forelimb than the hindlimb, however (B, C) there was no significant difference in azimuth angle or limb radial magnitude. During maximum *r*, (D) elevation angle is significantly different in the hindlimb, whereas (E) there was no significant difference in azimuth angle. Lastly, (F) relative radial magnitude is significantly different across species, however there was no difference between forelimb and hindlimb. These results suggest quadrupedal walking frogs effectively use similar proportions for their fore- and hindlimb lengths across a stride, while adjusting vertical extension in the fore- and hindlimb by increasing their elevation angle throughout a stride. *Denotes significant difference within the forelimb and hindlimb of a species, $P<0.05$. Significant forelimb pairwise comparisons across species indicated with letters a, ab, b, etc., and significant hindlimb pairwise comparisons indicasted with x, y, xy, etc. Means not sharing the same letters are significantly different (Tukey HSD, $P<0.05$). See Appendix A.7 for more detailed statistics.

1.6 REFERENCES

Aerts, P. (1998). Vertical jumping in *Galago senegalensis*: The quest for an obligate mechanical power amplifier. *Philosophical Transactions of the Royal Society B: Biological Sciences*, 353(1375), 1607–1620. https://doi.org/10.1098/rstb.1998.0313

Ahn, A. N., Furrow, E., & Biewener, A. A. (2004). Walking and running in the red-legged running frog, *Kassina maculata*. *Journal of Experimental Biology*, 207, 399–410. https://doi.org/10.1242/jeb.00761

Ashley-Ross, M. A. (1994). Hindlimb kinematics during terrestrial locomotion in a salamander (*Dicamptodon tenebrosus*). *Journal of Experimental Biology*, 193(1), 255–283.

Astley, H. C. (2016). The diversity and evolution of locomotor muscle properties in anurans. *Journal of Experimental Biology*, 219, 3163–3173. https://doi.org/10.1242/jeb.142315

Biewener, A. A. (1983). Allometry of quadrupedal locomotion: The scaling of duty factor, bone curvature and limb orientation to body size. *Journal of Experimental Biology*, 105, 147–171.

Biewener, A. A. (1989a). Mammalian terrestrial locomotion and size. *Bioscience*, 39(11), 776–783. https://doi.org/10.2307/1311183

Biewener, A. A. (1989b). Scaling body support in mammals: Limb posture and muscle mechanics. *Science*, 245(4915), 45–48. https://doi.org/ 10.1126/science.2740914

Biewener, A. A. (2005). Biomechanical consequences of scaling. *Journal of Experimental Biology*, 208(9), 1665–1676. https://doi.org/10.1242/ jeb.01520

Chen, J. J., Peattie, A. M., Autumn, K., & Full, R. J. (2006). Differential leg function in a sprawled-posture quadrupedal trotter. *Journal of Experimental Biology*, 209, 249–259. https://doi.org/10.1242/jeb.01979

Chen, J., Bever, G. S., Yi, H. Y., & Norell, M. A. (2016). A burrowing frog from the late Paleocene of Mongolia uncovers deep history of spade-foot toads (Pelobatoidea) in East Asia. *Scientific Reports*, 6, 19209. https://doi.org/10.1038/spe19209.

Choi, I., Shim, J. H., & Ricklefs, R. E. (2003). Morphologic relationships of take-off speed in anuran amphibians. *Journal of Experimental Zoology A*, 299(2), 99–102. https://doi.org/10.1002/jez.a.10293

Emerson, S. B. (1976). Burrowing in frogs. *Journal of Morphology*, 149(4), 437–458. https://doi.org/10.1002/jmor.1051490402

Emerson, S. B. (1979). The ilio-sacral articulation in frogs: Form and function. Biological *Journal of the Linnean Society*, 11, 153–168. https://doi.org/10.1111/j.1095-8312.1979.tb00032.x

Emerson, S. B. (1988). Convergence and morphological constraint in frogs: Variation in postcranial morphology. *Fieldiana Zoology*, 43, 1–19.

Emerson, S. B., & Koehl, M. A. R. (1990). The interaction of behavioral and morphological change in the evolution of a novel locomotor type: "Flying" frogs. *Evolution*, 44(8), 1931–1946. https://doi.org/10.1111/ j.1558-5646.1990.tb04300.x

Farley, C. T., & Ko, T. C. (1997). Mechanics of locomotion in lizards. *Journal of Experimental Biology*, 200(16), 2177–2188.

Fischer, M. S., Schilling, N., Schmidt, M., Haarhaus, D., & Witte, H. (2002). Basic limb kinematics of small therian mammals. *Journal of Experimental Biology*, 205(9), 1315–1338.

Frost, D. R., Grant, T., Faivovich, J., Bain, R. H., Haas, A., Haddad, C. F. B., ... Ward, C. (2006). The amphibian tree of life. *Bulletin of the American Museum of Natural History*, 297, 8–370.

Gans, C., & Parsons, T. S. (1966). On the origin of the jumping mechanism in frogs. *Evolution*, 20, 92–99. https://doi.org/10.1111/ j.1558-5646.1966.tb03345.x

Garland, T., Jr., & Ives, A. R. (2000). Using the past to predict the present: Confidence intervals for regression equations in phylogenetic comparative methods. *The American Naturalist*, 155(3), 346–364.

Gomes, F. R., Rezende, E. L., Grizante, M. B., & Navas, C. A. (2009). The evolution of jumping performance in anurans: Morphological correlates and ecological implications. *Journal of Evolutionary Biology*, 22(5), 1088– 1097. https://doi.org/10.1111/j.1420-9101.2009.01718.x

Grafen, A. (1989). The phylogenetic regression. *Philosophical Transactions of the Royal Society B: Biological Sciences*, 326(1233), 119–157. https://doi.org/10.1098/rstb.1989.0106

Hedrick, T. L. (2008). Software techniques for two- and three- dimensional kinematic measurements of biological and biomimetic systems. *Bioinspiration & Biomimetics*, 3(3), 034001. https://doi.org/10.1088/1748-3182/3/3/034001

Hildebrand, M. (1968). Symmetrical gaits of dogs in relation to body build. *Journal of Morphology*, 124(3), 353–360. https://doi.org/10.1002/ jmor.1051240308

Hildebrand, M. (1980). The adaptive significance of tetrapod gait selection. *American Zoologist*, 20(1), 255–267.

Hildebrand, M. (1985). Walking and running. In M. Hildebrand, D. M. Bramble, K. F. Liem, & D. B. Wake (Eds.), Functional vertebrate morphology (pp. 38–57). Cambridge, MA: Harvard University Press.

Isaac, N. J. B., Redding, D. W., Meredith, H. M., & Safi, K. (2012). Phylogenetically-Informed Priorities for Amphibian Conservation. *PLoS ONE*, 7(8), e43912. https://doi.org/10.1371/journal.pone.0043912

Jenkins, F. A. (1971). Limb posture and locomotion in the Virginia opossum (*Didelphis marsupialis*) and in other non-cursorial mammals. *Journal of Zoology*, 165(3), 303–315. https://doi.org/10.1111/ j.1469-7998.1971.tb02189.x

Jenkins, F. A., & Shubin, N. H. (1998). *Prosalirus bitis* and the anuran caudopelvic mechanism. *Journal of Vertebrate Paleontology*, 18(3), 495–510. https://doi.org/10.1080/02724634.1998.10011077

Jorgensen, M. E., & Reilly, S. M. (2013). Phylogenetic patterns of skeletal morphometrics and pelvic traits in relation to locomotor mode in frogs. *Journal of Evolutionary Biology*, 26(5), 929–943. https://doi.org/10.1111/jeb.12128

Kubow, T. M., & Full, R. J. (1999). The role of the mechanical system in control: A hypothesis of self-stabilization in hexapedal runners. *Philosophical Transactions of the Royal Society B: Biological Sciences*, 354(1385), 849– 861. https://doi.org/10.1098/rstb.1999.0437

Marsh, R. L. (1994). Jumping ability of anuran amphibians. *Advances in Veterinary Science Comparative Medicine*, 38B, 51–111.

Martins, E. P., & Hansen, T. F. (1997). Phylogenies and the comparative method: A general approach to incorporating phylogenetic information into the analysis of interspecific data. *The American Naturalist*, 149(4), 646–667. https://doi.org/10.1086/286013

Napier, J. R., & Walker, A. C. (1967). Vertical clinging and leaping—A newly recognized category of locomotor behavior of primates. *Folia Primatologica*, 6(3), 204–219. https://doi.org/10.1159/000155079

Orme, D., Frechketon, R. P., Thomas, G. H., Petzoldt, T., Fritz, S., Isaac, N., & Pearse, W. (2013). Caper: Comparative analysis of phylogenetics and evolution in R. version 0.5.2.

Paradis, E., Claude, J., & Strimmer, K. (2004). APE: Analysis of phyloge- netics and evolution in R language. *Bioinformatics*, 20(2), 289–290. https://doi.org/10.1093/bioinformatics/btg412

Peplowski, M. M., & Marsh, R. L. (1997). Work and power output in the hindlimb muscles of Cuban tree frogs *Osteopilus septentrionalis* during jumping. *Journal of Experimental Biology*, 200(22), 2861–2870.

Pinheiro, J., Bates, D., DebRoy, S., & Sarkar, D. & R Development Core Team. (2017). nlme: Linear and nonlinear mixed effects models. R package version, 3, 1–131.

Porro, L. B., Collings, A. J., Eberhard, E. A., Chadwick, K.P., & Richards, C. T. (2017). Inverse dynamic modelling of jumping in the red-legged running frog, *Kassina maculata*. *Journal of Experimental Biology*, 220, 1882–1893. https://doi.org/10.1242/jeb.155416

Preuschoft, H., Witte, H., & Fischer, M. (1995). Locomotion in nocturnal prosimians. In L. Alterman, G. A. Doyle, & M. Kay (Eds.), Creatures of the dark: The nocturnal prosimians (pp. 453–472). Boston, MA: Springer US. https://doi.org/10.1007/978-1-4757-2405-9_27

Reilly, S. M., & Jorgensen, M. E. (2011). The evolution of jumping in frogs: Morphological evidence for the basal anuran locomotor condition and the radiation of locomotor systems in crown group anurans. *Journal of Morphology*, 272(2), 149–168. https://doi.org/10.1002/jmor.10902

Reilly, S. M., McElroy, E. J., Odum, R. A., & Hornyak, V. A. (2006). Tuataras and salamanders show that walking and running mechanics are ancient features of tetrapod locomotion. *Proceedings of the Royal Society B: Biological Science*, 273(1593), 1563–1568. https://doi.org/ 10.1098/rspb.2006.3489

Riskin, D. K., & Hermanson, J. W. (2005). Independent evolution of running in vampire bats. *Nature*, 434(7031), 292. https://doi.org/10.1038/ 434292a

Rohlf, F. J. (2001). Comparative methods for the analysis of continuous variables: Geometric interpretations. *Evolution*, 55(11), 2143–2160.

Schmidt, M. (2005). Hind limb proportions and kinematics: Are small primates different from other small mammals? *Journal of Experimental Biology*, 208(17), 3367–3383. https://doi.org/10.1242/jeb. 01781

Schmitt, J., & Holmes, P. (2000). Mechanical models for insect locomotion: Dynamics and stability in the horizontal plane—II. Application. *Biological Cybernetics*, 83(6), 517–527. https://doi.org/10.1007/s004220000180

Shubin, N. H., & Jenkins, F. A. (1995). An early Jurassic jumping frog. *Nature*, 377, 49–52. https://doi.org/10.1038/377049a0

Steudel, K., & Beattie, J. (1993). Scaling of cursoriality in mammals. *Journal of Morphology*, 217(1), 55–63. https://doi.org/10.1002/jmor.1052170105

Swartz, S. M. (1997). Allometric patterning in the limb skeleton of bats: Implications for the mechanics and energetics of powered flight. *Journal of Morphology*, 234(3), 277–294. https://doi.org/10.1002/ (SICI)1097-4687(199712)234:3<277::AID-JMOR6>3.0.CO;2-6

Swartz, S. M., & Middleton, K. M. (2007). Biomechanics of the bat limb skeleton: Scaling, material properties and mechanics. *Cells Tissues Organs*, 187(1), 59–84. https://doi.org/10.1159/000109964

Zug, G. R. (1972). Anuran locomotion: Structure and function. I. Preliminary observations on relation between jumping and osteometrics of appendicular and postaxial skeleton. *Copeia*, 4, 613–624. https://doi.org/10.2307/1442720

Zug, G. R. (1978). Anuran locomotion— structure and function. 2: Jumping performance of semiaquatic, terrestrial, and arboreal frogs. *Smithsonian Contributions to Zoology*, 276, 1–31.

CHAPTER 2

Effects of compliance on jumping in Cuban tree frogs: disruption of the inertial latch mechanism and elastic energy storage

2.1 INTRODUCTION

In habitats where there is large variation in the environment, whether navigating dense foliage or other physical obstacles, it can be challenging for an organism to traverse. Organisms encounter naturally occurring obstacles all the time. For instance, during running many organisms use stabilizing mechanisms that can help adjust limb stiffness, posture, and muscle force in response to various perturbations to the COM or terrain (Daley and Biewener 2006, 2011; Daley et al., 2006; Biewener and Daley, 2007; Gordon et al. 2015). The mechanical properties of the environment can often shape locomotor patterns that can lead to changes in motor function or even muscle properties (Biewener and Gillis, 1999; Nauwelaerts and Aerts; 2003; Azizi and Roberts, 2010; Azizi, 2014; Cox and Gillis, 2016). However, sensory feedback is not the only avenue for modulation and control, the mechanical properties of the musculoskeletal system have been shown to also control whole-body and muscle kinetics (Dickinson et al, 2000; Roberts and Azizi, 2011). More specifically, the use of tendinous elastic structures can passively amplify muscle power or dampen, which have also been shown to aid in stability (Wilson et al. 2001; Wakeling et al. 2002; Roberts and Azizi, 2011).

These tested perturbations often revolve around cyclic behaviors that allow for recycling of kinetic energy from one hop or stride cycle to the next (McMahon 1985; Biewener and Gillis, 1999; Schnyer et al. 2014). For more impulsive systems, it remains unclear what differentiates an organism capable of recovering from a perturbation or dynamic change in substrate. Studies on

human movements on complaint surfaces have shown active modulation within the first step or hop on a dynamic surface; increasing leg stiffness, changes in joint angle, and metabolic rates, for greater locomotor efficiency (McMahon and Greene 1978; Ferris and Farley, 1997; Farley et al. 1998; Ferris et al., 1998, Ferris et al. 1999; Kerdok et al. 2002).

Effective use of a complaint substrate has not been limited to humans, but also other vertebrates, previous studies have shown gibbons and Cuban tree frogs, *Osteopilus septentrionalis*, recover some energy from compliant substrates when jumping or leaping (Channon et al., 2011; Astley et al. 2015). However, in the case of primate vertical clingers and leapers and anole lizards, these organisms leave prior to elastic recoil of the substrate, lose energy to substrate deformation, and therefore gave reduced efficiency and performance (Demes et al. 1995; Gilman et al., 2012; Gilman and Irschick, 2013). What differentiates an organism capable of recovering energy from a compliant substrate?

Substrates of varying mechanical properties from woody branch structures to sand have been modeled as in-series mass, spring, and/or dampers which have substantial effects on substrate interactions (James et al. 2006; Aguilar and Goldman, 2016). These substrates have some energy associated with them that can either be stored or absorbed. On elastic substrates, an organism uses several times its body weight to deform the substrate. Energy is stored within the substrate. However, it takes some time for the substrate to accelerate its mass due to inertia and recoil. Therefore, in order for an organism to regain the stored energy this requires correct take-off timing. Otherwise, the organism loses a portion of the energy stored to the substrate, decreasing efficiency. Jump performance off compliant substrates provides an interesting paradigm into studying the mechanical interactions between the spring-like properties within the

substrate and the spring-like properties within the whole organism at the scale of the muscle-tendon; an example of two mass-spring systems in-series.

Cuban tree frogs provide an excellent model to investigate dual mass-spring dynamics given previous studies have shown these species take advantage of the recoil energy in compliant substrates and use tendon elastic energy to amplify muscle power (Astley et al. 2015; Roberts et al., 2011). In our study we ask: "How do Cuban tree frogs optimize energy recovery from compliant substrates?" We test hypotheses on mechanisms that may allow for substrate energy recovery. Frogs may modulate their performance by slowing limb extension rates to slow down take-off timing. Effectively waiting for the substrate to accelerate its mass and then recoil to accelerate the frog. This may be reflected with changes in motor pattern, differentially recruiting muscles based upon changes in substrate compliance. A second possibility, muscles may be recruited similarly, not actively altering musculoskeletal function. Alternatively, the mechanical properties of the environment may govern locomotor performance and allow for substrate energy recovery. We measured substrate and jump kinetics and limb kinematics of jumps from a dynamically complaint substrate—a custom-made actuated substrate that allows for specific adjustments in the substrate spring constant, *k*. Additionally, we use *in vivo* measurements of EMG activity in the two joint extensor muscles, an ankle (*m. cruralis*) and knee extensor (*m. plantaris*), to understand muscle recruitment patterns in response to compliant substrates. We discuss the trade-offs in power amplified systems and the implications for understanding latch dynamics on variable substrates.

2.2. MATERIAL AND METHODS

2.2.1 Reactive motor set-up

To investigate jump performance and motor response of Cuban tree frogs from compliant surfaces, we designed a dynamic compliant substrate. The spring-like reactive behavior of the servomotor was controlled by a BeagleBone Black controller, used to simulate a linear spring. We used a feedback control system, programed based upon a linear spring equation,

$$F_{VGRF} = -kx, \qquad (2.1)$$

where F_{VGRF} is the vertical ground reaction force of the frog, k, is the spring constant, and x is the displacement of the platform. As a result, this reactive substrate directly tunes to the behavior of the animal during jump take-off. The reactive substrate consisted of a jumping platform, created with acrylic (6.0 x 0.3 x 5.0 cm; mass = 10.0 g), attached to the top the lever arm (mass = 25.3 g) of a 50N dual-mode servomotor (Aurora Scientific Inc., Ontario CA, USA; 305-C-LR) lever arm (Figure 2.1a). Servomotor force and length voltage outputs were calibrated relative to the center of the acrylic platform.

The spring behavior of the reactive motor is governed by an open feedback control loop implemented in C++ and running on a BeagleBone Black. F_{VGRF} measurements are broadcast by the Aurora Scientific mechanical stimulator as analog signals in the ± 10 V range. A peripheral 16-bit sampling A/D unit (Texas Instruments ADS7813, Dallas TX, USA) on a custom printed circuit board converted this signal to a digital force measurement, which is then passed via the serial peripheral interface bus to the BeagleBone, where it is smoothed with a software-implemented resistor-capacitor circuit filter. The smoothed force estimate, and a predetermined k are used to calculate the displacement of a linear spring (platform) with the given k in the

presence of the measured F_{VGRF}. The digital displacement value is then passed from the BeagleBone to a peripheral 16-bit multiplying digital-to-analog converter chip (Analog Devices AD7849, Norwood MA, USA), where it is converted to an analog control signal. The analog position signal is sent to the Aurora Scientific mechanical stimulator which, in turn, controls the position of the platform. This control loop executes at approximately 1.4 kHz. As a result, the platform responds to external forces in a linear spring fashion with programmable stiffness (Figure 2.2a, b). There was an approximate delay of 0.042 s due to hitting the limits of the length step time response of the servomotor. Taking this delay into account, the inertial mass of the compliant substrate was approximately 0.075 kg. This dynamic substrate does not act as an ideal spring-mass, but a spring-mass-damper. However, the material properties of tree trunks and subsequent branches naturally act as in-series spring-mass-dampers (James 2003; James et al., 2006). Therefore, these frogs are less likely to experience a perfect spring mass system, but rather a dampened spring mass.

Prior to entering the spring behavior control loop, the BeagleBone samples and averages 1000 force measurements. This average was used as a passive force estimate and subtracted from forces measured within the control loop. Therefore, the displacement of the platform is a function of active force in excess of the passive ground reaction force exerted on the platform prior to a jump. All force and length data were collected at 10000 Hz using a 16-bit A/D converter (National Instruments, TX, USA) and Igor Pro Software (Wavemetrics Corp., Lake Oswego, OR, USA) for data acquisition.

2.2.2 Jump trials

This study used eight, wild-caught, female Cuban tree frogs (*O. septentrionalis*), purchased from a herpetological vendor (mean ± SEM; SNVL = 79.26 ± 2.27 mm, mass = 31.71 ± 3.07 g). Five individuals where used for kinetics and kinematics jump trials and six individuals were used for EMG jump trials. To standardize across frogs and each compliant condition, a predetermined *k*, was calculated relative to BW for each frog based on a desired displacement of 0.0, 0.3, 0.6, and 0.9 mm BW^{-1} that allowed us to test a range of *k* values from 237 - 1217 N/m. The range of *k* values were constrained by the response time of the servomotor; *k* values smaller than 100 N m^{-1} required too rapid of a time step for the servomotor to operate optimally. Despite these constraints, the tested range of *k* values are representative of biologically relevant ranges tested in various tree branch species that can span even greater stiffnesses (Kerzenmacher and Gardiner, 1998; James 2003).

Frogs were placed on the platform and allowed to jump the distance of the arena (61.0 x 29.0 x 60.5 cm), which included places for refuge to incentivize jumping. The frogs were encouraged to jump with a gentle tap on the pubis-ischium with a cotton swab, however many frogs jumped off the substrate voluntarily without probing. Experiments were performed in temperatures ranging between 21.9 - 27.9 °C and percent humidity range between 31 - 47%. We filmed jumping events using two high-speed video cameras (Phantom M120 Cameras, Vision Research Inc., Wayne NJ, USA) positioned posteriorly and laterally to the individual and the compliant surface (Figure 2.1b). Cameras recorded at 1000 frames s^{-1}. All servomotor force-length data were synchronized to high-speed video data using an external trigger.

Each individual performed 5 jumps at each compliance (0.0, 0.3, 0.6, and 0.9 mm BW^{-1}). Jump trials from a given compliance were selected at random, however each frog jumped off a

single compliance during a jump session to detect any learning or increase in performance due to experience on a certain compliance. Individual and jump sequences were accounted as factors during statistical analyses. Jumps were chosen based upon robust performance with no foot or limb slippage from the platform. Analyzed content was based upon the criteria that both limbs began on the platform and ended with both hindlimb phalanges on the platform until the instant of toe-off.

2.2.3 Hindlimb kinematics and kinetics

For each jump, we used MATLAB to calculate the three-dimensional (3D) position of the left hindlimb relative to the platform. To calibrate the jumps, we used a custom calibration cube with 48 non-planar points with direct-linear transformation software from Hedrick (2008) in MATLAB (The MathWorks, Natick MA, USA). Using the direct-linear transformation scripts we manually tracked the tip of the longest phalange, metatarsal, ankle, knee and hip on the left leg, the limb closest to the lateral view camera. In addition, we digitized the frog COM and five separate landmarks on the substrate to characterize the position of the platform relative to the frog.

Video data were used to determine the rate of limb extension and onset of joint extension over a jump to characterize timing of elastic energy storage. Rate of limb extension was characterized as the rate of change in the vector magnitude originating from the hip directed to the tip of the longest phalange. Initially, limb extension traces were interpolated in Igor Pro to minimize any noise due to manual digitization. 3D coordinates were used to calculate relative knee and ankle joint angles during a jump within the local reference frame. Joint angles were

also interpolated to reduce any noise, then differentiated with respect to time to calculate joint angular velocities during jumps and determine timing of joint extension onset.

Total frog and substrate energies were calculated using both high-speed video footage and force-length servomotor outputs. Servomotor force and length traces were interpolated using Igor Pro to minimize noise. To characterize energy during loading and unloading phases of the substrate, jumps were divided into two different phases: (1) the loading phase, defined as the start of the jump until the time of maximum substrate deflection and (2) the unloading phase was characterized as the time after maximum substrate deflection until right before the foot left contact with the substrate (toe-off). Total substrate energy was calculated as the sum of the inertial rotational energy and the spring potential energy of the platform,

$$E_{sub} = (m_{sub}\Delta x_{sub}a_{sub}) + (\tfrac{1}{2}kg(\Delta x_{sub})^2) \qquad (2.2),$$

where m_{sub} is the total mass of the acrylic platform and servomotor lever arm. E_{sub} was characterized for the loading and unloading phases of the jump. The proportion of energy used from the platform was characterized as efficiency (η); the proportion of energy recovered before toe-off relative to the total energy loaded into the substrate,

$$\eta = \frac{E_{recovered}}{E_{loaded}} \qquad (2.3).$$

Total frog energy was calculated as the sum of the kinetic and potential energy of the COM,

$$E_{frog} = (\tfrac{1}{2}m_{frog}(V_{com})^2) + (m_{frog}g\,\Delta x_{com}) \qquad (2.4),$$

where V_{com} and x_{com} were calculated from the digitized COM of the frog. Lastly, F_{VGRF} was differentiated with respect to time to characterize jump power. We calculated frog efficiency to detect any increase in jump performance with increased exposure to a certain compliance, as the proportion of energy recovered from the platform and the total energy of the frog COM at toe-off.

2.2.4 Electromyography

We studied two joint extensor muscles, *m. cruralis* and *m. plantaris*; a knee and an ankle extensor. These muscles play an important role during the jump take-off phase. EMG transducers were made with fine-wire bipolar electrodes (Medwire, Corp., Mt. Vernon NY, USA), by twisting two bipolar wires together with the insulation stripped-off about 1 mm, with an approximate offset of 1 mm. Customized ground wire and EMG electrode lengths were determined based upon SNVL and limb segment lengths. A ground wire and two EMG bipolar electrodes were soldered into a 6 pin microtech strip connector (Microtech, inc., Boothwyn PA, USA) and cemented with epoxy, creating a transducer connector to carry signals, amplified at x1000 (A-M systems, WA, USA).

Tree frogs were anaesthetized with immersion in 2L of tricaine methanesulphonate solution (MS-222, 2.0g L^{-1}) for 20 minutes. Following anesthesia, EMG transducers were surgically implanted into muscles of interest. Incisions were made by scalpel over the dorsal midline and along the skin covering each muscle. EMG transducers were fed under the skin and along the left leg to each muscle. One electrode was implanted per muscle using a 22-gauge hypodermic needle. Electrodes were sutured in place at the surface of each muscle using 6.0 suture silk. The ground wire was implanted subdermal along the dorsal side of the frog. All three skin incisions were sutured closed with 4.0 suture silk, with the transducer sutured onto the animals' back. Frogs were allowed to recover for 24 h before jump trials were performed. Muscle activities were recorded during compliant jump trials at all four compliant conditions. While instrumented, frogs were recorded using the same previously explained experimental set-up with high-speed video and force actuated platform. Five jumps per compliance were analyzed

for each of the six individuals. After EMG jump trials tree frogs were euthanized by MS-222 submersion and a double pithing protocol.

EMG signals were filtered with a finite impulse response filter (Figure 2.2c, d) and rectified using Igor Pro. EMG signals were normalized to the average maximum amplitude of the rectified signal relative to each muscle (electrode). Muscle activity onset and offset timing were identified and evaluated with respect to take-off timing. Then, rectified and normalized muscle activity signals were integrated between onset and offset of muscle activity to calculate muscle activation intensity during a jump. Previously mentioned joint extension velocities were used to determine the timing of elastic energy storage defined as the start of extensor muscle activation until the onset of the corresponding joint extension.

2.2.5 Statistical analysis

All subsequent statistical analyses were run in RStudio (v. 1.0.136, Boston, MA, USA). For each variable, mean values per individual were calculated and used for mean and standard error calculations across the different compliant substrates. To examine the effect of substrate compliance on energy efficiency, max V_{limb}, and max jump power, we used a mixed-model analysis of variance (ANOVA) to compare performance across compliance, accounting for variance within individuals and jump sequence. Post-hoc comparisons were made with Bonferroni corrections to examine the affect between various complaint substrates. To detect whether there was learning or increased performance with exposure to a particular compliance we performed linear regressions for each compliance. We used one-way analysis of variance (ANOVA) to compare muscle recruitment intensities across compliance relative to each muscle. In addition, we performed repeated measures two-way ANOVAs on muscle activation onset and

offset accounting for variance within individuals. In addition, two-way repeated measures ANOVA was also performed to test for changes in joint onset across extension timing across compliance.

2.3 RESULTS

A total of 220 jumps were analyzed between six animals, with a total of 120 jumps collected for EMG analysis. Frogs generally loaded about 3 - 4 times their body weight (Figure 2.2a). For compliant conditions, platform deflections ranged from a minimum of 0.5 – 2.5 mm. Across all compliances, about 50% of the original energy stored into the substrate was recovered before toe-off (Figure 2.3a). Therefore, not all energy stored was recovered prior to take-off. There were no relationships between previous experience with a certain compliance and frog efficiency performance (Appendix B Figure B.1). Therefore, we found regardless of exposure to a particular substrate effective use of recoil energy did not change. Furthermore, these comparisons were run across all performance variables tested with mixed-model ANOVAs, such as V_{limb} and jump power. Regardless of the metric, these frogs did not improve their performance with increased experience or repetitions on a particular compliance.

We examined limb kinematics and jump performance to determine whether there were any changes in performance across these compliant substrates. We found a 20% decrease in limb extension velocity with compliance ($P < 0.001$; Figure 2.3b). V_{limb} tended to decrease for substrate compliances of 0.3 and 0.6 mm BW^{-1} ($P = 0.003$; $P = 0.0025$). Although, V_{limb} on 0.9 mm BW^{-1} compliant substrates were not statistically different from either solid jumps or compliant jumps at 0.3 and 0.6 mm BW^{-1}. This was largely driven by one individual on average

having greater V_{limb} and high force and powered jumps on the most compliance substrate (Figure 2.3b, 2.4b).

These changes in limb velocity were also reflected in jump power. Jump power decreased across compliance ($P = 0.014$; Figure 2.4). Jump power on solid substrates were statistically higher than on compliant substrates 0.6 mm BW^{-1} ($P = 0.025$). However, at the most compliant condition, 0.9 mm BW^{-1}, did not differ significantly between the solid substrate nor less compliant substrates (0.3 and 0.6 mm BW^{-1}). Given this observed decrease in jump performance, we examined whether this performance was actively modulated by muscle activation.

The *m. plantaris* and *m. cruralis* roughly activated at similar times prior to any body or joint movement across all compliance (Figure 2.2, 2.5). Despite nonsignificant relationships, a later onset of muscle activation timing on more compliant substrates, tended to show a shorter jump duration (Figure 2.5). However, muscle activation offset differed between muscles within compliance ($P = 0.027$), although not a clear pattern on 0.3 and 0.9 mm BW^{-1} substrates *m. plantaris* and *m. cruralis* tended to continue activation until the timing of toe-off. Whereas, on solid and 0.6 mm BW^{-1} offset occurred milliseconds prior to toe-off. Muscle activation intensities did not change across compliance for both *m. plantaris* and *m. cruralis* (Figure 2.5a). Despite no clear active modulation in the two joint extensor muscles jump performance was compromised with decreased power on more compliant substrates.

Our results suggest the early onset of limb extension may be due to the displacement of the compliant substrate, which in turn decreases power output by nearly half. Knee and ankle joint extension onset appeared to be decoupled on compliant substrates (Figure 2.5b). Ankle and knee joint extension onset occurred at significantly different times at compliances of 0.3 and 0.6 mm BW^{-1} (Figure 2.5b). We characterized the timing between EMG onset and onset of relative

joint extension (prior to any change in mechanical advantage) as the approximate timing of elastic energy storage. On solid substrates, we found frogs have a greater time frame to store elastic energy (Figure 2.5c), therefore introducing more energy to the system, which results in higher force and power outputs, and thus a faster limb extension.

2.4 DISCUSSION

We examined jumps from various compliant substrates to investigate how the mechanical properties of a substrate impact limb and muscle function. We hypothesized frogs may actively optimize for energy recovery by modulating muscle activation patterns and therefore adjust limb kinematics to recover elastic energy stored within a substrate. On average Cuban tree frogs recovered about half the energy stored for each compliance. Decreases in the rate of limb extension with compliance suggest these frogs are modulating limb kinematics, however muscle activation patterns did not reflect these changes. We provide evidence that suggests Cuban tree frog jumps operate via a feedforward control program, where once initiated there is likely little modulation or adjustment at the muscle level. Joint kinematics and muscle activity show how the interaction with a compliant substrate may be responsible for early on-set of joint extension. We demonstrate a trade-off on compliant substrates, which reduces the timing for elastic energy storage. However, a decreased timing in elastic energy and jump power allows for a slower rate of limb extension and therefore slows down the timing of take-off. In turn, this allows for greater energy recovery from the substrate. As a result, it is likely the inertial catch mechanism is compromised on complaint substrates, which performs optimally on solid substrates.

Cuban tree frogs utilize substrate elastic energy, though they lose a portion of that energy previously loaded during take-off (Figure 2.2). There was no significant change in performance

due to increased exposure or repetition with a particular substrate (Appendix Figure B.1). Given the large variation in substrate variability within a habitat, it may be more beneficial to adapt a single jump mechanism regardless of the variable mechanical properties of the substrate. Our experimental set-up and efficiency results validate previous research demonstrating the use of elastic recoil energy from surgical tubing (Astley et al., 2015). Given the limited range of tested compliance, we did not find a clear trade-off in energy recovery, efficiency, or optimal performance for a certain compliance. However, Astley, et al. (2015) has shown this apparent trade-off on substrates may be apparent on substrates up to double our experimented compliance. We note our tested perturbations are relatively small displacements, however we still find a significant effect of compliance on performance. This shows the critical influence of compliances on ballistic systems. We suspect to find even more pronounced trends with greater displacement perturbations.

In the case of organisms that utilize substrate recoil energy, we find evidence that passive muscle properties of the Cuban tree frog may play a larger role over active modulation. Initially, we proposed to optimize energy recovery an organism must slow down the rate of limb extension to await the substrate recoil; which must accelerate its own mass prior to recoil. This lag between loading and unloading requires an organism to remain on the substrate long enough to recover all recoil energy. We found rate of limb extension slows down with increased compliance (Figure 2.3). A decrease in rate of limb extension allows these frogs to remain on the platform until substrate recoil to regain a portion of the stored energy. Previously, Astley, et al. (2018) showed a decreasing trend in take-off velocity of the COM, it is possible this may be a result of changes in limb extension rate and timing.

2.4.1 Feedforward jump mechanism

Across all substrates, we recorded muscle activation patterns to detect any changes in recruitment intensity, onset, or offset. Given the significant decrease in the rate of limb extension, we expected active modulation to coordinate with these changes. However, we found no significant patterns in activation intensity or onset across both extensor muscles (Figure 2.5). These results support the idea that Cuban tree frogs do not prioritize feedback information during jump take-off but operate with a feedforward control program. At this timescale the performance may be too short for active modulation (Kagaya and Patek 2016). Once a jump is initiated the frog is no longer able to adjust performance. It is possible antagonistic muscle activation patterns may play an active role resisting change in limb mechanical advantage.

Previous work on variable substrates have described the kinetics (Astley et al., 2015) of the system and interactions, however our work uses variable substrates to provide additional support for a feedforward mechanism and demonstrate the limited role of feedback and/or proprioception during jump take-off. Our results provide evidence that visual, vestibular, and proprioceptive feedback may not play a direct role in Cuban tree frog jumps. Organisms that use elastic elements potentially give up the ability to respond to perturbations. It remains untested the extent of visual, vestibular, and proprioceptive feedback incorporated in other species that do not predominately use elastic energy storage, for example in toads. Cuban tree frogs have been shown to use elastic energy to produce up to four times the power output of toads (Roberts et al., 2011). This may change depending on how heavily an organism relies on elastic energy storage to power a jump. In addition, toad species have been shown to modulate activation patterns in anticipation for landing (Gillis et al., 2010; Akella and Gillis, 2011; Azizi and Abbott, 2012; Cox

and Gillis, 2016, 2017). We propose the use of elastic elements comes at the cost of the ability to respond to perturbations after the loading phase.

2.4.2 Trade-off in power amplified systems

Additionally, we found substrate compliance negatively impacted jump power (Figure 2.4). These frogs used the same jump motor program, however did not amplify power as well on compliant surfaces. This highlights the fundamental trade-off between using the same locomotor mode on power output. Cuban tree frogs are known for their high-powered jump performance (Marsh and John-Alder 1994; Peplowski and Marsh 1997). A locomotor performance that surpasses the limits of muscle force production (Roberts and Marsh, 2003; Roberts, et al. 2011). To overcome these constraints, Cuban tree frogs use an inertial catch mechanism to amplify power by storing energy via elastic strain within the tendon (Astley and Roberts, 2012, 2014). This allows for up to seven times the amplification of power (Roberts, et al. 2011). Our results show how the mechanical properties of the substrate affect power amplification

We characterized the timing between onset of EMG and joint extension to approximate the timing of elastic energy storage. We suspect a dynamic change in mechanical advantage may cause a decoupling in joint extension, therefore variably 'unlatching' the catch mechanism. We observed a significant difference between ankle and knee joint extension times with increased compliance (figure 2.5b). A previous study by Astley and Roberts (2014) demonstrated the role of poor mechanical advantage and high joint moments as possible mechanisms responsible for power amplification in *Rana pipiens*, a frog species shown to use elastic recoil energy. Although a physical latch has not been found, these resistive forces likely act as a catch or latching mechanism that allow for elastic energy storage (Astely and Roberts, 2014). This poor

mechanical advantage allows for the muscle to shorten and the tendon to stretch, storing elastic energy all before any change in mechanical advantage or onset of joint extension in the limb (Astley and Roberts, 2012). Once a force threshold is reached this results in a dynamic change in mechanical advantage and release of energy from the tendon at a far more rapid rate than can be stored or produced by the muscle alone. Given this, frogs on a solid substrate are able to maintain a flexed limb with a small mechanical advantage, which allows for elastic energy storage. While on a compliant substrate, the joint may be forced to extend sooner and begin limb extension earlier, prematurely 'unlatching' the system. As a result, this increases mechanical advantage and truncates the time of elastic energy storage. The sooner the 'unlatching' (onset of one joint) the less time the extensor muscle has to store energy, the slower rate of joint and limb extension, and therefore decreased jump power. We provide the first evidence of how an organisms' environment or substrate may interfere with the catch or inertial latching mechanisms, thus creating a less effective latch.

2.4.3. Latch quality and variable substrates

Despite this trade-off, the use of elastic structures for optimal performance with greater power outputs on solid substrates still provides benefits to jump performance on compliant substrates. On a solid substrate we saw the example of an ideal latching mechanism that allows for rapid energy release (Ilton et al., 2018). A similar timing in joint extension may allow for more time to store energy, introducing more energy to the system upon release, ultimately producing greater power output and fast limb extension. Whereas, a compliant substrate essentially creates a less effective or less rigid latch, which dynamically slows down the rate of energy release. This is analogous to increasing latch radius (creating a more rounded latch) in a

recent power amplification model proposed by Ilton et al. (2018). Our results show the frog latching mechanism can be manipulated by the mechanical properties of a substrate and performs best under a poor latch condition that allows for slower release of energy in order to remain on the substrate. A reduced rate of limb extension allows the frog to recover more energy from a compliant substrate, since elastic energy storage timing has been disrupted, power output decreases, and slows down the rate of limb extension enough to keep the frog on the substrate in order to regain energy from the substrate. Recent work by Ilton et al. (2018) demonstrates the importance of latch dynamics, which incorporates a motor, latch, mass/projectile, and spring in-series. Our findings suggest these latch dynamics may be significantly effected during the interaction of variable substrate properties. For example, by including an additional mass-spring to model the substrate in-series with the actuated motor, mass-spring latching model the optimal latch properties may change for optimal energy efficiency.

Here we demonstrate that recruitment intensity, and onset and offset timing of *m. plantaris* and *m. cruralis* are not modulated with changes in substrate compliance. Additionally, we use *in vivo* observations to experimentally show the first evidence of latch manipulation. Our study provides further support, as well as others, for an inertial catch mechanism, suggesting this dynamic change in mechanical advantage within the limb effectively acts as the latching mechanism. Antagonistic muscle activation patterns may play a role in changes in limb mechanical advantage and 'unlatching'. Our study highlights the importance of further investigation in understanding the dynamic interactions between latch mechanisms and substrates. For instance, frog jumps from lily pads may provide a different latching interaction when considering a highly viscous and dampening force from the environment (Aguilar and Goldman 2016). Additionally, it is likely non-linear or exponential springs may have different

effects on the latching mechanisms and therefore change performance. In light of these dynamic changes in an organisms' environment it raises the question of whether the evolution of a power-amplified mechanism provides the most robust performance regardless of the type of substrate or the environment.

2.5 LIST OF ABBREVIATIONS

A/D, analogue-to-digital;

a_{sub}, substrate acceleration;

BW, body weight;

COM, center of mass;

E_{frog}, total frog energy;

E_{loaded}, energy loaded into platform;

$E_{recovered}$, platform energy recovered during jump unloading phase;

E_{sub}, total substrate energy;

EMG, electromyography;

F_{VGRF}, vertical ground reaction force;

g, acceleration of gravity;

k, spring constant;

m_{frog}, *frog mass;*

m_{sub}, substrate mass;

SNVL, snout-vent length;

x_{com}, frog center of mass displacement;

x_{sub}, substrate displacement;

V_{com}, frog center of mass velocity;

η, energy efficiency;

2.6 ETHICS

Animal husbandry and experimental procedures were approved by the University of California, Irvine Institutional Animal Care and Use Committee (Protocol AUP-17-170).

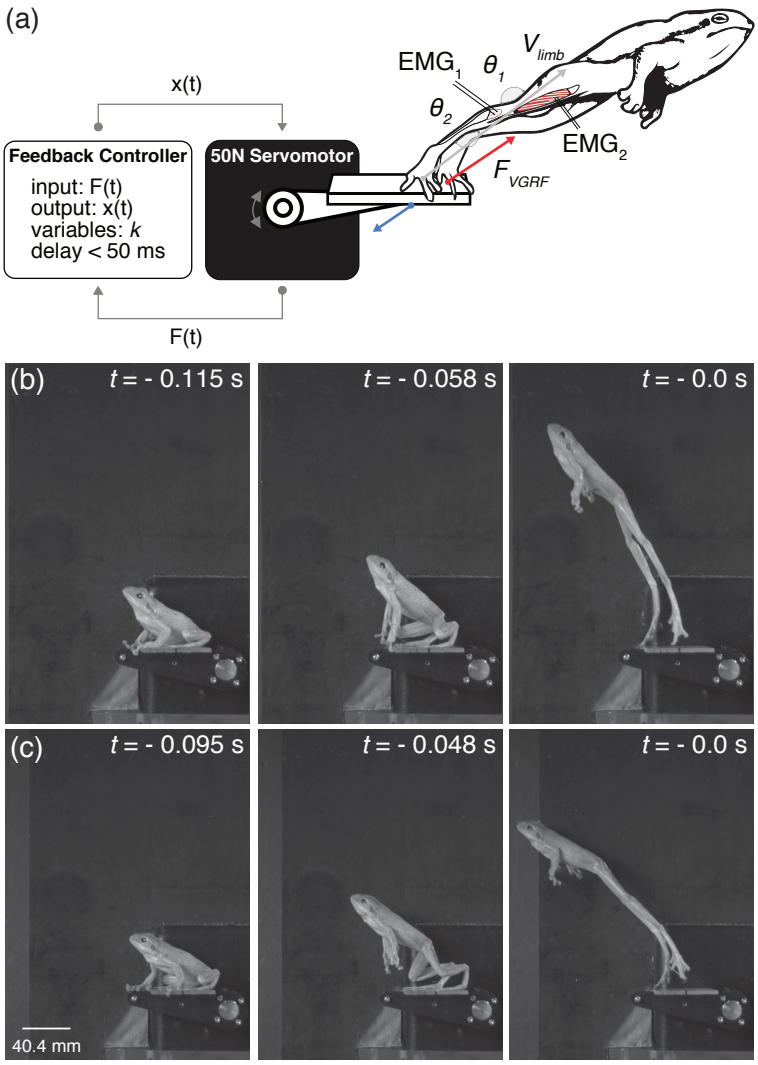

Figure 2.1. Experimental set-up for the dynamically compliant substrate. (a) The reactive motor set-up built from a 50N Aurora servomotor and BeagleBone Black computer controller. The BeagleBone controller was programed to function as a linear spring equation based upon a predetermined spring constant, *k*, relative to body weight. Vertical ground reaction force (F_{VGRF}) voltage inputs were sent from the servomotor to the BeagleBone. In response, the BeagleBone voltage outputs were sent to the servomotor with a calculated length change relative to the programed linear spring equation. Lateral and dorsal views of jumps were filmed using two high-speed video cameras, recording at 1000 frames s^{-1} to measure rate of limb extension (V_{limb}), changes in relative ankle (θ_A) and knee (θ_K) joint angle, and timing of jump. Electromyography (EMG) electrodes were surgically implanted to record muscle activity patterns in an ankle extensor (*m. cruralis*) and a knee extensor (*m. plantaris*). Sample lateral view high-speed video frames of a Cuban tree frog from (b) solid substrate and (c) the most compliant condition (0.9 mm BW^{-1}).

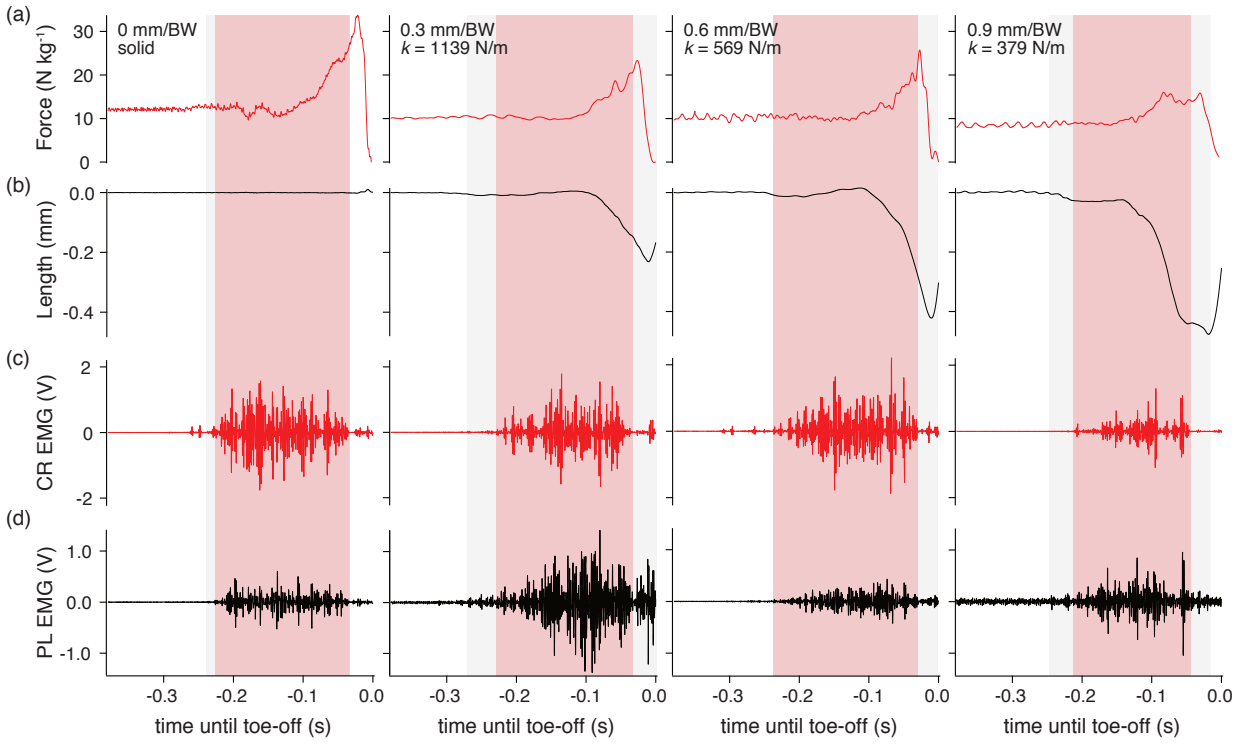

Figure 2.2. *In vivo* representative traces of recorded (a) vertical ground reaction forces and (b) dynamic substrate length change in response to the feedback controller at four different compliances: 0.0, 0.3, 0.6, and 0.9 mm per body weight (BW). (c, d) Relative electromyography (EMG) activity patterns during the four complaint conditions for the *m. cruralis* (CR) and *m. plantaris* (PL) muscles.

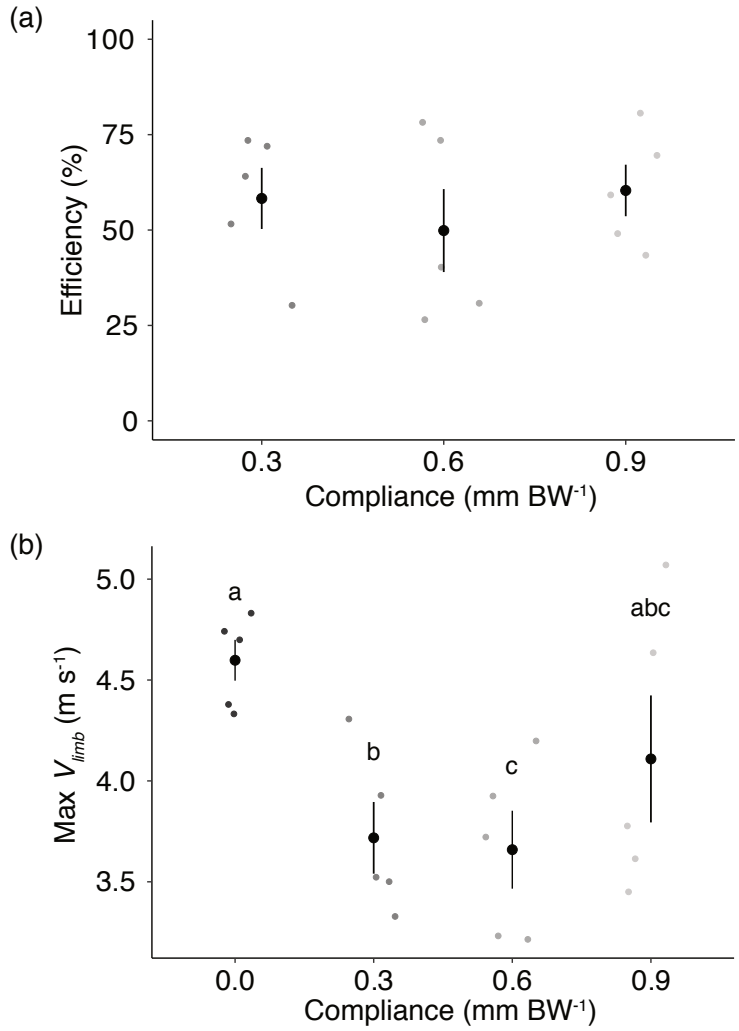

Figure 2.3. *O. septentrionalis* kinetics and limb kinematics across variably compliances (N = 5; mean SEM). (a) Energy recovery efficiency across variable compliant substrates. Across all compliances *O. septenrionalis* recovered about 50% of the energy stored in the substrate before jump take-off. (b) Maximum limb extension velocity across variable compliant substrates. Rate of limb extension tends to decrease with increasing compliance ($P < 0.001$). Significant differences across compliance are denoted with letters a, ab, b, etc., compliances not sharing the same letters are significantly different ($P < 0.05$).

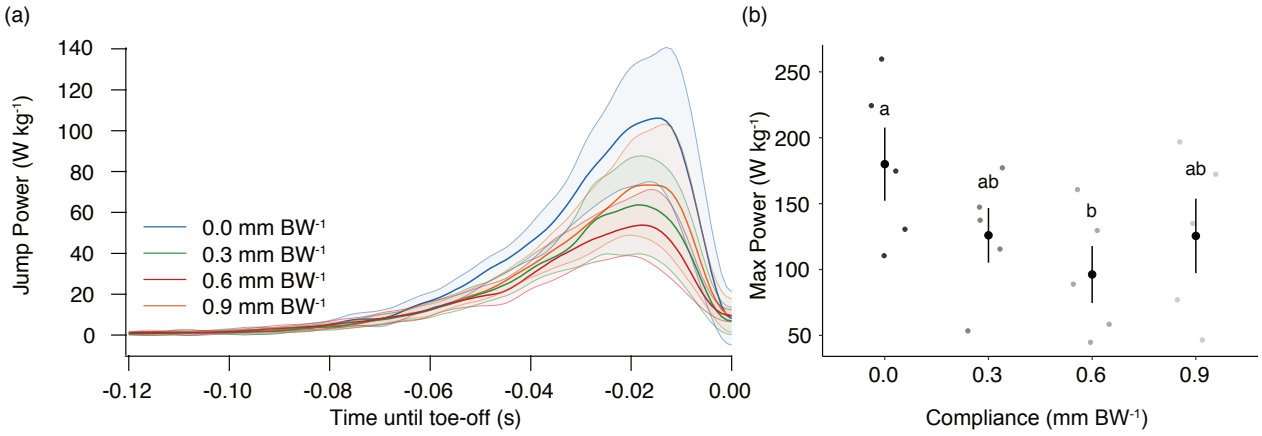

Figure 2.4. Jump power across four compliant conditions (N = 5). (a) Average jump power profile during a jump. All averaged data are shown as a bolded line with 95% confidence intervals denoted with like-color shaded regions around the averaged traces. (b) Maximum jump power with averaged individual data points represented as swarm plots with scatter plots (mean ± SEM) overlaid. Maximum jump power decreases with increasing compliance (P = 0.014). Significant comparisons are indicated with a, b, and ab; means not sharing the same letters are significantly different (P < 0.05).

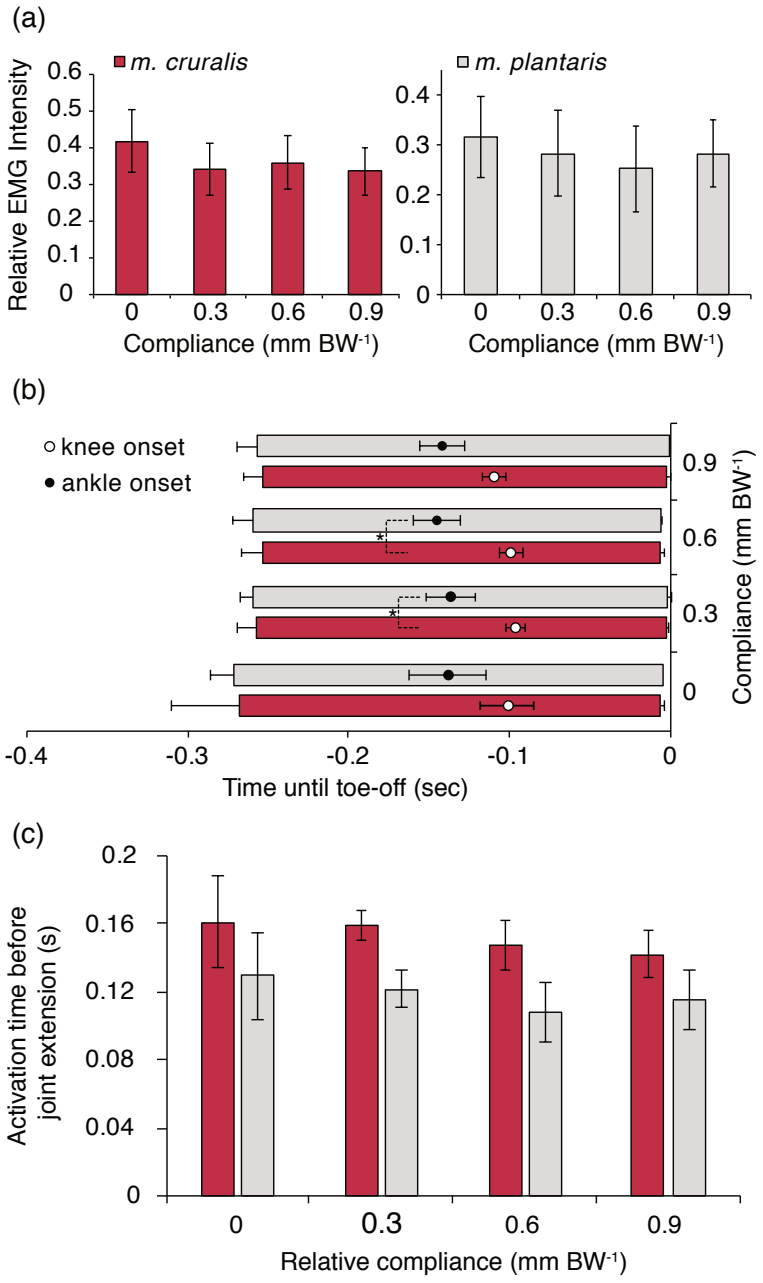

Figure 2.5. Average muscle activation patterns for *m. cruralis*, and *m. plantaris* during jumps from various compliant substrates (N = 6; mean SEM). (a) There was no difference in muscle activation intensity across compliance for both joint extensor muscles. (b) Bar graphs represent EMG extensor muscle onset and offset, with onset of relative joint extensions represented scatter plots. Muscle activation occurred around similar times across compliance, however offset differed significantly (P = 0.033). Joint angle onset decoupled with greater compliances at 0.3 and 0.6 mm BW^{-1} (P = 0.046; 0.039).

2.8 REFERENCES

Aguilar, J. and Goldman, D. I. (2016). Robophysical study of jumping dynamics on granular media. *Nature Physics* 12, 278-284.

Akella, T. and Gillis, G. B. (2011). Hopping isn't always about the legs: Forelimb muscle activity patterns during toad locomotion. *Journal of Experimental Zoology* 315, 1-11.

Astley, H. C. and Roberts, T. J. (2012). Evidence for a vertebrate catapult: elastic energy storage in the plantaris tendon during frog jumping. *Biology Letters* 8, 386-389.

Astley, H. C. and Roberts, T. J. (2014). The mechanics of elastic loading and recoil in anuran jumping. *Journal of Experimental Biology* 217, 4372-4378.

Astley, H. C., Haruta, A., and Roberts, T. J. (2015). Robust jumping performance and elastic energy recovery from compliant perches in tree frogs. *Journal of Experimental Biology* 218, 3360-3363.

Azizi, E. (2014). Locomotor function shapes the passive mechanical properties and operating lengths of muscle. *Proceedings of the Royal Society B: Biological Science* 281, 20132914

Azizi, E. and Abbott, E. M. (2013). Anticipatory motor patterns limit muscle stretch during landing in toads. *Biology Letters* 9, 20121045. DOI: http://dx.doi.org/10.1098/rsbl.2012.1045

Azizi, E. and Roberts, T. J. (2010). Muscle performance during frog jumping: influence of elasticity on muscle operating lengths. *Proceedings of the Royal Society B*: *Biological Science* 277, 1523-1530.

Biewener, A. A. and Daley, M. A. (2007). Unsteady locomotion: integrating muscle function with whole body dynamics and neuromuscular control. *Journal of Experimental Biology* 210, 2949-2960.

Biewener, A. A. and Gillis, G. B. (1999). Dynamics of muscle function during locomotion: accommodating variable conditions. *Journal of Experimental Biology* 202, 3387-3396.

Channon, A. J., Günther, M. M., Crompton, R. H., D'Août, K., Preuschoft, H., and Vereecke, E. E. (2011). The effect of substrate compliance on the biomechanics of gibbon leaps. *Journal of Experimental Biology* 214, 687-696.

Cox, S. M. and Gillis, G. B. (2016). Sensory feedback and coordinating asymmetrical landing in toads. *Biology Letters* 12, 20160196. DOI: http://dx.doi.org/10.1098/rsbl.2016.0196

Cox, S. M. and Gillis, G. (2017). Evidence toads may modulate landing preparation without predicting impact time. *Journal of Experimental Biology* 6, 71-76.

Daley, M. A. and Biewener, A. A. (2006). Running over rough terrain reveals limb control for intrinsic stability. *PNAS* 103 (42), 15681-15686.

Daley, M. A. and Biewener, A. A. (2011). Leg muscles that mediate stability: mechanics and control of two distal extensor muscles during obstacle negotiation in the guinea fowl. *Philosophical Transactions of the Royal Society B*: *Biological Science* 366, 1580-1591.

Daley, M. A., Felix, G., and Biewener, A. A. (2007). Running stability is enhanced by a proximo-distal gradient in joint neuromechanical control. *Journal of Experimental Biology* 210, 383-394.

Demes, B., Jungers, W. L., Gross, T. S. and Fleagle, J. G. (1995). Kinematics of leaping primates: influence of substrate orientation and compliance. *American Journal of Physiological Anthropology* 96, 419-429.

Dickinson, et al. (2000). How animals move: An integrative view. *Science* 288, 100-106.

Farley, C. T., Houdijk, H. H. P., Van Strien, C. and Louie, M. (1998). Mechanism of leg stiffness adjustment for hopping on surfaces of different stiffnesses. *The American Physiological Society* 1044-1055.

Ferris, D. P. and Farley, C. T. (1997). Interaction of leg stiffness and surface stiffness during human hopping. *The American Physiological Society* 15-22.

Ferris, D. P., Louie, M., and Farley, C. T. (1998). Running in the real world: adjusting leg stiffness for different surfaces. *Proceedings of the Royal Society B: Biological Science* 265, 989-994.

Ferris, D. P., Liang, K. and Farley, C. T. (1999). Runners adjust leg stiffness for their first step on a new running surface. *Journal of Biomechanics* 32, 787-794.

Gillis, G. B., Akella, T., and Gunaratne, R. (2010). Do toads have a j ump on how far they hop? Pre-landing activity timing and intensity in forelimb muscles of hopping *Bufo marinus*. *Biology Letters* 6, 486-489.

Gilman, C. A. and Irschick, D. J. (2013). Foils of flexion: the effects of perch compliance on lizard locomotion and perch choice in the wild. *Functional Ecology* 27, 374-381.

Gilman, C. A., Bartlett, M. D., Gillis, G. B., and Irschick, D. J. (2012). Total recoil: perch compliance alters jumping performance and kinematics in green anole lizards (*Anolis c arolinensis*). *Journal of Experimental Biology* 215, 220-226.

Gordon, J. C., Rankin, J. W., and Daley, M. A. (2015). How do treadmill speed and terrain visibility influence neuromuscular control of guinea fowl locomotion? *Journal of Experimental Biology* 218, 3010-3022.

Hedrick, T. L. (2008). Software techniques for two- and three-dimensional kinematic measurements of biological and biomimetic systems. *Bioinspir. Biomes.* 3, 034001. DOI: http://dx.doi.org/10.1088/1748-3182/3/3/034001

Ilton, M., Bhamla, M. S., Ma, X., Cox, S. M., Fitchett, L. L., Kim, Y., Koh, J., Krishnamurthy, D., Kuo, C., Temel, F. Z., Crosby, A. J., Parkash, M., Sutton, G. P., Wood, R. J., Azizi, E., Bergbreiter, S., and Patek, S.N. (2018). The principles of cascading power limits in small, fast biological and engineering systems. *Science* 360, eaao1082.

James, K. (2003). Dynamic loading of trees. *Journal of Arboriculture* 29 (3): 165-171.

James, K. R., Haritos, N., and Ades, P. K. (2006). Mechanic stability of trees under dynamic loads. *American Journal of Botany* 93 (10): 1522-1530.

Kagaya, K. and Patek, S. N. (2016). Feed-forward motor control of ultrafast, ballistic movements. *Journal of Experimental Biology* 219, 319-333.

Kerdok, A. E., Biewener, A. A., McMahon, T. A., Weyand, P. G., and Herr, H. M. (2002). Energetics and mechanics of human running on surfaces of different stiffnesses. *The American Physiological Society* 92, 469-478.

Kerzenmacher, T. and Gardiner, B. (1998). A mathematical model to describe the dynamic response of a spruce tree to the wind. *Trees* 12: 385-394.

Marsh, R. L. and John-Alder, H. B. (1994). Jumping performance of hylid frogs measured with high-speed cine film. *Journal of Experimental Biology* 188, 131-141.

McMahon, T. A. and Green, P. R. (1978). The influence of track compliance on running. *Journal of Biomechanics* 12, 893-904.

McMahon, T. A. (1985). The role of compliance in mammalian running gaits. *Journal of Experimental Biology* 115, 263-282.

Nauwelaerts, S. and Aerts, P. (2003). Propulsive impulse as a covarying performance measure in the comparison of the kinematics of swimming and jumping in frogs. *Journal of Experimental Biology* 206, 4341-4351.

Peplowski, M. M. and Marsh, R. L. (1997). Work and power output in the hindlimb muscles of Cuban tree frogs *Osteopilus septemtrionalis* during jumping. *Journal of Experimental Biology* 200, 2861-2870.

Roberts, T. J. and Marsh, R. L. (2003). Probing the limits of muscle-powered accelerations: lessons from jumping bullfrogs. *Journal of Experimental Biology* 206, 2567-2580.

Roberts, T. J., and Azizi, E. (2011). Flexible mechanisms: the diverse roles of biological springs in vertebrate movement. *Journal of Experimental Biology* 214, 353-361.

Roberts, T. J., Abbot, E. M. and Azizi, E. (2011). The weak link: do muscle properties determine locomotor performance in frogs? *Philosophical Transactions of the Royal Society B: Biological Science* 366, 1488-1495.

Schnyer, A., Gallardo, M., Cox, S., and Gillis, G. (2014). Indirect evidence of elastic energy playing a role in limb recovery during toad hopping. *Biology Letters* 10, 20140418.

Wakeling, J. M., Nigg, B. M., and Rozitis, A. I. (2002). Muscle activity damps the soft tissue resonance that occurs in response to pulsed and continuous vibrations. *The American Physiological Society* 93, 1093-1103.

Wilson, A. M., McGuigan, M. P., Su, A., and van den Bogert, A. J. (2001). Horses damp the spring in their step. *Nature* 414, 895-899.

CHAPTER 3

Trade-offs of power amplification on compliant substrates

3.1 INTRODUCTION

Many biological systems utilize power amplification to achieve fast ballistic movements. This allows an organism to perform greater power outputs than what is possible at the muscle level alone (Roberts and Marsh 2003; Roberts, et al. 2011). These mechanisms have been uniformly characterized as a series of motors, elastic elements (springs), and latches (Ilton et al., 2018). Broadly, latch mechanisms act as a resistive force that allows for the motor to develop force and store energy in an elastic element. Upon unlatching, this stored energy can be rapidly released at far faster rates than can be produced instantaneously (Roberts and Marsh, 2003; Roberts et al. 2011). However, this performance can be affected by the radial latch qualities, or rate at which energy is released, which ultimately affects the power output (Ilton et al., 2018). These fundamental properties driving power amplification are still largely unknown and black boxed. For example, it remains unclear what physical anatomical structures may characterize each component. Whereas, the role of springs and elastic structures (e.g. tendons) in power amplification has been well demonstrated (Roberts and Marsh 2003; Roberts and Azizi 2011; Astley and Roberts 2012, 2014; Ilton et al., 2018), although decoupling these structures (the latch, motor, and spring) is a continued challenge. Thus, we present a hypothetical model that provides a unique opportunity to test the latch, spring, and motor interactions on variable substrates, providing further insight into the latching mechanism. We validate our hypothetical model using a biological analogue and novel experimental design using the plantaris muscle-tendon-unit (MTU) of a bullfrog (*Lethobates catesbeianus*).

We use the latch model from Ilton and colleagues (2018) to better understand substrate interactions by placing a simple latch model on a compliant substrate (Figure 3.1). With this model we decouple the latching components and ask questions like: If we change the quality of a latch by making it less rigid, will it change energy recovery of the projectile spring (k_1) and mass (m_1) from the substrate spring (k_2) and mass (m_2)? Modeling the dynamics between the mass (m_1) and substrate (m_2, k_2) also allows us to understand how substrates of a particular mass (m_2) and stiffness (k_2) may affect latch dynamics and energy recovery (Figure 3.1). With our model we predict a less effective latch would allow for a slower rate of energy release and greater energy recovery from the recoil of a compliant substrate. We hypothesize this trade-off additionally depends on the mass and inertia of the substrate and how long it takes for the substrate to recoil. We take a reductionist approach to investigate this trade-off between the type of latch and total energy recovery during power amplification. We design a dual servomotor set-up that tests a range of latch types, controlled by the rate at which elastic energy stored is released from the tendon of the plantaris MTU, and quantify energy recovery within the system. The aim of this study is to further understand optimal latch dynamics and energy conservation when dealing with compliant substrates.

3.2 MATERIAL AND METHODS

3.2.1 In vitro muscle preparations

Eight adult American bullfrogs (*Lithobates catesbeianus*, 92-126 g) were used in this experiment. Frogs were purchased from Rana Ranch (Twin Falls, ID), a bullfrog vendor. Animals were housed, and experiments were performed at the University of California, Irvine

(UCI) according to the UCI Institutional Animal Care and Use Committee (IACUC) protocol. We used an *in vitro* isolated muscle-tendon-unit (MTU) preparation approach using the bullfrog *m. plantaris*. All frogs were euthanized with a double pithing protocol. A single leg was skinned and isolated from the frog body by cutting through the acetabulum. Dissections were done at room temperature (21.5 - 22.2 °C) in Ringer's solution. The *m. plantaris* MTU was carefully isolated from the proximal muscles of the leg. The proximal muscle attachment at the knee was kept intact to minimize any potential nerve damage. Sonomicrometry transducers (1 mm, Sonometrics Inc., London, Ontario, Canada) were implanted along a muscle fascicle to measure fascicle length changes, $L_{fascicle}$ (e.g. figure 2b). One transducer was implanted at the apex of the muscle and another above the aponeurosis. Transducers were secured in place with 6-0 suture. The sciatic nerve was isolated from the surrounding femur muscle tissue and instrumented with a nerve cuff, made from silver wire and plastic tubing for stimulation. The tibia fibula was cut and separated from the muscle. To mount the muscle, the plantaris tendon was cut above the ankle, and secured to a custom-made tendon clamp. The femur was clamped and tied with Kevlar to a rigid acrylic post, which kept the knee in place to avoid slippage. The tendon clamp was attached to a 50N dual-mode servomotor lever arm (Aurora Scientific., Ontario CA, USA) using steal cable. The 50N servomotor simulated spring-like reactive behavior, which was controlled by a BeagleBone Black controller used to simulate different compliances relative to tendon compliance (spring constant, *k*) (figure 3.1b). For more detailed information on the reactive spring motor set-up reference Chapter 2.2 Methods and Materials. The femur post was tightly screwed to the end of the 100N servomotor lever arm. The 100N servomotor simulated a latch-like behavior that shortened by 30% Lo at four different shortening velocities (e.g. Figure 3.2e). Slack and additional compliance were minimized from the system. Servomotor lever-arms where

oriented side-by-side so that the MTU was mounted horizontally between the two lever arms. *In vitro* contractions were done at room temperature in an oxygenated ringer's solution bath.

All dynamic muscle contractions were performed at optimum muscle lengths, determined by fixed-end contractions under maximum twitch conditions. An optimum passive tension was determined based upon a force-length curve. Optimum length (L_o) was defined at the plateau region, where muscle force production was highest. The plantaris was stimulated via the sciatic nerve using a Grass Stimulator (S48; Grass, West Warwick, RI; train duration, 600 ms; stim rate, 60 ms; pulse duration, 0.2 ms; amplitude, 9V). Continuous data acquisition (1000 Hz) of the dual servomotor forces, lengths, and fascicle length were recorded during activations using a 16-bit A/D converter (National Instruments, TX, USA) and Igor Pro Software (Wavemetrics Corp., Lake Oswego, OR, USA). Once *Lo* was determined a fixed-end tetanus contraction was performed. Force was plotted against length to determine the *k* of the tendon, the slope between force and length. Following, the reactive spring motor was programed to use the same measured *k* of the tendon. A series of randomized dynamic muscle contractions were tested with the programed reactive spring motor and the latch motor in-series (V_L = 0, 0.05, 0.1, 0.2, 0.5 m s^{-1}). Muscle preparations used for each latch velocity varied: n = 8 contractions for V_L = 0, 0.05 and 0.2 m s^{-1} and n = 4 for V_L = 0.1 and 0.5 m s^{-1}. The muscle contractions occurred in two distinct phases, pre- and post-latch phases. During the pre-latch phase, the plantaris was stimulated for 500 ms prior to servomotor unlatching to achieve full tetanus. After 500 ms, the post-latch phase occurred at a predetermined velocity. These latch velocities were subsequently tested with $k_{substrate}$ values set at values ½ and ¼ of k_{tendon}.

3.2.1 Analysis

All data analyses were run in MATLAB (The MathWorks, Natick, MA) with a custom-made script, which calculated variables of interest from acquired data. Whole fascicle length measurements were corrected for by multiplying the ratio of measured sonomicrometry crystal length by whole caliper measured fascicle length at L_o. Tendon length changes were extrapolated based upon muscle fiber shortening lengths, as well as latch and substrate servomotor length changes. Total tendon energy was characterized as the product of the tendon length (L_{ten}) change and force output from the compliant motor (F_{sub}),

$$E_{ten} = L_{ten} F_{sub} \qquad (2.1).$$

Where F_{sub} was measured from the force of the reactive spring servomotor and was representative of muscle force output (e.g. Figure 3.2a). Tendon energy was differentiated with respect to time to characterize tendon power. Total substrate energy was calculated as,

$$E_{sub} = \tfrac{1}{2} k_{sub} {L_{sub}}^2 \qquad (2.2),$$

where k_{sub} is the predetermined k constant for the compliant substrate and L_{sub} is the length change of the compliant substrate servomotor. Substrate efficiency (η) was characterized as,

$$\eta = 1 - \left(\frac{E_{recovered}}{E_{stored}}\right) \qquad (2.3),$$

where $E_{recovered}$ is the total energy at the end of the post-latch phase and E_{stored} is the total energy stored prior to the latch initiation phase (pre-latch phase).

Statistical analyses were performed in RStudio (v 1.0.136, Boston, MA). Mixed-model ANOVAs were performed for substrate efficiency and power, accounting for individual as a random factor and interaction between latch velocity and substrate compliance. Tukey HSD post-hoc analyses were run to test for differences within latch type and substrate compliance.

3.3 RESULTS

We found energy recovery from a compliant substrate decreased with a more 'ideal', high velocity latch. For a fast latch energy remained in the substrate by the end of the phase of rapid energy release, which resulted in energy loss to the substrate (Figure 3.2d). The less 'ideal', slower latch allowed for almost complete energy recovery during tendon recoil. Whereas, with a high velocity latch the MTU lost nearly 40% of the energy stored, therefore making a perfect latching mechanism less efficient in recovering energy in compliant environments (Figure 3.4a). Latch shortening velocity had a significant impact on the energy efficiency ($p < 0.0001$), latch velocities half as fast as the 'ideal' fast latch proved to be slow enough to recover even ~ 92% of the energy stored (Figure 3.4). However, k_{sub} did not have a significant effect on efficiency, demonstrating the k of the tendon may only impact the loading phase of power amplified systems (Figure 3.3). Further demonstrating the importance of latch quality on compliant substrates for efficient performance.

We found latch velocity and relative substrate compliance significantly affected tendon power output (V_L, $p < 0.0001$; k_{sub}, $p < 0.0001$). There was also a significant interaction between latch quality and k_{sub} with tendon power ($p = 0.0001$), suggesting the springier the substrate the lower the effect the quality of the latch has on tendon power (Figure 3.4). The same amount of energy is loaded into the tendon during the pre-latch phase (Figure 3.4). This demonstrates the trade-offs and cascading effects of latch quality are only important during the post-latch phase. Lastly, in force traces and subsequent energy traces there were small irregular peaks after the start of the latch, we suspect this is the result of the acceleration of the muscle mass and the delay in reactive movement of the substrate servomotor arm that has a delay of about 17 ms, which corresponds with the timing of the irregular peak from latch onset.

3.4 DISCUSSION

Our work demonstrates how impulsive systems interact with dynamic substrates. Efficiency of energy recovery from a compliant substrate decreases with a more rigid latch (faster latch velocities). Additionally, tendon power is increasingly lost to the substrate at faster latch velocities. This strongly suggests that the slower the latch, the lower the rate of energy loss to the substrate. We discovered a trade-off in power amplified systems between latch quality, power output, and efficiency on variable substrates. Whereas, on solid substrates latch quality does not have the same effect, a more rigid latch allows for greater power amplification on solid substrates (Ilton, et al. 2018). Relative compliance of the substrate to tendon compliance did not affect efficiency, however made a significant effect on tendon power outputs at the highest latch velocity, where springier substrates decreased power output to the substrate with the use of the same latch.

Our previous work (Chapter 2) also exemplifies this at the whole organism scale. Cuban tree frog jumps off compliant substrates compromise the latching mechanism by inducing premature limb extension. This truncating in timing of elastic energy storage and subsequently decrease power output and rate of limb extension, is analogous to the slower velocity, 'less ideal' latch, hence the slower rate of limb extension. While on solid substrates, a non-complaint environment provides the ideal conditions for elastic energy storage and a more 'rigid latch'. Hence, our work provides further support in the role of dynamic changes in mechanical advantage, which changes elastic energy recovery on compliant substrates, effectively changing the latch or catch properties (Astley and Roberts, 2012).

We found less-rigid latches allow for greater elastic energy recovery from compliant substrates. We characterize the flow of energy in impulsive systems and provide a fundamental

understanding of how biological systems, from the whole animal to the muscle level, interact with their physical environments. Our research provides the potential to characterize latch quality used by various biological and engineered systems using kinetics and compliant substrates. Understanding how power amplified systems may be uniquely tuned for optimal performance across variable substrates is currently unknown. However, by probing additional questions around unique perturbations to impulsive systems and their latching mechanism may further uncouple the individual components and dynamics (Aguilar and Goldman 2016). Future work exploring mathematical latch models and physical robot models may allow for greater manipulation of the latch and will greatly advance our understanding of the general principals driving impulsive systems.

3.5 LIST OF ABBREVIATIONS

$E_{recovered}$, energy recovered from substrate;

E_{stored}, energy stored in substrate;

F_{sub}, muscle force measured from compliant servomotor;

k_{ten}, tendon spring constant;

k_{sub}, substrate spring constant;

L_o, optimal muscle length;

L_{ten}, tendon length;

MTU, muscle-tendon-unit;

V_L, latch velocity

3.6 ETHICS

Animal husbandry and experimental procedures were approved by the University of California, Irvine Institutional Animal Care and Use Committee (Protocol AUP-17-170).

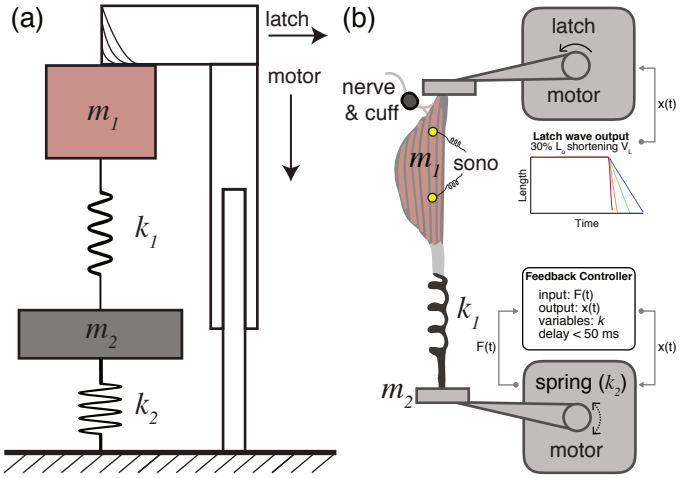

Figure 3.1. (a) Duel spring-mass and actuated latch schematic model. The latch fastens the mass, m_1, in place and allows the mass to keep potential energy in the attached spring, k_1. Below m_1 and k_1 is a compliant substrate, modeled as a fixed secondary mass (m_2) and spring (k_2). An accelerating motor loads both springs, and once the latch slides and releases, the energy stored is also released from the system. The latch rigidity controls the rate of energy release from the system. (b) Schematic of the analog in vitro muscle-tendon-unit (MTU) experimental prep using the bullfrog plantaris muscle. The MTU was clamped and mounted between two servomotors. One 100N motor simulates latch-like behavior, and the second, 50 N motor, simulates reactive spring-like behavior. The analogues latches in the in vitro prep were tested by adjusting the velocity (V_L) of a 30% L_o length change. The muscle was maximally stimulated using a nerve cuff. Sonomicrometry was used to measure fascicle length changes.

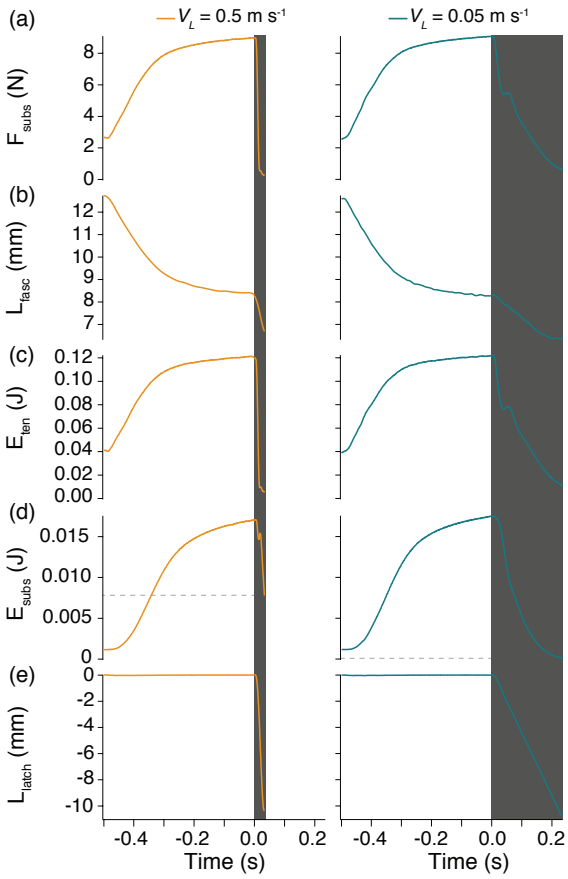

Figure 3.2. Representative in vitro plantaris tetanus measurements taken at fast (0.5 m s^{-1}) and slow (0.05 m s^{-1}) latch velocities. The first 500 ms of the tetanus is the pre-latch phase, characterized as the time leading up to unlatching, where energy is loaded into the system as the muscle achieves complete tetanus, as (a) force, $F_{substrate}$, plateaus. The shaded area, time after t = 0 represents latch duration. This results in 30% (c) muscle fascicle shortening, $L_{fascicle}$. Analysis terminated at the end of unlatching (30% L_o). Energy dynamics between the (d) compliant substrate, $E_{substrate}$, and (e) tendon, E_{tendon}, were characterized from changes in tendon length and muscle force output, also $F_{substrate}$. Note the dashed lines comparing energy left in the substrate with a fast latch versus a slower latch. About half the energy remains in the substrate with a fast latch, however with a slower latch all energy is returned back to the muscle.

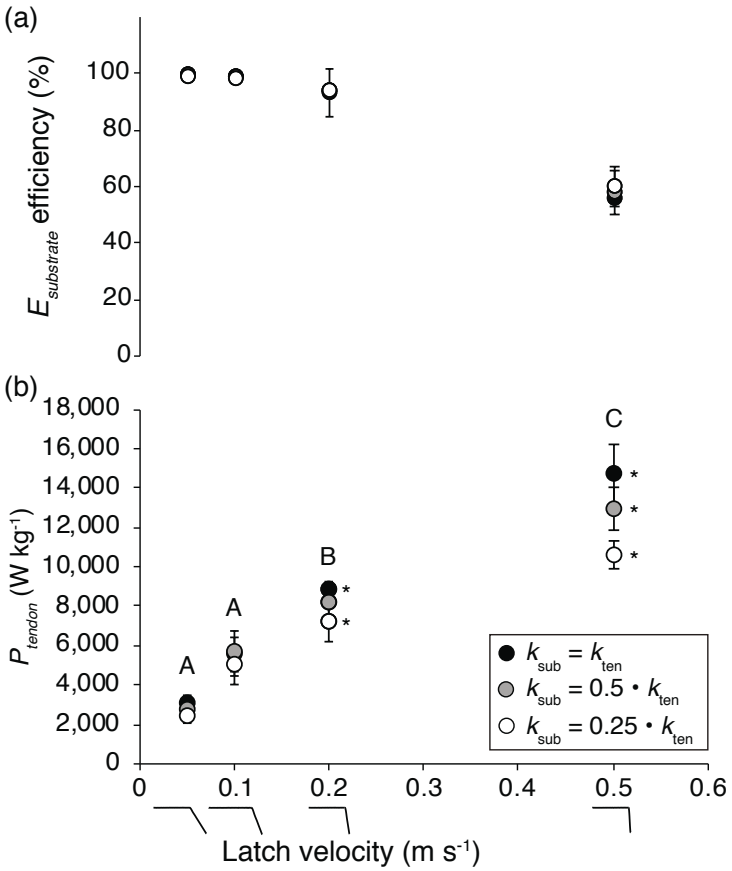

Figure 3.3. Representative traces of tendon power (a) stored prior to latch release and (b) tendon power lost to the substrate after latch on-set. Representative traces are from a fast latch condition (0.5 m s-1) and a slow latch (0.05 m s-1). Power stored in pre-latch phase is the same across latch conditions, however a fast latch loses a dramatically larger portion of power to the substrate.

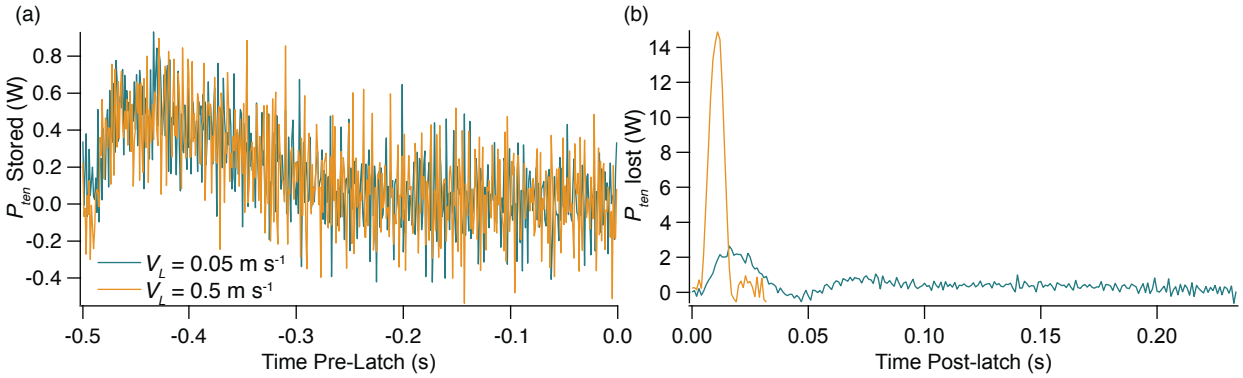

Figure 3.4. Effects of latch velocity on (a) percent energy recovered from the substrate and (b) tendon power output. Grayscale data points correspond with changes in $k_{substrate}$ relative to k_{tendon}. Summary data for N = 8 muscle preparations with n = 8 contractions for V_L = 0, 0.05 and 0.2 m s^{-1} and n = 4 for V_L = 0.1 and 0.5 m s^{-1}. All data are means with s.e.m. ± error bars. Illustrations of latches under x-axis correspond to 30% fascicle length and shortening velocities. Greater latch velocities (or more rigid latches) result in decreased energy recovery and increased tendon power output. Energy recovery is truncated by half with greater latch velocities. The effect of variable stiffnesses between the substrate and tendon separate out with fast latch velocities.

3.8 REFERENCES

Aguilar, J. and Goldman, D. I. (2016). Robophysical study of jumping dynamics on granular media. *Nature Physics* 12, 278-284.

Astley, H. C. and Roberts, T. J. (2012). Evidence for a vertebrate catapult: elastic energy storage in the plantaris tendon during frog jumping. *Biology Letters* 8, 386-389.

Astley, H. C. and Roberts, T. J. (2014). The mechanics of elastic loading and recoil in anuran jumping. *Journal of Experimental Biology* 217, 4372-4378.

Ilton, M., Bhamla, M. S., Ma, X., Cox, S. M., Fitchett, L. L., Kim, Y., Koh, J., Krishnamurthy, D., Kuo, C., Temel, F. Z., Crosby, A. J., Parkash, M., Sutton, G. P., Wood, R. J., Azizi, E., Bergbreiter, S., and Patek, S.N. (2018). The principles of cascading power limits in small, fast biological and engineering systems. *Science* 360, eaao1082.

Roberts, T. J. and Marsh, R. L. (2003). Probing the limits of muscle-powered accelerations: lessons from jumping bullfrogs. *Journal of Experimental Biology* 206, 2567-2580.

Roberts, T. J., and Azizi, E. (2011). Flexible mechanisms: the diverse roles of biological springs in vertebrate movement. *Journal of Experimental Biology* 214, 353-361.

Roberts, T. J., Abbot, E. M. and Azizi, E. (2011). The weak link: do muscle properties determine locomotor performance in frogs? *Philosophical Transactions of the Royal Society B: Biological Sciences* 366, 1488-1495.

APPENDICES

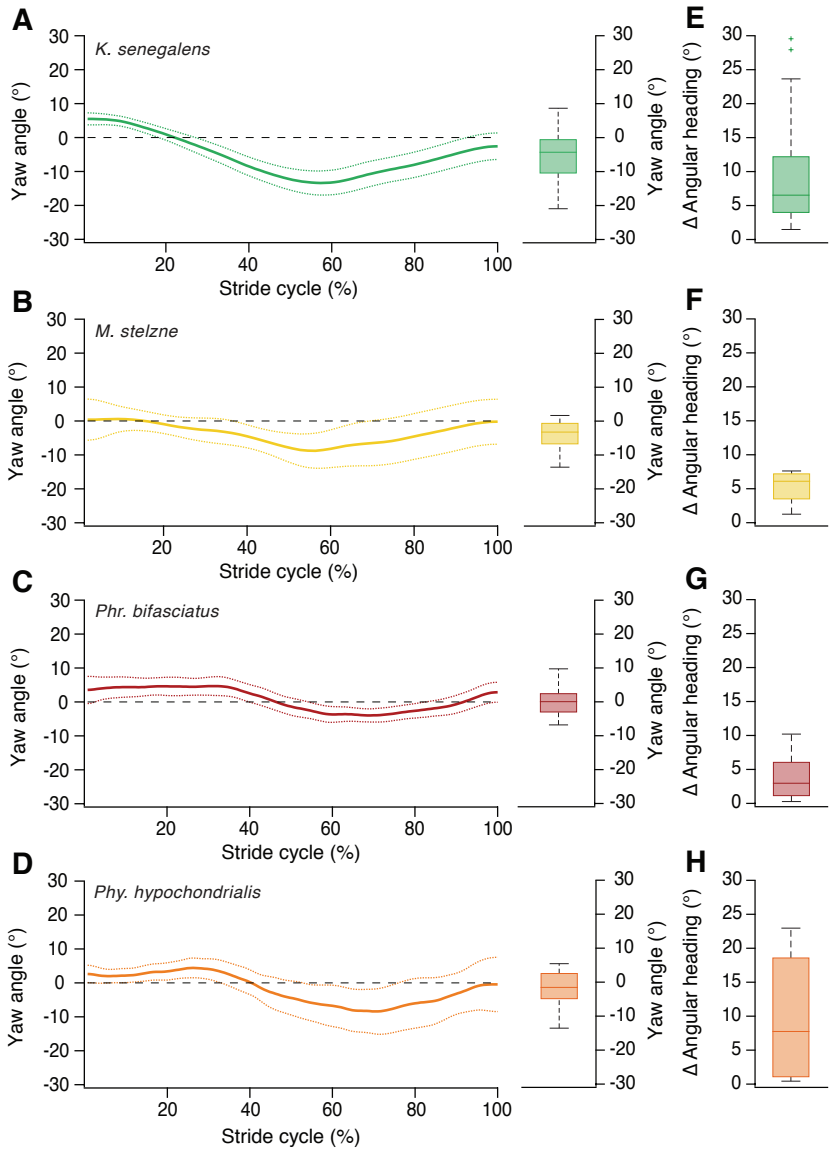

Appendix Figure A.1. A comparison of average body yaw and heading angle over a single stride. (A, E) *Kassina senegalensis* (green; *n*=5), (B, F) *Melanophryniscus stelzneri* (yellow; *n*=2), (C, G) *Phrynomantis bifasciatus* (maroon; *n*=3), and (D, H) *Phyllomedusa hypochondrialis* (orange; *n*=2). Traces correspond to changes in yaw angle over a single stride. Stride cycle is defined as the first point of contact for the lead forelimb, to just before the lead forelimb touched back down to start a new stride. All averaged data are shown by a solid line, with dotted lines representing 95% confidence intervals. Changes in heading (E - H) demonstrate when yaw did not return back to original stride start position frogs had changed heading direction. The box and whisker plots represent 50% of the data range and interquartile ranges. Bold horizontal lines represent the median, while box height and whisker asymmetry indicate skewness of observation. In all four species, the start of a stride was characterized by a negative change in yaw to about 50% of the stride cycle, followed by a positive change in yaw to conclude the stride.

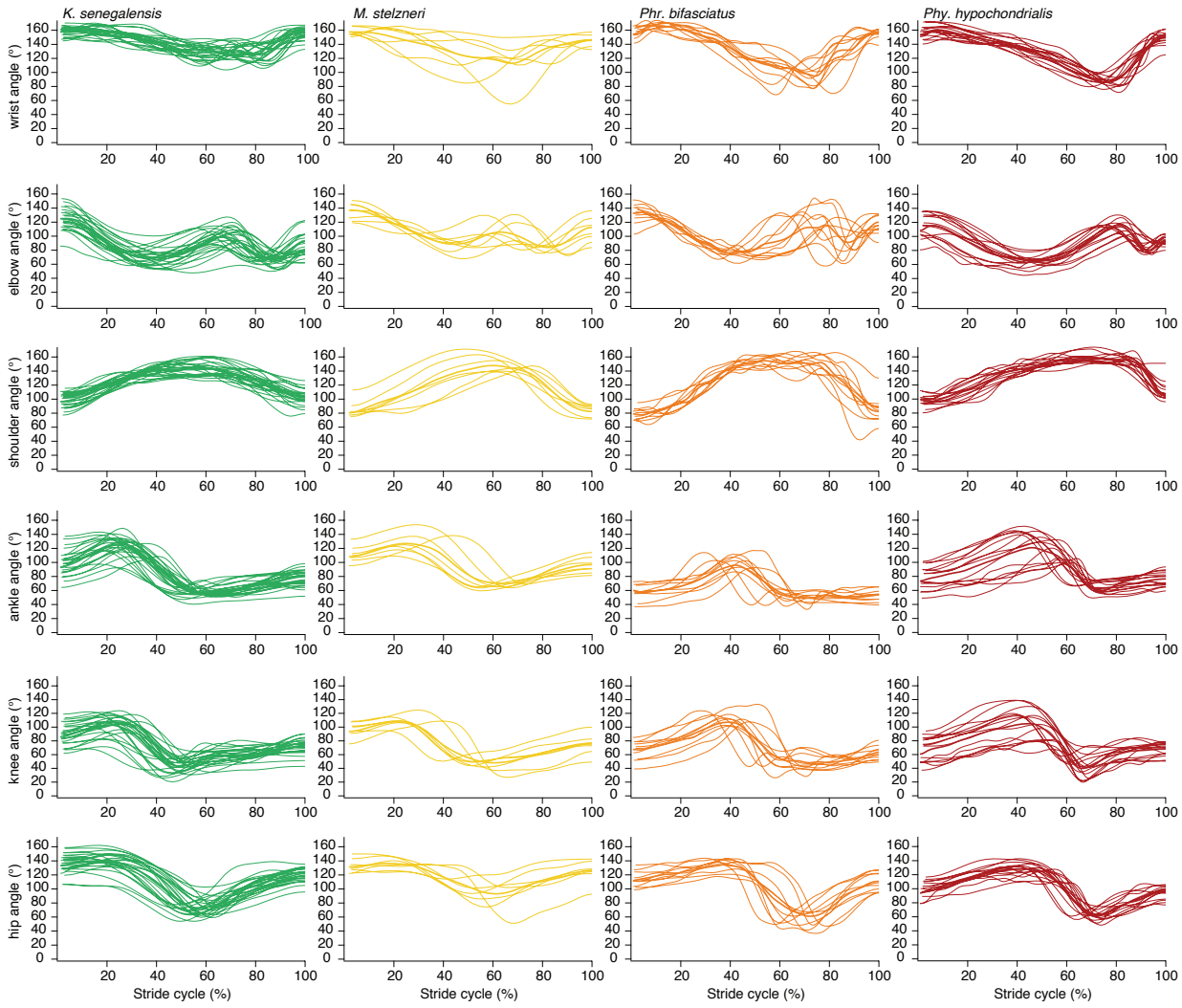

Appendix Figure A.2. Average relative joint angle changes over a stride in the fore- and hindlimb— a reproduction of Figure 8. *Kassina senegalensis* (green; *n*=5), *Melanophryniscus stelzneri* (yellow; *n*=2), *Phrynomantis bifasciatus* (maroon; *n*=3), and *Phyllomedusa hypochondrialis* (orange; *n*=2). A complete stride cycle is defined from the first point of contact of the leading forelimb to just before the same leading forelimb touches back down. All averaged data are shown as a bold line. Thinner lines show individual trail traces.

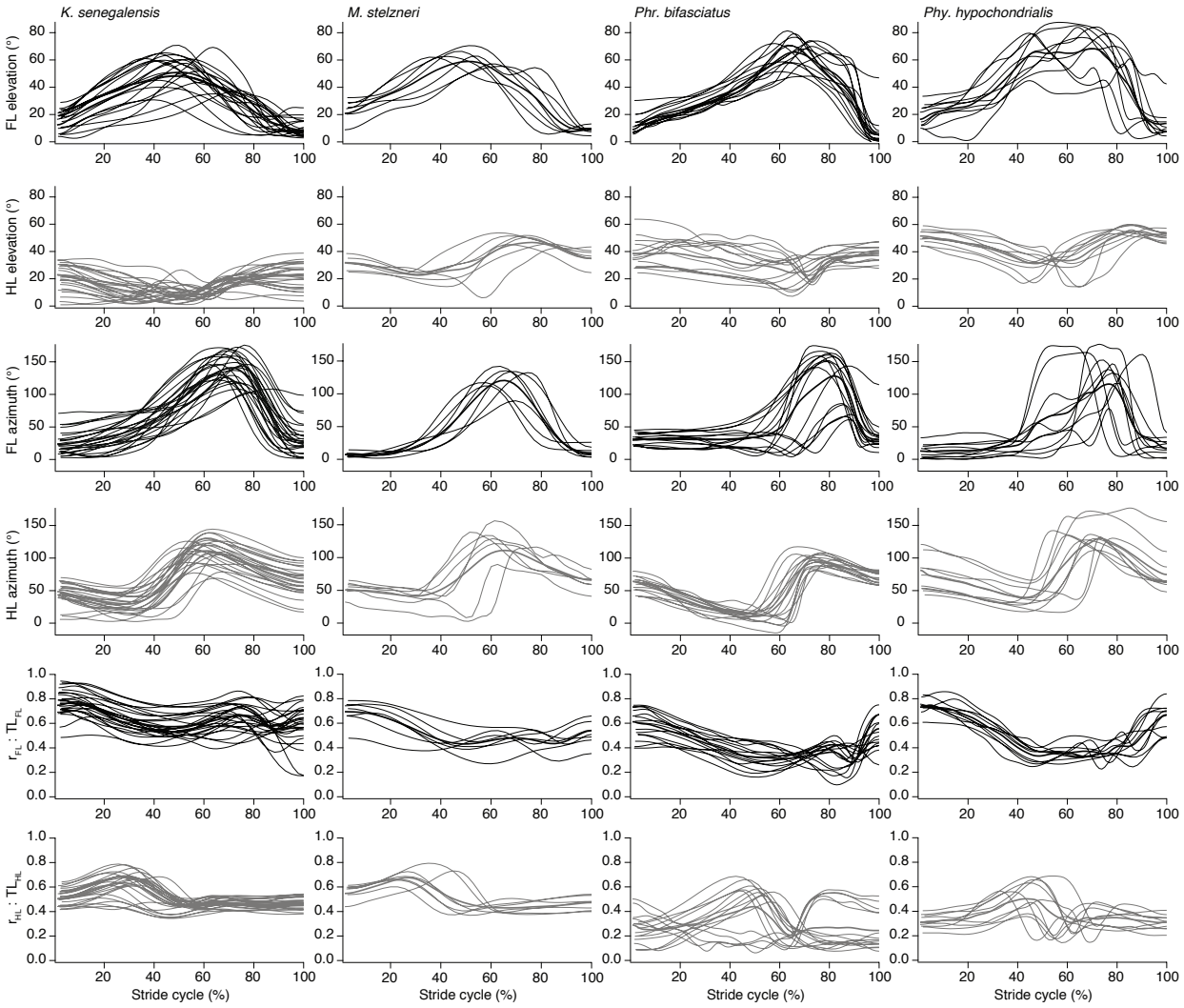

Appendix Figure A.3. Average polar angles and relative radial distance changes over a stride in the fore- (FL) and hindlimb (HL). *Kassina senegalensis* (first column, *n*=5), *Melanophryniscus stelzneri* (second column, *n*=2), *Phrynomantis bifasciatus* (third column *n*=3), and *Phyllomedusa hypochondrialis* (fourth column, *n*=2). The top two rows of graphs show the elevation angle changes in the fore- and hindlimb across a stride. The middle two rows show azimuth angle changes, and the bottom two rows show radial distance (*r*) changes relative to respective total limb lengths (TL) within a stride. Stride cycle was defined as the point of first contact of the leading forelimb until the leading forelimb touched back down. Bolded lines are averaged traces. Thinner lines show individual trail traces. See Figure 1.9 for more summary analyses of midstance and maximum extension of each limb.

Supplementary Table S1 Anuran specimen information and species limb length mean values.

Family	Species	*n*	SVL ± SE †	FL ± SE †	HL ± SE †	Preparation	Collection‡	ID§
Brachycephalidae	*Eleutherodactylus guentheri*	1	38.31	26.47	87.56	X-ray CT	DM	
Bufonidae	*Anaxyrus canorus*	6	30.95 ± 2.34	18.60 ± 1.17	33.68 ± 2.62	C&S	LACM	11881 11867 1083 11122 11079 11278
Bufonidae	*Atelopus cruciger*	1	39.62	25.27	45.39	C&S	LACM	127301
Bufonidae	*Atelopus ignescens*	3	40.76 ± 5.43	23.64 ± 2.12	41.95 ± 3.91	C&S	LACM	127307 127306 127305
Bufonidae	*Atelopus spurrelli*	1	31.19	21.71	34.41	C&S	LACM	45780
Bufonidae	*Atelopus varius*	2	39.87 ± 0.55	23.62 ± 0.31	42.85 ± 1.04	C&S	LACM	64440 64437
Bufonidae	*Incilius periglenes*	1	44.91	33.10	66.71	X-ray CT	DM	
Bufonidae	*Melanophryniscus stelzneri*	2	25.75 ± 3.40	18.94 ± 0.48	26.00 ± 0.59	C&S	HCA	1 2
Centrolenidae	*Centrolene prosoblepon*	2	24.25 ± 0.97	22.05 ± 3.52	40.83 ± 1.04	Skeletal	LACM	162367 168371
Ceuthomantidae	*Ceuthomantis smaragdinus*	1	19.76	12.70	34.80	X-ray CT	DM	
Craugastoridae	*Craugastor vulcani*	3	66.37 ± 0.98	39.18 ± 1.43	100.13 ± 1.45	C&S	LACM	178067 178066 178065
Craugastoridae	*Haddadus binotatus*	1	39.51	29.54	85.68	X-ray CT	DM	
Dendrobatidae	*Adelphobates quinquevittatus*	1	17.95	13.51	24.09	C&S	LACM	42307
Dendrobatidae	*Allobates talamancae*	2	23.50 ± 2.54	16.40 ± 1.23	34.21 ± 1.79	C&S	LACM	60969 43943
Dendrobatidae	*Ameerega bilinguis*	1	21.03	13.52	25.79	C&S	LACM	60980
Dendrobatidae	*Ameerega pulchripecta*	1	27.37	20.08	33.44	C&S	LACM	42302
Dendrobatidae	*Ameerega trivittata*	1	40.11	29.59	59.61	C&S	LACM	60981
Dendrobatidae	*Ameerega picta*	1	21.84	16.87	31.33	C&S	LACM	60997

Family	Species	*n*	SVL ± SE[†]	FL ± SE[†]	HL ± SE[†]	Preparation	Collection[‡]	ID[§]
Dendrobatidae	*Colostethus inguinalis*	1	25.76	19.16	39.79	C&S	LACM	42507
Dendrobatidae	*Colostethus embena*	1	21.77	14.92	30.87	C&S	LACM	43969
Dendrobatidae	*Colostethus pratti*	1	49.12	38.22	59.99	C&S	LACM	44144
Dendrobatidae	*Dendrobates tinctorius*	1	39.94	23.00	42.93	C&S	LACM	43923
Dendrobatidae	*Dendrobates truncatus*	1	25.34	16.99	33.13	C&S	LACM	44265
Dendrobatidae	*Mannophryne trinitatis*	1	36.08	28.76	45.96	C&S	LACM	60971
Dendrobatidae	*Oophaga histrionica*	1	20.64	18.58	30.95	C&S	LACM	43732
Dendrobatidae	*Oophaga pumilio*	1	13.79	10.17	19.28	C&S	LACM	60992
Dendrobatidae	*Ranitomeya ventrimaculata*	1	43.78	39.70	73.15	C&S	LACM	438227
Dendrobatidae	*Rhenobates palmatus*	1	19.20	11.83	24.79	C&S	LACM	44175
Eleutherodactylidae	*Eleutherodactylus diastema*	2	25.90 ± 0.75	21.93 ± 0.10	34.16 ± 0.81	C&S	LACM	178005 178062
Eleutherodactylidae	*Eleutherodactylus angustidigitorum*	2	21.67 ± 0.50	13.34±1.13	35.07 ± 0.06	C&S	LACM	178145 178100
Eleutherodactylidae	*Eleutherodactylus gossei*	1	22.29	13.41	40.02	X-ray CT	DM	
Eleutherodactylidae	*Syrrhophus angustidigitorum*	2	25.90 ± 0.50	21.93 ± 1.13	34.16 ± 0.06	C&S	LACM	178145 178100
Hylidae	*Acris gryllus*	2	31.10 ± 4.63	22.92 ± 1.76	52.68 ± 5.27	C&S	LACM	12220 178029
Hylidae	*Hyla walkeri*	2	67.41 ± 2.50	50.52 ± 1.47	104.82 ± 3.66	C&S	LACM	45048 8432
Hylidae	*Litoria caerulea*	2	26.81 ± 3.86	18.00 ± 8.20	45.29 ± 17.56	C&S	LACM	167447 167446
Hylidae	*Phyllomedusa hypochondrialis*	2	38.00 ± 1.45	28.61 ± 0.57	50.50 ± 0.74	C&S	HCA	1 2
Hylidae	*Pseudacris brachyphona*	3	24.47 ± 0.36	18.72 ± 0.42	41.67 ± 0.95	C&S	LACM	166892 166893 166894
Hylidae	*Pseudacris cadaverina*	3	29.23 ± 0.24	19.18 ± 0.88	41.57 ± 1.14	C&S	LACM	AG431 AG433 AG432

Family	Species	*n*	SVL ± SE[†]	FL ± SE[†]	HL ± SE[†]	Preparation	Collection[‡]	ID[§]
Hylidae	*Pseudacris crucifer*	3	25.64 ± 0.55	14.34 ± 0.50	32.60 ± 2.46	C&S	LACM	166863 166862 166859
Hyperoliidae	*Kassina senegalensis*	10	31.87 ± 0.79	24.74 ± 0.70	40.01 ± 0.74	C&S	AL	1 2 3 4 5 6 7 8 9 10
Microhylidae	*Gastrophryne mazatlanensis*	4	30.49 ± 0.48	20.65 ± 0.84	53.15 ± 0.23	Skeletal	LACM	162698 162699 162700 162696
Microhylidae	*Hamptophryne boliviana*	1	23.23	13.87	29.89	X-ray CT	DM	
Microhylidae	*Gastrophryne usta*	4	18.72 ± 0.73	9.58 ± 0.29	15.64 ± 0.18	X-ray CT	DM	
						Skeletal	LACM	162865 162862 162863
Microhylidae	*Phrynomantis bifasciatus*	2	44.00 ± 1.29	30.33 ± 0.64	43.67 ± 0.62	C&S	HCA	1 2 3
Myobatrachidae	*Metacrinia nichollsi*	2	63.06 ± 2.27	32.95 ± 1.84	58.52 ± 1.63	Skeletal	LACM	162913 162912
Odontophrynidae	*Odontophrynus americanus*	2	24.78 ± 9.92	16.02 ± 2.25	42.23 ± 3.44	C&S	LACM	178120 1788113
Ranidae	*Rana boylii*	2	75.36 ± 1.90	46.08 ± 2.59	121.13 ± 2.70	C&S	LACM	178128 178135

Family	Species	*n*	SVL ± SE [†]	FL ± SE [†]	HL ± SE [†]	Preparation	Collection[‡]	ID[§]
Ranidae	*Lithobates pipiens*	3	61.18 ± 16.98	41.17 ± 15.10	107.30 ± 29.10	Skeletal	LACM	162684 162142 162683
Rhacophoridae	*Buergeria oxycephala*	1	46.31	29.59	72.54	X-ray CT	DM	
Rhacophoridae	*Chiromantis rufescens*	1	27.24	21.62	38.88	X-ray CT	DM	
Rhacophoridae	*Kurixalus idiootocus*	1	35.30	27.69	62.27	X-ray CT	DM	
Rhacophoridae	*Nyctixalus pictus*	1	48.12	33.60	89.68	X-ray CT	DM	
Rhacophoridae	*Polypedates cruciger*	1	61.16	42.54	110.02	X-ray CT	DM	
Rhacophoridae	*Polypedates leucomystax*	1	27.84	19.63	46.05	X-ray CT	DM	
Rhacophoridae	*Philautus femoralis*	1	36.95	24.60	65.59	X-ray CT	DM	
Rhacophoridae	*Philautus microtympanum*	1	24.14	15.33	38.24	X-ray CT	DM	
Rhacophoridae	*Philautus signatus*	1	64.04	45.47	100.45	X-ray CT	DM	
Rhacophoridae	*Rhacophorus reinwardtii*	1	33.60	24.09	62.83	X-ray CT	DM	
Rhacophoridae	*Polypedates eques*	1	34.13	23.79	59.40	X-ray CT	DM	
Rhacophoridae	*Theloderma stellatum*	1	30.40	17.39	53.36	X-ray CT	DM	
Strabomantidae	*Eleutherodactylus pulvinatus*	1	21.71	13.62	28.97	X-ray CT	DM	

Abbreviations: SVL, snout-vent-length; FL, forelimb length; HL, hindlimb length; SE, standard error of the mean.

[†]Measurements are given in millimeters.

[‡]Collection abbreviations are as follows: DM is DigiMorph online database; LACM is Natural History Museum of Los Angeles County; HA is personal collection of Henry C. Astley; AL is personal collection of the Azizi Lab.

[§]ID numbers correspond to collection acquisition number.

Appendix Table A.5. Regression models of anuran $\log_{10}$ hindlimb length with $\log_{10}$ forelimb length as the covariate.

Statistical Model	*N*	Slope (± SE)	*y*-intercept (± SE)	AIC
Conventional ANCOVA:				
FL Length + Locomotor Type	56	1.113 ± 0.066	Other Anura 0.186 ± 0.089	-107.62
			Walkers -0.157 ± 0.040	
PGLS:				
FL Length + Locomotor Type	54	0.941 ± 0.047	Other Anura 0.402 ± 0.082	-137.22
Pagel's λ = 1.0			Walkers -0.125 ± 0.043	

Note: Analysis of covariance (ANCOVA) indicates the non-phylogenetic model. Phylogenetic generalized least squares (PGLS) indicates phylogenetic model analysis. Slope is the regression slope and allometric exponent, with the standard error (SE), which was not significantly different between locomotor types. Akaike Information Criterion (AIC) is used to compare models, a smaller value indicates a better fit. For both models locomotor type was always significant in intercept (all $P<0.001$), indicating limb lengths are more symmetric in specialized anuran walkers.

Appendix Table A.6. Summary of three-dimensional relative joint angle kinematics (*mean* ± *s.e.m*) during minimum and maximum limb extension, *r*, of a stride in quadrupedal walking species: *Kassina senegalensis* (*n=5*), *Melanophryniscus stelzneri* (*n=2*), *Phrynomantis bifasciatus* (*n=3*), and *Phyllomedusa hypochondrialis* (*n=2*).

	Joint angles at limb phase			
Joint comparisons	Maximum *r* (°)	Mid-stance (°)	Range (°) †	Average (°) §
K. senegalensis				
Wrist	156.09 ± 2.15	145.25 ± 1.94	13.10 ± 2.23	144.05 ± 0.64
Elbow	126.02 ± 4.32	67.87 ± 4.33 [a]	58.15 ± 5.25	90.21 ± 3.22
Shoulder	96.12 ± 3.04	138.77 ± 2.78	42.65 ± 5.33	129.55 ± 1.89
Ankle	119.18 ± 1.26	113.11 ± 3.86	9.07 ± 2.05	84.42 ± 1.45 [a]
Knee	89.89 ± 2.26	85.48 ± 4.43	11.28 ± 2.46	71.62 ± 1.67
Hip	130.84 ± 3.33	128.27 ± 4.02	45.36 ± 4.6 [a]	111.07 ± 1.92
M. stelzneri				
Wrist	159.37 ± 9.66	136.41 ± 7.04	27.53 ± 1.96	134.27 ± 8.86
Elbow	138.00 ± 5.62	96.08 ± 5.34 [b]	41.92 ± 0.28	109.65 ±2.81
Shoulder	76.13 ± 3.39	120.23 ± 6.63	44.10 ± 3.25	120.43 ± 4.00
Ankle	130.65 ± 15.08	123.80 ± 18.43	8.60 ± 2.62	98.25 ± 6.47 [a]
Knee	113.53 ± 6.33	98.89 ± 15.89	14.64 ± 9.57	74.90 ± 1.81
Hip	133.09 ± 0.51	128.07 ± 3.67	34.21 ± 16.40 [ab]	116.59 ± 5.32
Phr. bifasciatus				
Wrist	154.41 ± 7.15	131.98 ± 4.34	22.44 ± 2.86	126.72 ± 2.99
Elbow	112.30 ± 8.82	63.14 ± 3.26 [a]	49.17 ± 6.53	89.06 ± 7.21
Shoulder	97.76 ± 3.92	145.07 ± 4.52	47.31 ± 0.61	136.63 ± 2.85
Ankle	118.84 ± 11.47	118.31 ± 15.69	12.19 ± 2.66	88.57 ± 7.14 [a]
Knee	75.69 ± 25.57	103.72 ± 14.17	29.33 ± 10.70	74.96 ± 8.65
Hip	113.05 ± 10.55	127.83 ± 4.26	9.91 ± 6.05 [b]	100.96 ± 2.15
Phy. hypochondrialis				
Wrist	151.18 ± 4.02	136.17 ± 0.72	17.72 ± 2.03	132.08 ± 0.64
Elbow	129.45 ± 4.25	73.98 ± 1.01 [ab]	55.47 ± 5.26	103.03 ± 0.45
Shoulder	80.54 ± 6.57	145.35 ± 0.23	64.81 ± 6.79	127.45 ± 1.66
Ankle	95.59 ± 2.12	98.33 ± 6.77	11.30 ± 0.33	64.71 ± 0.29 [b]
Knee	97.25 ± 6.22	108.15 ± 2.47	16.13 ± 3.46	71.35 ± 1.97
Hip	128.25 ± 5.51	133.61 ± 3.05	21.73 ± 6.34 [ab]	104.32 ± 4.50

Superscript letters: Designate significant ($P < 0.05$) relative joint comparisons across species. Means not sharing the same letters are not significantly different.

†Joint angle range was calculated as the difference in joint angle between maximum *r* and mid-stance.

§Joint angle average was calculated during the stance phase for each limb across a stride.

Appendix Table A.7. Analysis of variance (ANOVA) false discovery rate *post-hoc* tests of elevation angle, azimuth angle, and relative radial magnitude (*r:* total limb length) use during minimum and maximum limb extension, *r*, of a stride in quadrupedal walking species: *Kassina senegalensis* (*n=5*), *Melanophryniscus stelzneri* (*n=2*), *Phrynomantis bifasciatus* (*n=3*), and *Phyllomedusa hypochondrialis* (*n=2*).

	Elevation Angle		Azimuth Angle		*r:* total limb length	
	Stride phase		Stride phase		Stride phase	
	Mid-stance	Maximum *r*	Mid-stance	Maximum *r*	Mid-stance	Maximum *r*
Limb comparisons	*P*	*P*	*P*	*P*	*P*	*P*
Forelimb						
K. senegalensis						
M. stelzneri	0.611	0.197	0.002**	0.017*	0.465	0.80
Phr. bifasciatus Phy.	0.544	0.570	0.008**	0.078	0.061	0.46
hypochondrialis	0.154	0.409	0.002**	0.085	0.148	0.99
M. stelzneri						
Phr. bifasciatus Phy.	0.374	0.109	0.434	0.001**	0.364	0.63
hypochondrialis	0.374	0.626	0.984	0.529	0.513	0.84
Phr. bifasciatus						
Phy. hypochondrialis	0.087	0.240	0.447	0.006**	0.789	0.49
Hindlimb						
K. senegalensis						
M. stelzneri	0.154	0.098	0.434	0.065	0.789	0.63
Phr. bifasciatus Phy.	0.004**	0.006**	0.105	< 0.001**	0.061	0.45
hypochondrialis	0.006**	0.002**	0.434	0.219	0.390	0.63
M. stelzneri						
Phr. bifasciatus Phy.	0.154	0.408	0.040*	< 0.001**	0.069	0.33
hypochondrialis	0.154	0.110	0.984	0.567	0.376	0.49
Phr. bifasciatus						
Phy. hypochondrialis	0.807	0.377	0.045*	< 0.001**	0.389	0.63

*Significance at $P<0.05$
**Significance at $P<0.01$

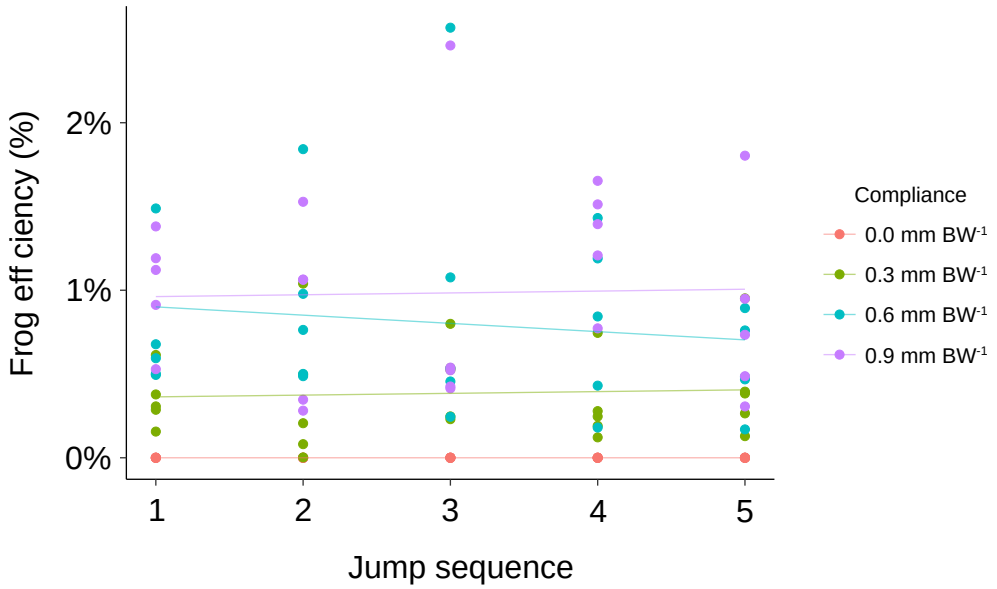

Appendix Figure B.1. The relationship between jump sequence and frog efficiency. Each color represents a different compliant condition. Each frog jumped off a single compliance. Experience with a given compliance was accounted for to detect any increase in performance or potential for learning. Linear regressions show not relationships between jump performance variable, frog efficiency, and experience with a given compliance across all individuals (N=5).